NASA CR 72732

CRYOGENIC POSITIVE EXPULSION DIAPHRAGMS

by

C. L. Lofgren and Dale Gieseking

THE BOEING COMPANY

Prepared for

NATIONAL AERONAUTICS AND SPACE ADMINISTRATION

NASA Lewis Research Center
Contract NAS 3-11204
R. F. Lark, Project Manager

NASA CR 72732

NASA CR 72732

Final Report

CRYOGENIC POSITIVE EXPULSION DIAPHRAGMS

by
C. L. Lofgren and D. E. Gieseking

THE BOEING COMPANY
Aerospace Operations

Prepared for
NATIONAL AERONAUTICS AND SPACE ADMINISTRATION
October 1970
Contract NAS3-11204

NASA Lewis Research Center
Cleveland, Ohio
R. F. Lark, Project Manager
Liquid Rocket Technology Branch
Chemical Rocket Division

FOREWORD

This report was prepared by The Boeing Company, Aerospace Operations, under NASA Contract NAS3-11204. The work was administered by the Lewis Research Center, Liquid Rocket Technology Branch, Chemical Rocket Division, Cleveland, Ohio with Mr. Raymond F. Lark as Program Manager.

Contract NAS3-11204, "Cryogenic Positive Expulsion Diaphragm" was a 33-month program (October 1967 to June 1970) consisting of five separate but related tasks. This final report covers the work performed on that program.

Performance of this contract was under the direction of the Manufacturing Technology Section, Aerospace Operations of The Boeing Company. Mr. C. L. Lofgren was Program Manager and Mr. D. E. Gieseking Technical Leader.

TABLE OF CONTENTS

NASA CR 72732

CRYOGENIC POSITIVE EXPULSION DIAPHRAGMS

by

C. L. Lofgren and D. E. Gieseking

ABSTRACT

This report covers the design fabrication and test of twenty polymeric film expulsion diaphragms for liquid hydrogen. The diaphragms, of single ply vapor barrier construction, failed during the liquid hydrogen test cycling.

LIST OF ILLUSTRATIONS

LIST OF TABLES

1.0 SUMMARY

The object of this program was the design, fabrication and testing of polymeric diaphragms capable of expelling liquid hydrogen under zero gravity conditions. The goal of the program was the development of a diaphragm capable of 25 failure-free cycles of liquid hydrogen expulsion.

The work was performed in two distinct progressive phases; prototype and improved. Each phase involved specific tasks of design, fabrication, and test of experimental diaphragms. Task I provided for the design configuration of the diaphragm and the evaluation and selection of promising materials. The second subtask was the development of manufacturing and quality assurance plans. The third subtask was the redesign and modification of the test apparatus and instrumentation to fulfill the requirements of the program. Task II consisted of the fabrication of two prototype units of each of eight approved designs. Task III involved cycle testing the prototype diaphragms in liquid hydrogen.

None of the 16 diaphragms or additional alternates performed as expected. All units failed during the initial liquid hydrogen expulsion cycle due to developed leaks in the basic material or in the seam joints of gored diaphragms.

Task IV function was the analysis of test results of Task III and the selection of material for four additional diaphragms, and the fabrication of the four units. In addition, the test container and tooling was redesigned and modified to incorporate a different configuration which would give less severe flexure during liquid hydrogen testing. Task V was the test phase for the four diaphragms designed and fabricated in Task IV.

None of the diaphragms tested in Task V survived cycle testing in liquid hydrogen. The final diaphragm was used as a control unit. A bladder with identical construction was successfully tested in liquid nitrogen and liquid hydrogen on other programs. This diaphragm was one of those which failed in Task V in identical manner as other units.

Although the program goal of 25 failure-free cycles in liquid hydrogen was not approached with any of the diaphragms tested, some of the results gave an insight into previous multiply diaphragms and bladder failures.

A positive result of the program was the test cryostat which allowed direct, undistorted view and photographic recording of the diaphragm during the test operation. This unit, with minor modification, could easily be adapted for advanced studies.

2.0 INTRODUCTION

The development of a suitable light-weight, multi-cycling diaphragm or bladder had been the object of a number of previous NASA and Air Force programs. Cryogenic expulsion under zero gravity conditions first received concentrated attention at Boeing during the design phases of the X-20 program to replace high-pressure super-critical systems. Initial studies were devoted to one-shot and multi-cycling metallic diaphragms, bladders, and metallic bellows. The metallic units could not withstand repeated folding without pin-holing and tearing. Follow-on programs which designed and placed reinforcing rings on the diaphragms allowed control of the collapsing pattern and improved their performance. Even though metallic units are now capable of multiple cycles, they impose weight and volumetric efficiency penalties and geometric limitations.

Polymeric diaphragms and bladders (references 1 and 2) have been investigated for liquid nitrogen and liquid hydrogen service. These programs have shown that Mylar film and Kapton film are the best materials for polymeric expulsion devices for cryogens. Test data has been accumulated from the previous programs for material selection and most of the processing limitations have been defined and fabrication methods developed. The porosity of the polymeric films to the cryogens has posed a problem during initial filling and cycling. Although the diffusion rates of the liquid hydrogen through multiple plies of a polymeric bladder are small, minute quantities of liquid hydrogen became entrapped between plies. Thermal gradients can cause plys to balloon, resulting in filling and expulsion problems (references 1 and 3).

This program employed single ply diaphragms to demonstrate the capability of a single ply polymeric film to perform repetitive filling and expulsion cycling. Reinforcing felt plies and reinforcing hoops were used to increase reliability of the single ply concept.

3.0 TEST PROGRAM

The test program was divided into tasks and subtasks to perform a specific function related to the total effort. Each area of work will be determined in the following paragraphs.

3.1 PROGRAM DEVELOPMENT

The initial phase in Task I was the design of the diaphragms and the selection of materials. The designs were divided into four categories:

a. The diaphragms were fabricated of a single ply of polymeric film, thermal vacuum formed to contour, reinforced with felt.

b. The diaphragms were fabricated of a single ply of polymeric film, assembled from flat gores and joined to the required contour, reinforced with felts.

c. Category A or B diaphragms with reinforcing hoops to control flexing of the diaphragms.

d. Diaphragms of metallic-polymeric laminates, assembled from flat gores and joined to the required contour, reinforced with felts.

The materials selected for diaphragm fabrication are shown in Table 1 "Material Selection." Basis for selection was the previous investigations by The Boeing Company and NASA contracts (references 1, 2, and 3) in which promising materials were identified.

3.2 DIAPHRAGM CONFIGURATION

The diaphragms for Task II consisted of a single polymeric film vapor barrier laminated between two dacron felt abrasion plies. Mylar and Kapton films of various thicknesses and polymeric film-metal laminates shown in Table 2 were the barrier ply materials. A typical diaphragm is illustrated in Figure 1.

Each diaphragm was nominally 15 inches in diameter with a 5.875 inch radius. A two inch truncated conical section joined the clamping flange radius to that of the hemispherical dome.

Each major component of the diaphragm is defined as follows:

Barrier Ply---The layer of polymeric film used to separate the liquid hydrogen from the helium pressurizing gas. This is the structural film of the diaphragm. The Barrier Ply was constructed of gores of polymeric material individually adhesively bonded together or by thermal-vacuum forming of the polymeric film.

Table 1: MATERIAL SELECTION

Material	Thickness (Mils)	Description	Source
Mylar Film Type A	1.0, 1.5, 2, 3, & 4.0	Poly (ethylene terephthalate) film	E. I. DuPont
Mylar Film Type C	1.0	Poly (ethylene terephthalate) film	E. I. DuPont
Kapton Film Type H	1.0 & 2.0	Polyimide Film	E. I. DuPont
G. T. -100 Adhesive	0.50	Polyester Adhesive	G. T. Schjeldahl
G. T. -300 Adhesive	1.0	0.5 Mil Polyester Adhesive 0.5 Mil Mylar Film	G. T. Schjeldahl
Dacron Felt		S4-23096 15P32 Felt - 32 oz.	Troy Mills
Zeroperm Laminate	0.50 Mylar 0.50 Aluminum Foil 0.50 Mylar	0.50 Mylar 0.50 Aluminum Foil 0.50 Mylar	Foilwrap, Inc.
Liquid Polyester Adhesive 46971		with RC-805 curing agent	E. I. DuPont

Table 2: DIAPHRAGM CONFIGURATIONS

Diaphragm	Material	Material Thickness (Mil)	Formed or Gores	Convolute Rings
1A	Mylar C	1.0	Gores	None
1B	Mylar A	1.5	Gores	None
2A	Mylar A	1.0	Formed	None
2B	Mylar A	2.0	Formed	None
3A	Kapton	1.0	Gores	None
3B	Kapton	2.0	Gores	None
4A	Mylar A	1.0	Formed	None
4AX	Mylar A	1.0	Formed	None
4B	Mylar A	2.0	Formed	None
4BX	Mylar A	2.0	Formed	None
5A	Kapton	2.0	Formed	None
5B	Kapton	3.0	Formed	None
6A	Mylar-Aluminum-Mylar Laminate	0.5-0.5-0.5	Gores	Bonded to felts
6B	Mylar-Lead-Mylar Laminate	0.5-1.0-0.5	Gores	Bonded to felts
7A	Mylar C	1.0	Gores	
7B	Mylar C	2.0	Gores	
8A	Mylar A	3.0	Formed	Bonded to Film
8AX	Mylar A	3.0	Formed	None
8B	Mylar A	4.0	Formed	Bonded to felts but removed

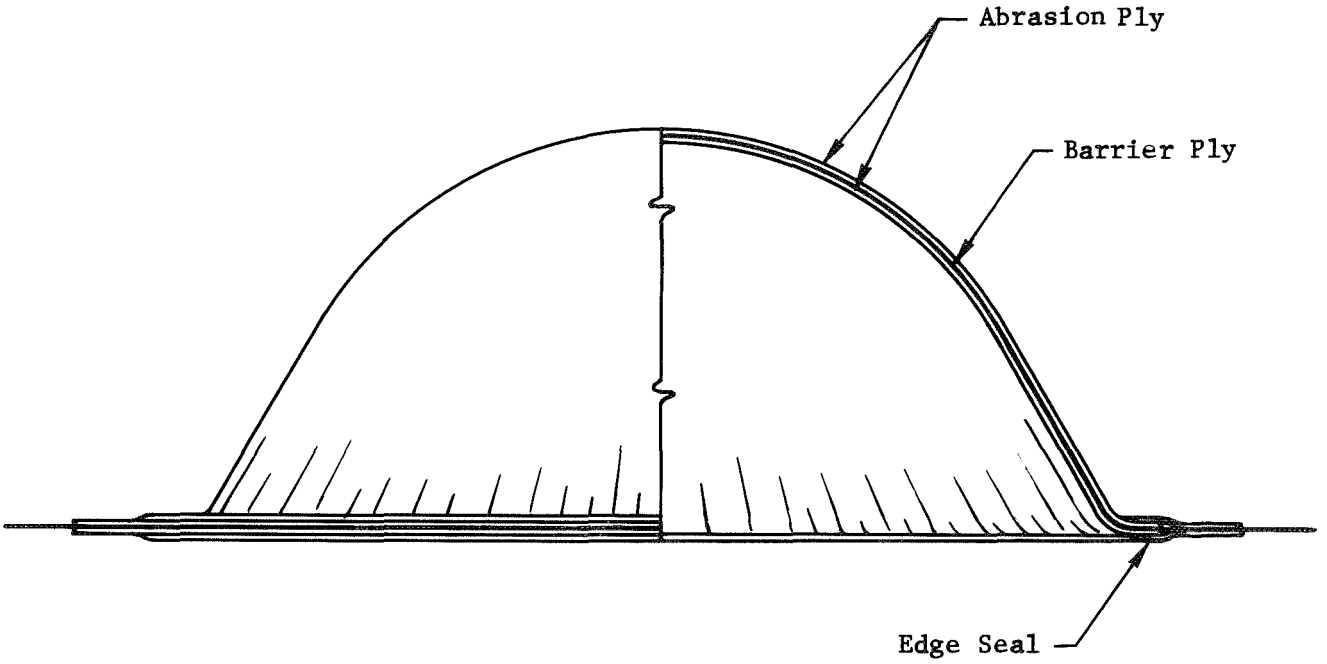

Figure 1 : TYPICAL EXPULSION DIAPHRAGM

Abrasion Ply---The abrasion plies are a layer of dacron felt bonded to the interior and exterior of the diaphragm to protect the barrier ply and reduce the three corner folding of the polymeric barrier ply.

Flange Seal---The flange seal is fabricated of washers of Mylar or Kapton bonded to the periphery of the abrasion ply extending over the abrasion plies to prevent gas leakage from the pressurization side to the cryogen side.

3.3 FABRICATION PLANS

The second phase of Task I was the development of fabrication plans and quality assurance plans for the program. The fabrication techniques are basically identical in all diaphragms as follows:

Materials---The materials used for diaphragm fabrication are shown in Table 2. All materials were standard commercial grades and inspected for quality by The Boeing Company prior to use.

Abrasion Plies---The abrasion plies of the diaphragms were fabricated by thermal-vacuum forming the dacron felted material in a fiberglass tool shown in Figure 2. The parent material was clamped in the forming fixture and a vacuum was slowly drawn (approximately 3-5 psi per minute while heat was applied with a hot air gun (300-350°F fabric temperature) shown in Figure 3. When the material contacted the mold surface, the heat was removed and the formed fabric was allowed to cool in the tool. The formed hemispherical shape was removed from the tool, trimmed, and protective packaged until assembly with the barrier film.

Barrier Plies---The barrier plies listed in Table 2 were fabricated by two means, thermal-vacuum forming of the modified hemispherical shape or by adhesive joining flat pattern gores.

The flat pattern gores were cut from the visually inspected parent material into the segments shown in Figure 4. These flat pattern segments were joined on the plaster mandrels shown in Figures 5 and 6. The hemispherical mandrel had six flat sections as shown, one for each gore. The flat section enabled the assembler to apply the tape adhesive without wrinkling either the barrier film or the adhesive which minimized adhesive ridges, stress concentrations, and possible leak paths. The gores were sealed using GT-100 or GT-300 adhesive on both sides of the butt joint. The laminate diaphragms had a spider cut from the parent material and GT-100 was used on these particular diaphragms. The sealing iron was set at 310 ± 10°F. Vapor barrier plies are shown in Figure 7 with a completed unit.

The formed hemispherical barrier plies were formed in the facility shown in Figures 8, 9, and 10. The facility is a thermal-vacuum unit composed of a gold plated cabinet, heat source and control unit, and the vacuum forming mandrel assembly. The process developed to form

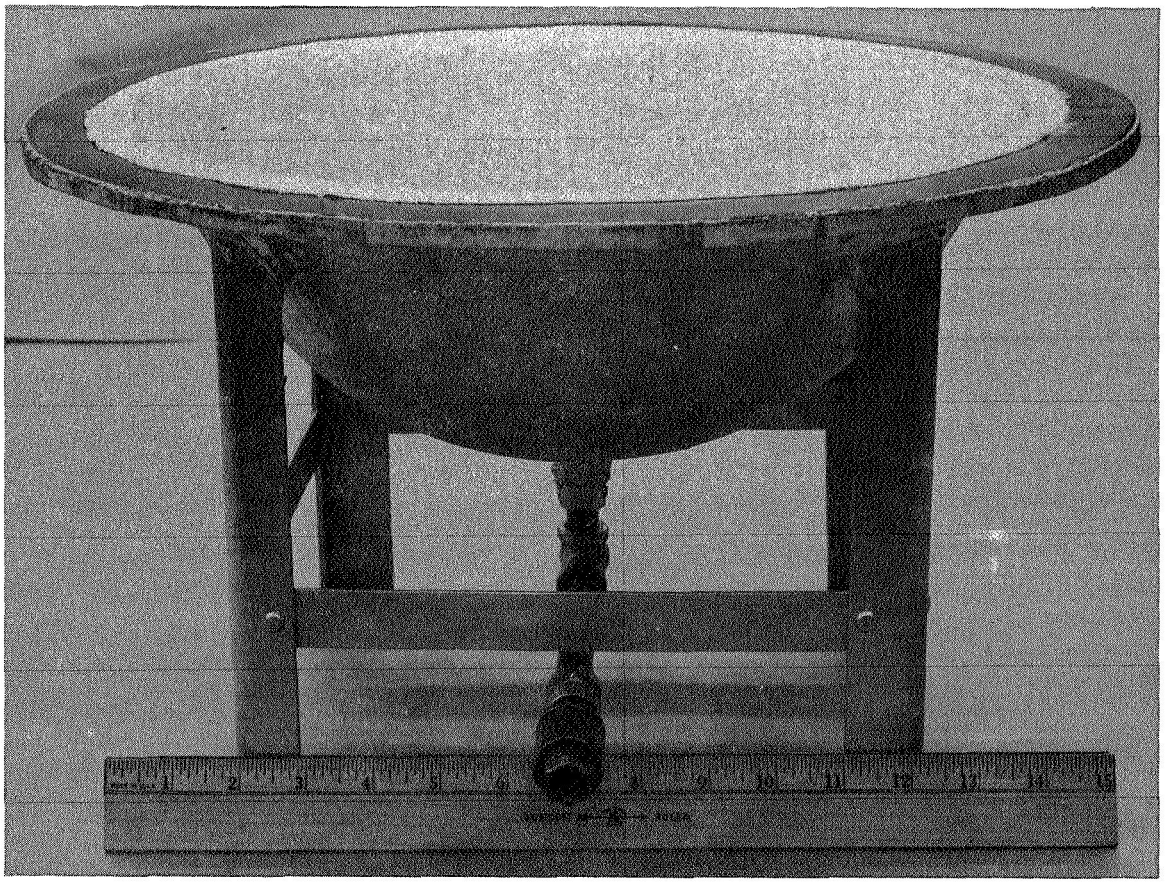

Figure 2: FELT FORMING TOOL

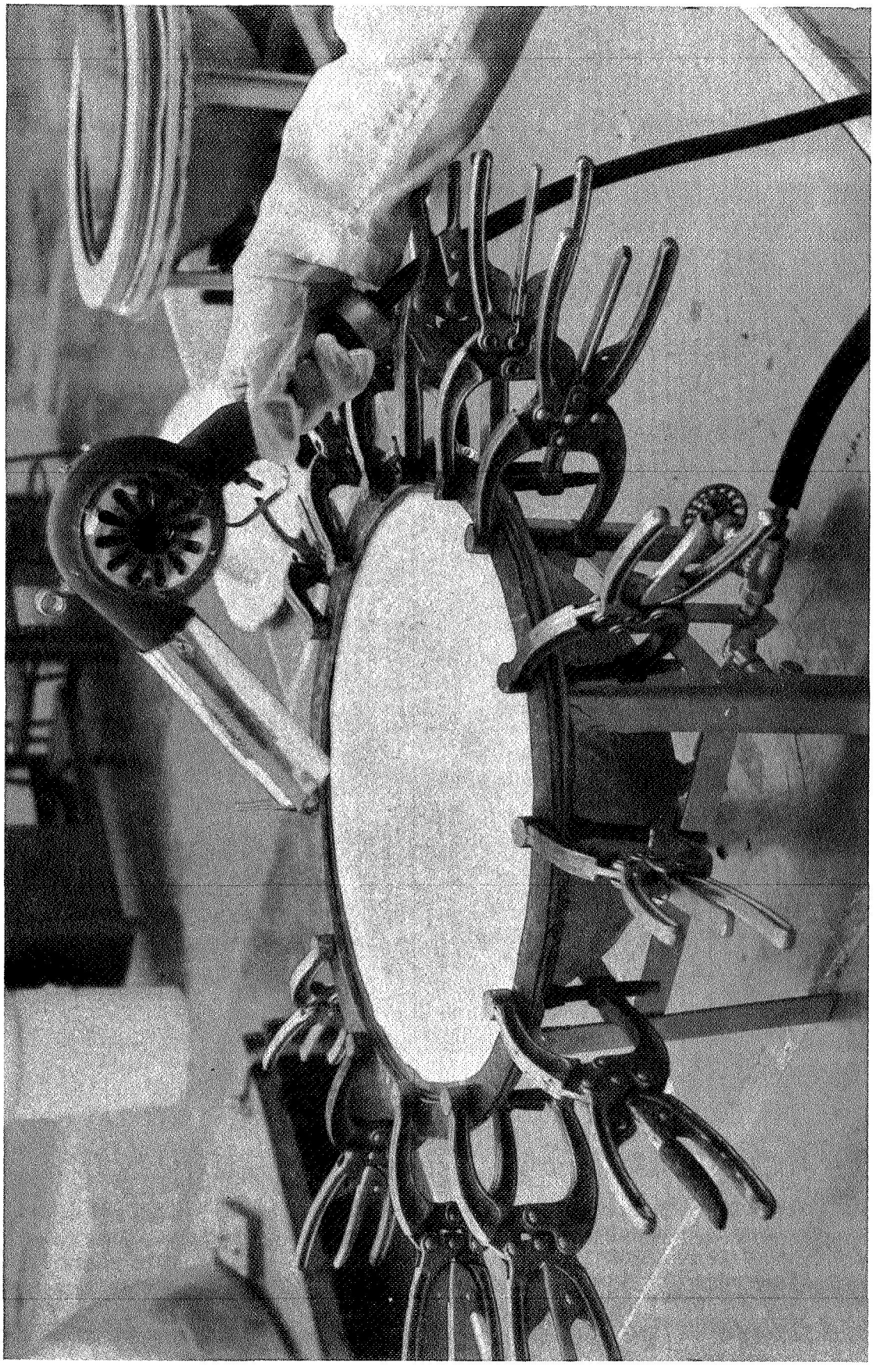

Figure 3: FELT FORMING OPERATION

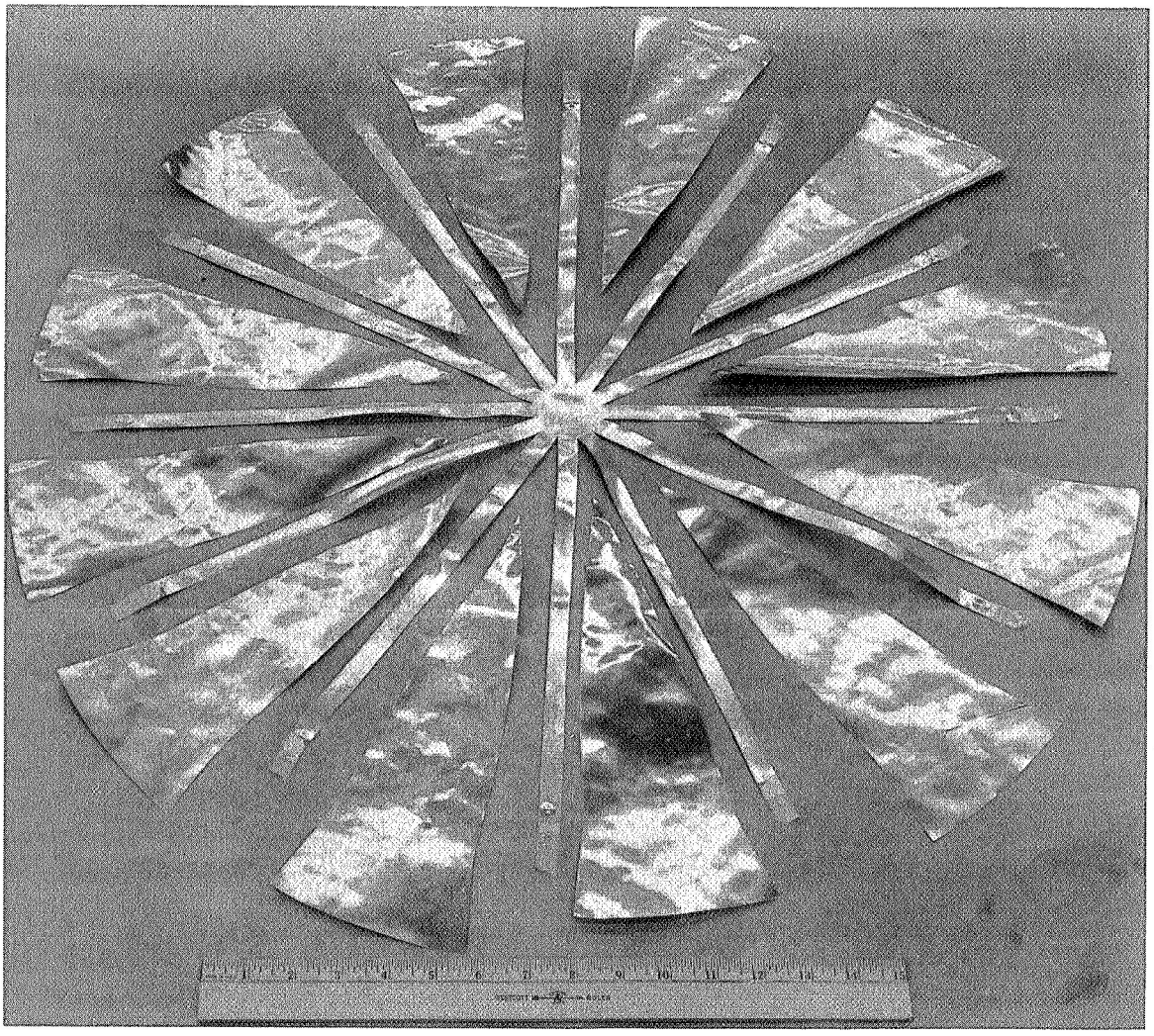

Figure 4: VAPOR BARRIER COMPONENTS

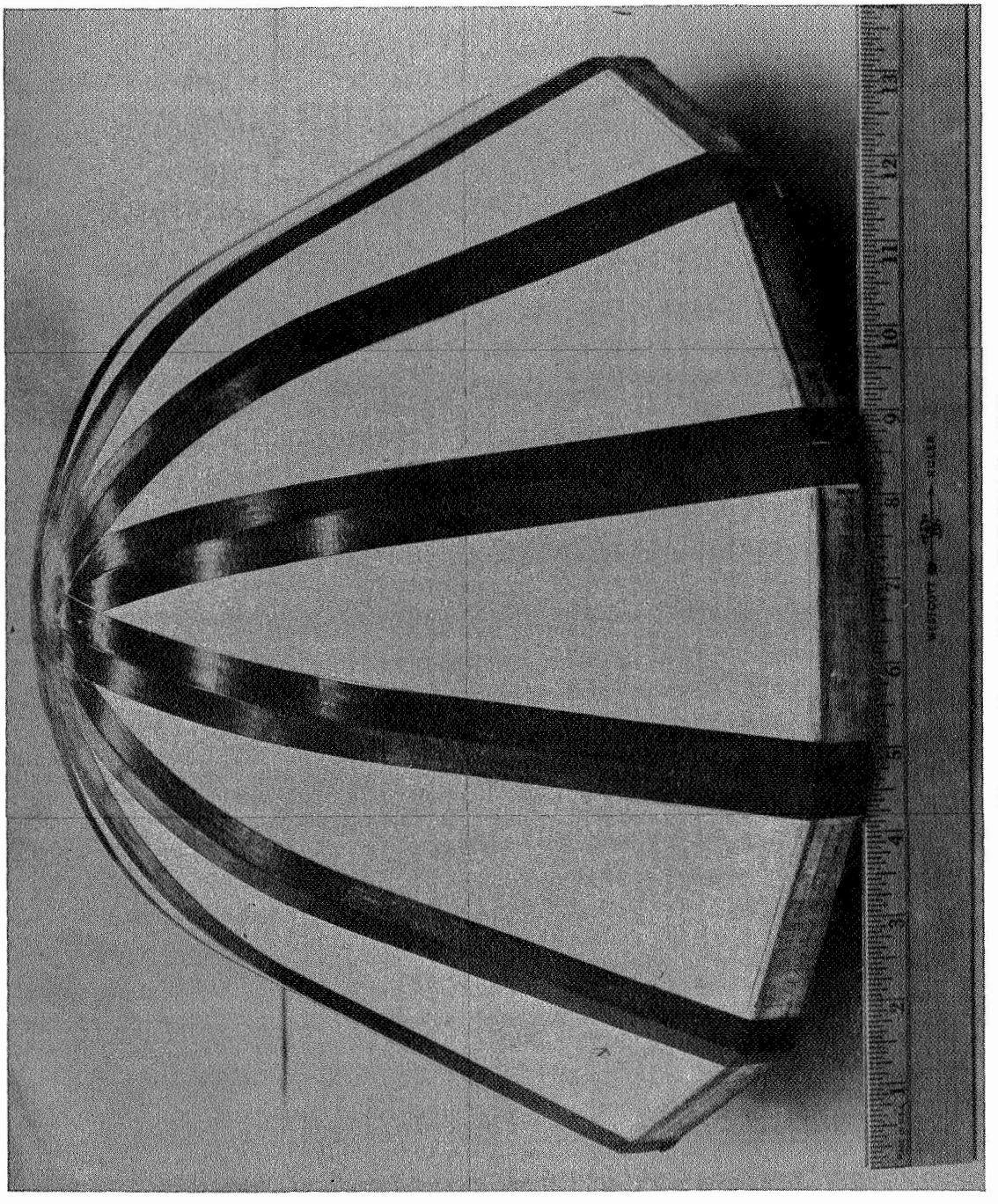

Figure 5: GORE ASSEMBLY TOOL

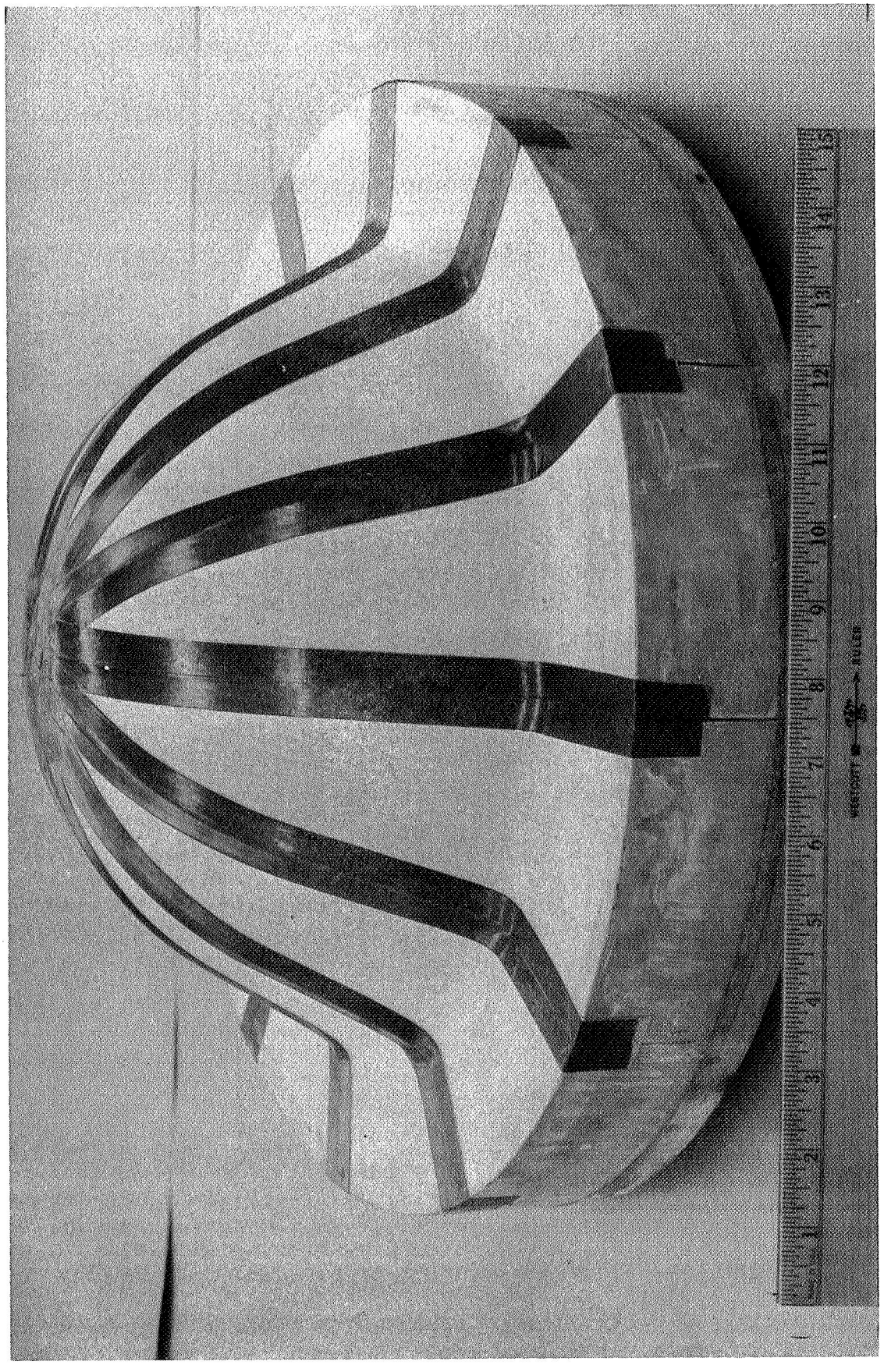

Figure 6: RADIUS JOINING FIXTURE

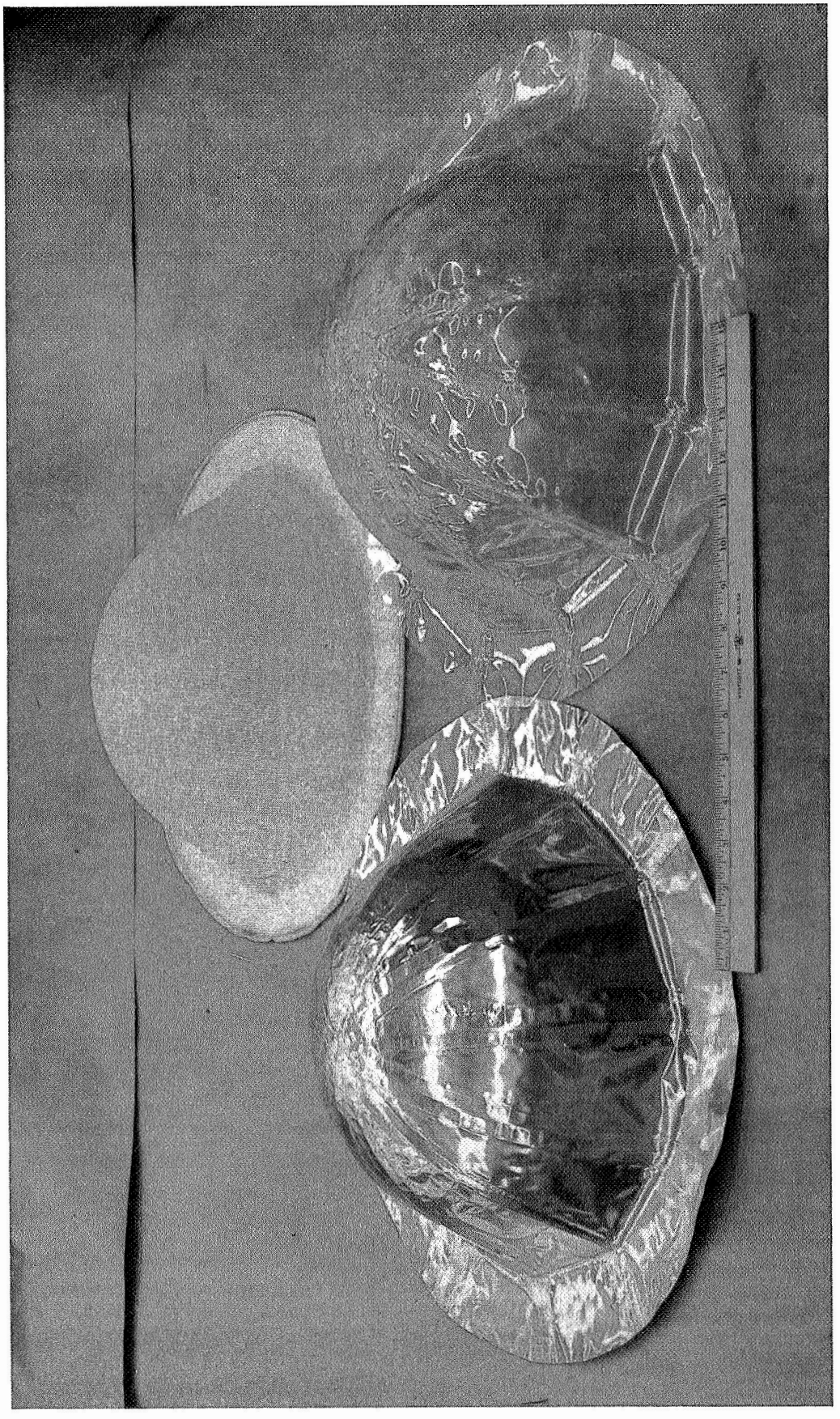

Figure 7: BARRIER PLIES

the modified hemispherical vapor barriers was to clamp the parent barrier material in the forming tool. Slight positive pressure was applied to the polymeric film as the film was heated to near its softening point by the radiant heating unit. The heat was removed after the "buble" was formed and the film was allowed to cool. A vacuum was drawn on the polymeric film bubble which pulled it down on the male aluminum mandrel to the exact contour of the diaphragms. Wrinkles were worked out by hand and heat was re-applied to complete the contour forming. The heat was then removed and the film allowed to cool on the mandrel before removal. The forming process described decreases the thickness gradient which results from vacuum forming alone.

Barrier Ply and Final Leak Checks---Each barrier ply was leak checked with a helium mass spectrometer leak detector. To perform this check, the vapor barrier was sealed and clamped to a base plate. Helium gas was injected into the cavity to 1/2 psi differential pressure and the entire diaphragm surface checked with a helium leak detector.

A standard helium mass spectrometer leak detector C.E.C. model 24-120A was used to perform the check. A zero division rise on the X-1 scale was used for acceptance after the leak detector had been calibrated to less than 2×10^{-10} std. cc/sec/division. Although the sniffer allows dilution of the sensing gas to approximately 1×10^{-8} std. cc/sec., the sensitivity was adequate for thin film leak detection.

The barrier ply was accepted if no leaks were detected in the unit. If a leak was detected in a seamed (gored) diaphragm, an attempt was made to reseal the GT-100 or GT-300. No patches were applied. If a leak existed in the parent material of the seamed vapor barrier or in a formed vapor barrier, the unit was scrapped and replaced.

The final leak check was conducted on the diaphragm after the abrasion plies and edge seals were applied. An identical leak check to that described above was used on the completed unit. Zero leakage was the criteria for acceptance.

Flange Seal---The flange seals for the diaphragms were fabricated of two identical discs of Mylar bonded to the vapor barrier film with 46971 adhesive as shown in Figure 11, did not make provisions for sealing the Mylar discs to the vapor barrier ply thus allowing the helium gas and liquid hydrogen to pass through the lower felt, around the vapor barrier through the top felt. Sealing the vapor barrier to the Mylar discs eliminated the flange leakage. Bonding is shown in Figure 12.

Convolute Rings---Convolute rings, used to control diaphragm flexing action and to prevent or reduce three corner folding of the vapor barrier, were fabricated by cutting spring steel wire to the required length and placing it in the holding fixture shown in Figure 13. The ends of the wire lengths were welded to form hoops of the four sizes. The rings were sprayed with a release agent, wound spirally with

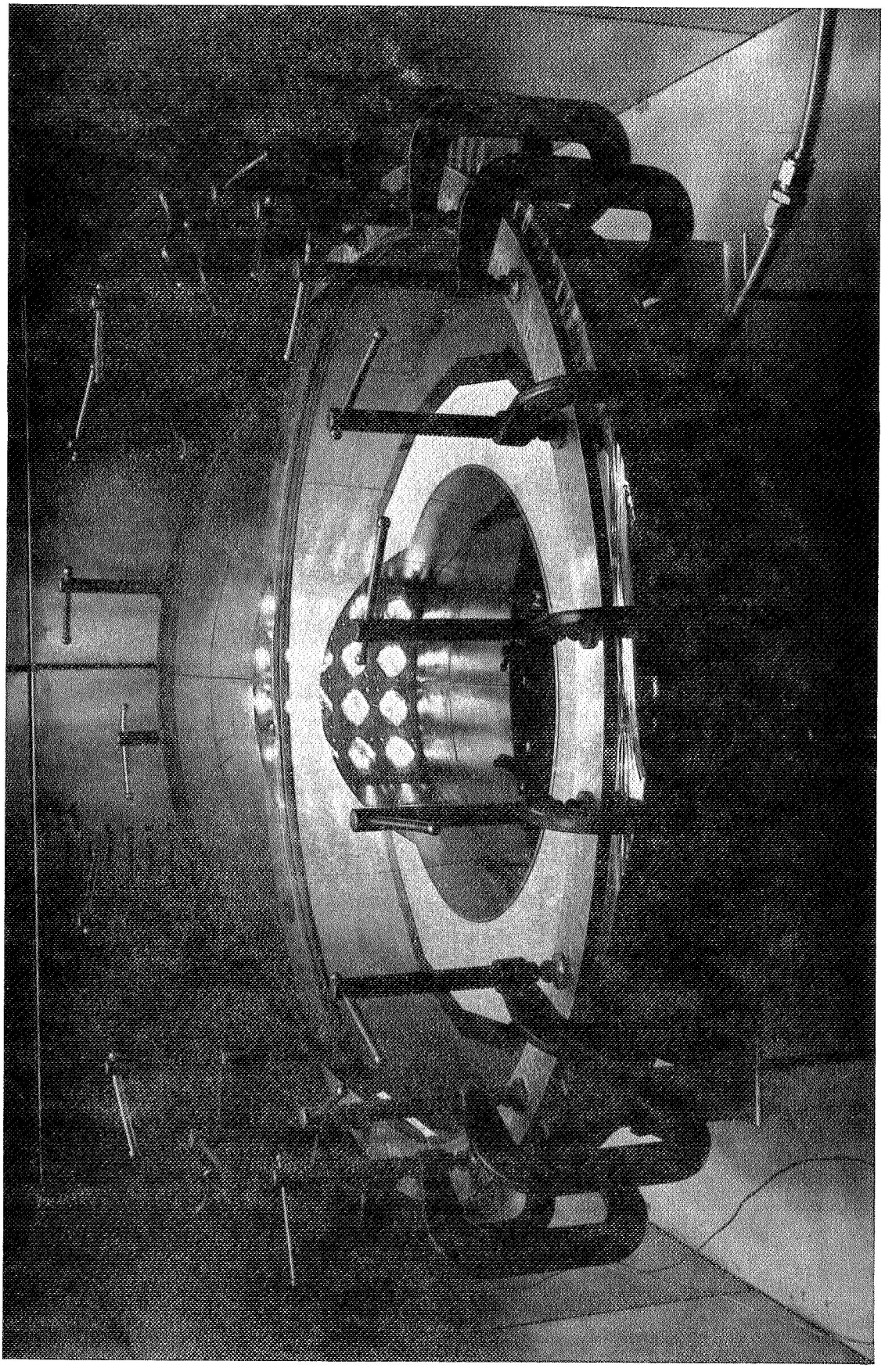

Figure 8: VAPOR BARRIER FORMING

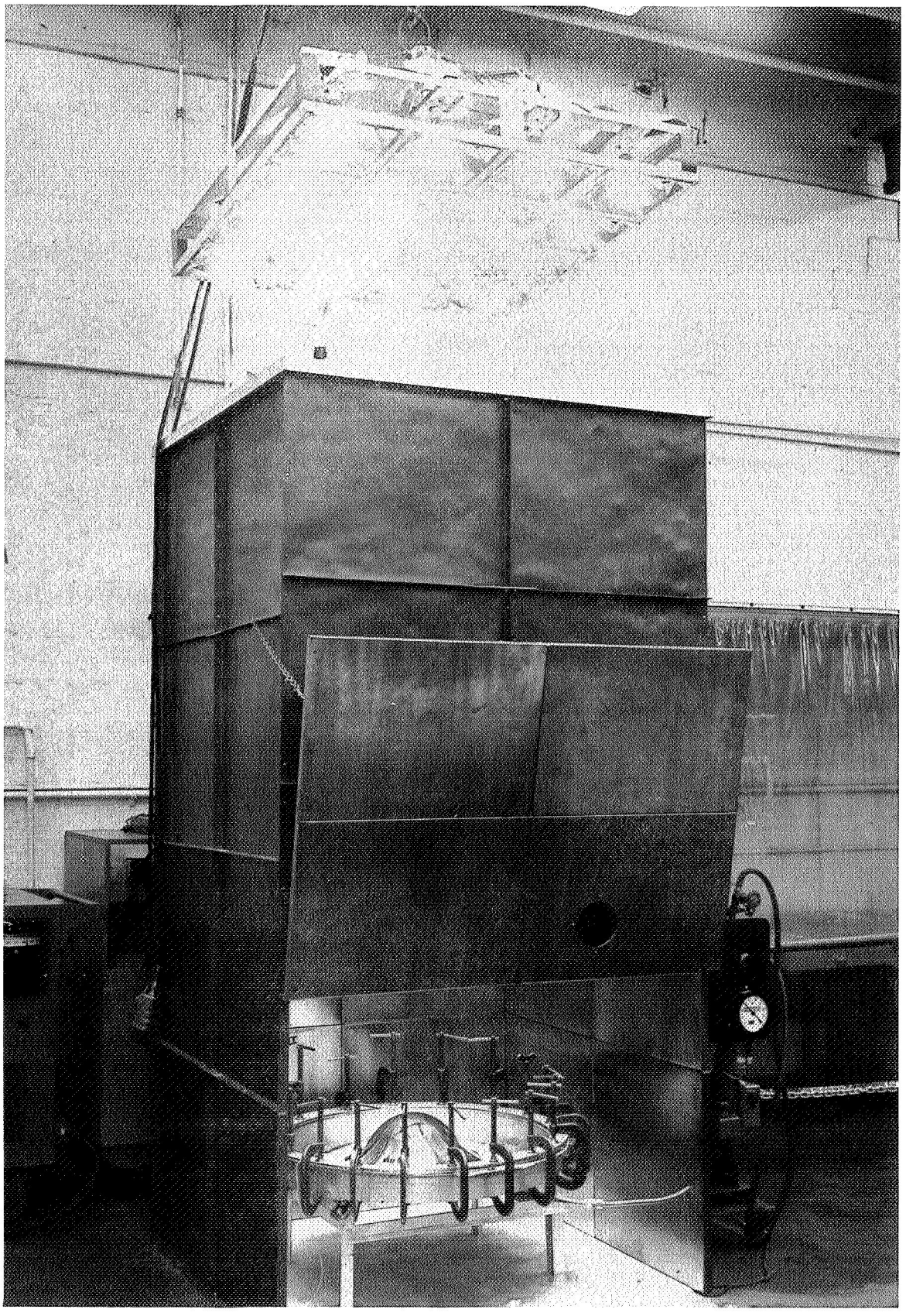

Figure 9: FILM FORMING FACILITY

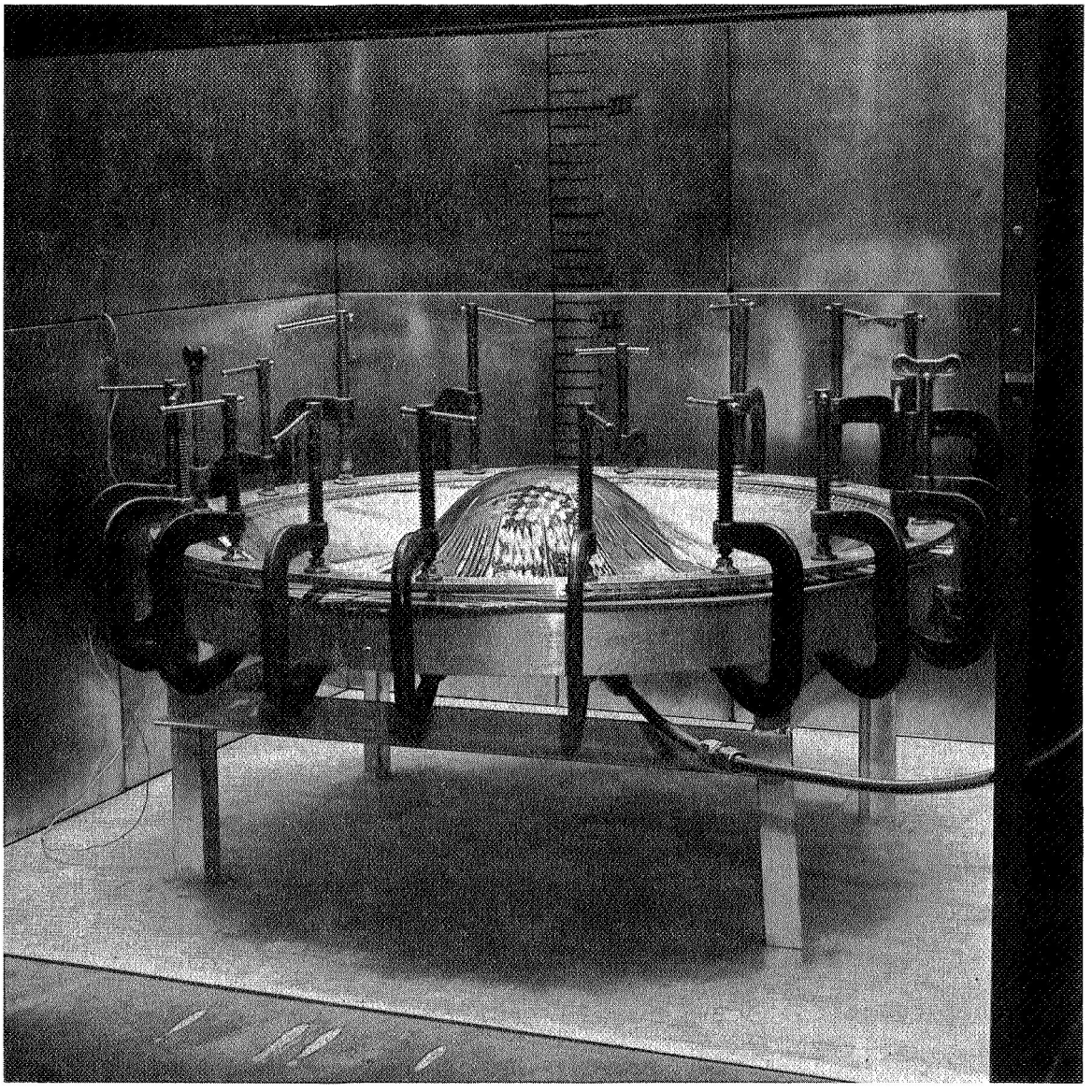

Figure 10: FILM FORMING CYCLE

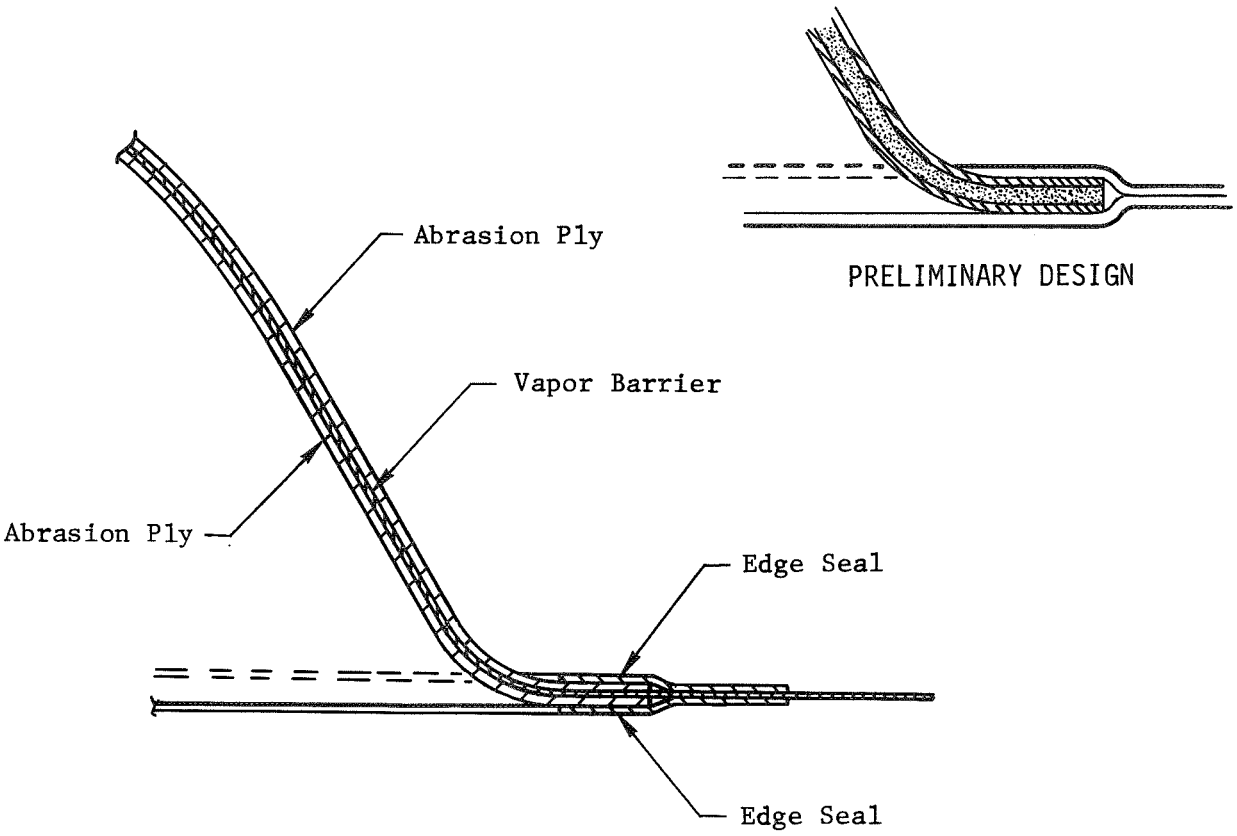

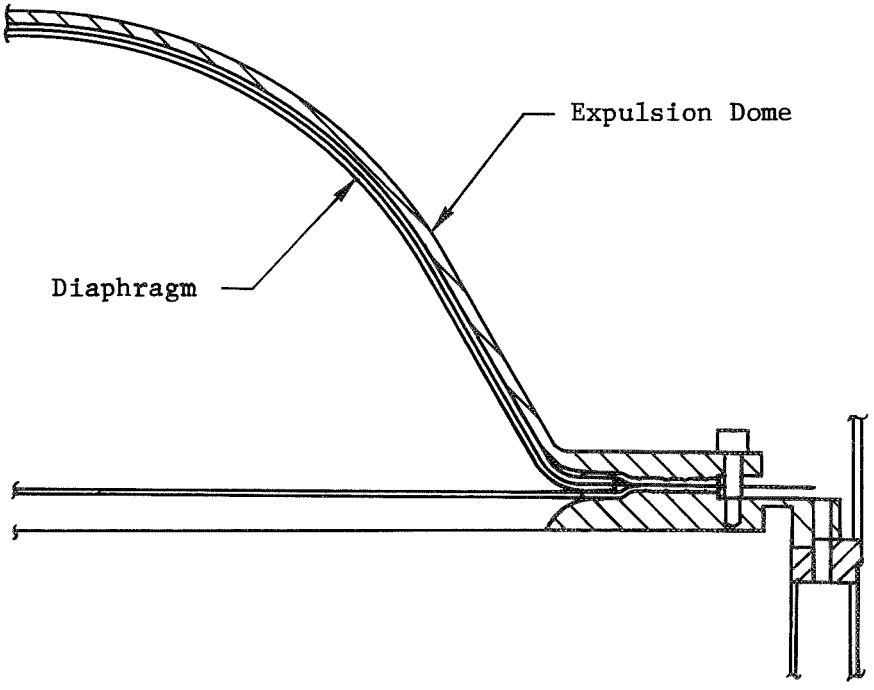

Figure 11: FLANGE SEAL

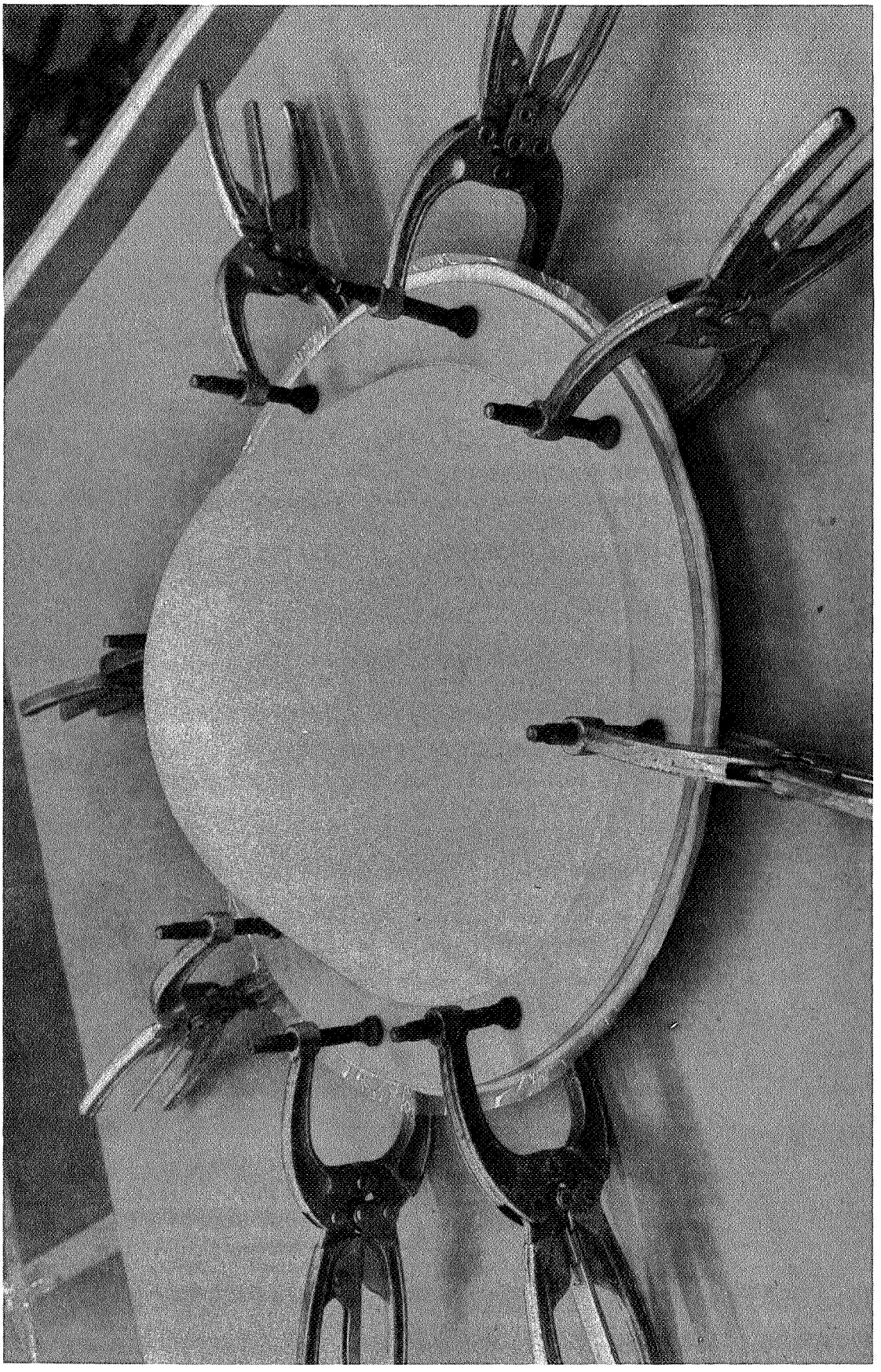

Figure 12: FLANGE SEAL BONDING

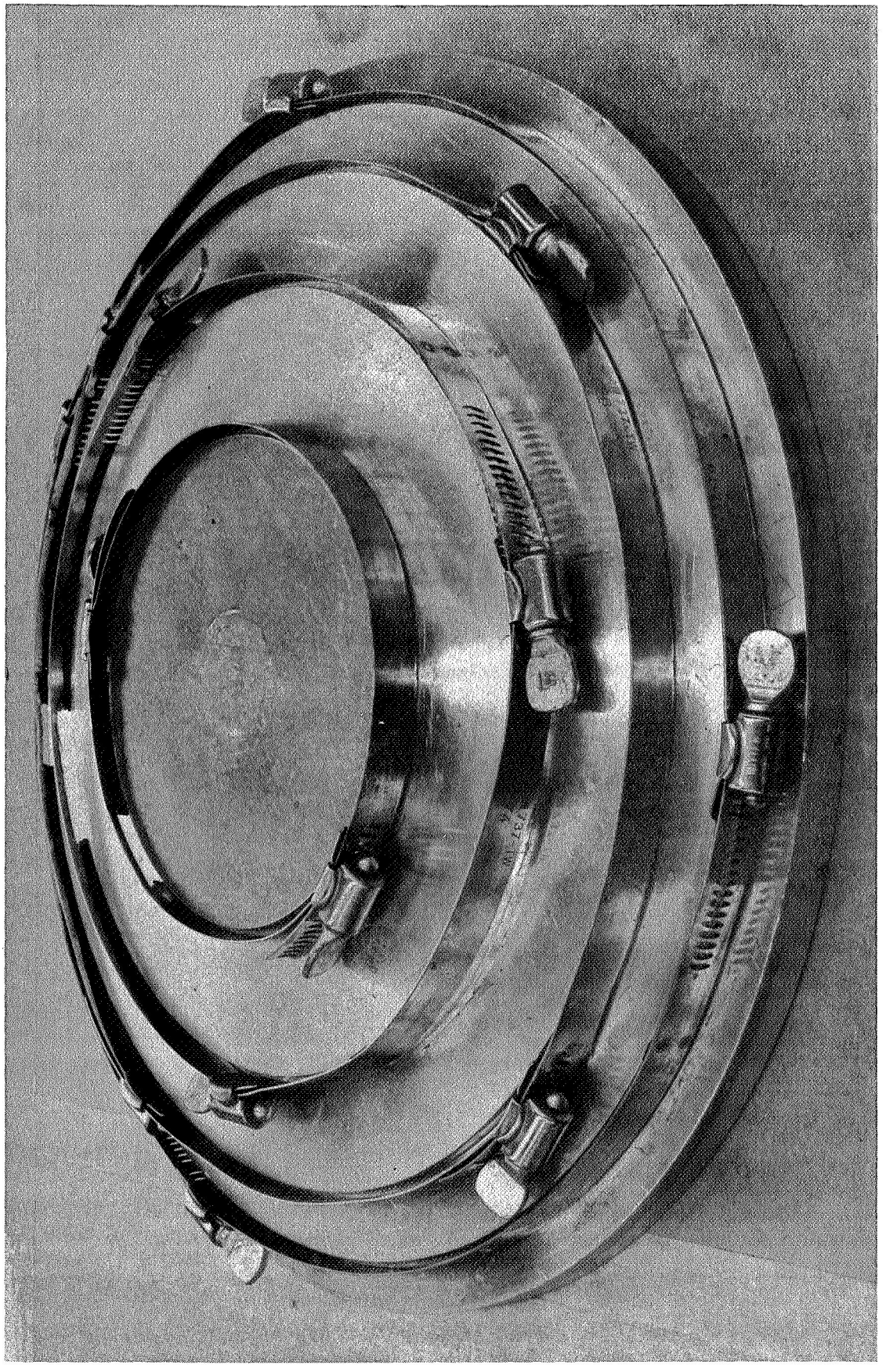

Figure 13: RING WELD FIXTURE

GT-300 and heated to 310°F to cure the adhesive. The resultant ring was capable of turning within the cover. Without this ability, the ring would resist turning while attached to the diaphragm which would result in material rupture.

The rings were bonded to the vapor barrier or the dacron felt, as the case may be, by placing the rings on the grooved male hemispherical bonding tool shown in Figure 14.

The diaphragms were assembled by sequentially placing on the aluminum mandrel (shown in Figures 15 and 16) a dacron felt which received a thin spray coat of polyester resin, a vapor barrier ply which received a thin spray of polyester resin, and a dacron felt ply. This composite was clamped at the edge and cured at about 300°F. The edge seal was applied by secondary bonding the edge seal disc to the vapor barrier. A completed diaphragm is shown in Figures 17 and 18.

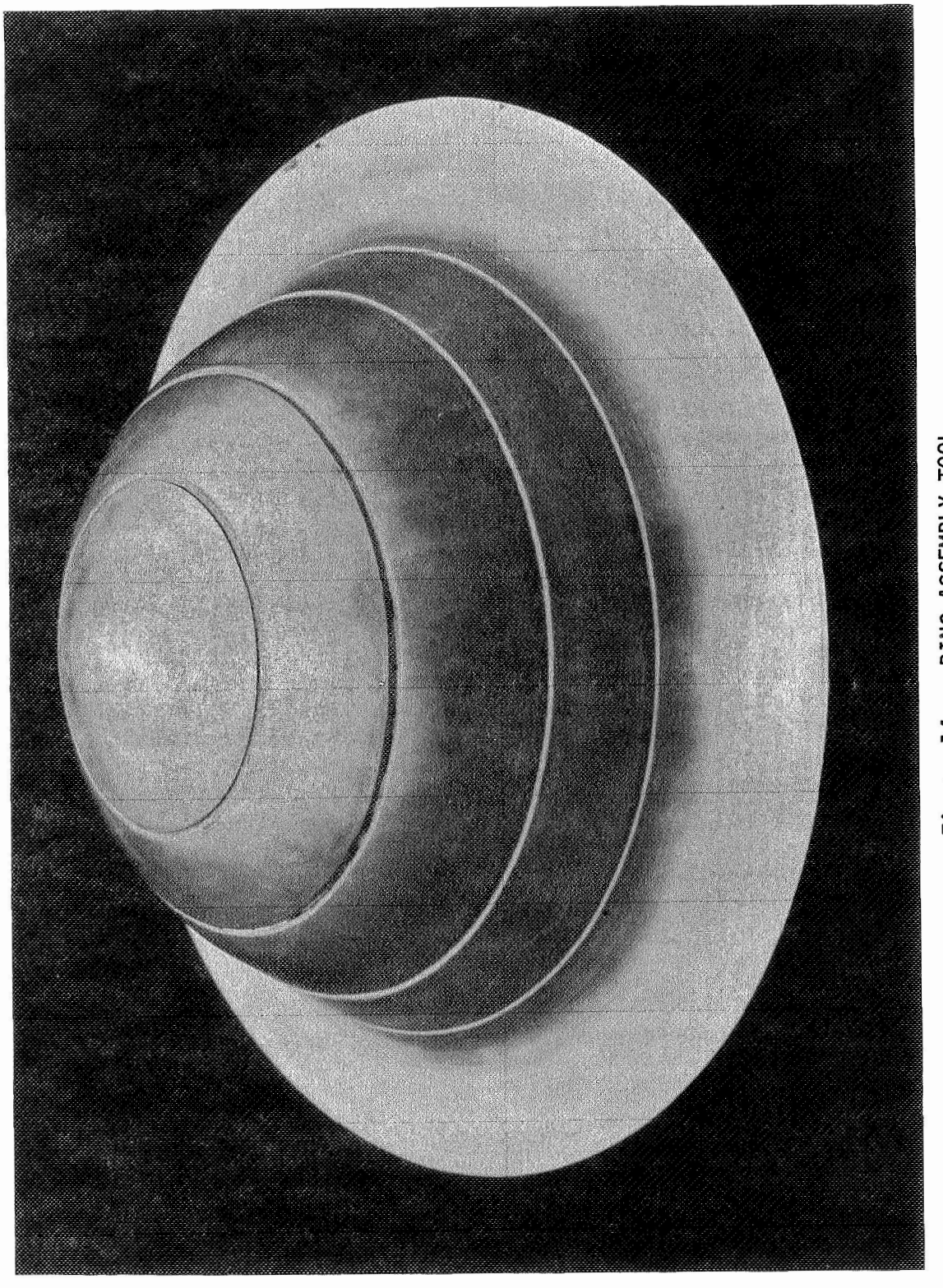

Figure 14: RING ASSEMBLY TOOL

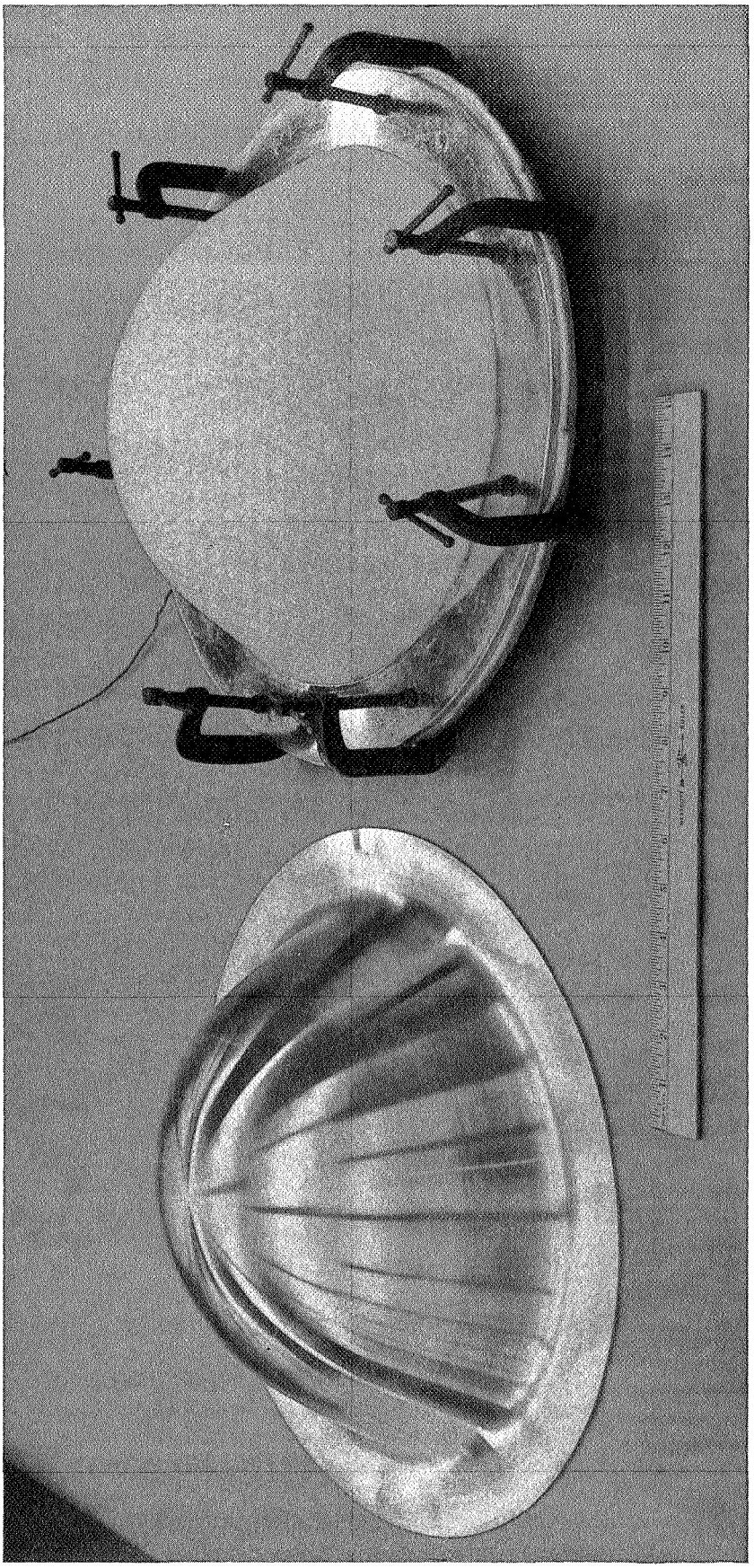

Figure 15: DIAPHRAGM ASSEMBLY

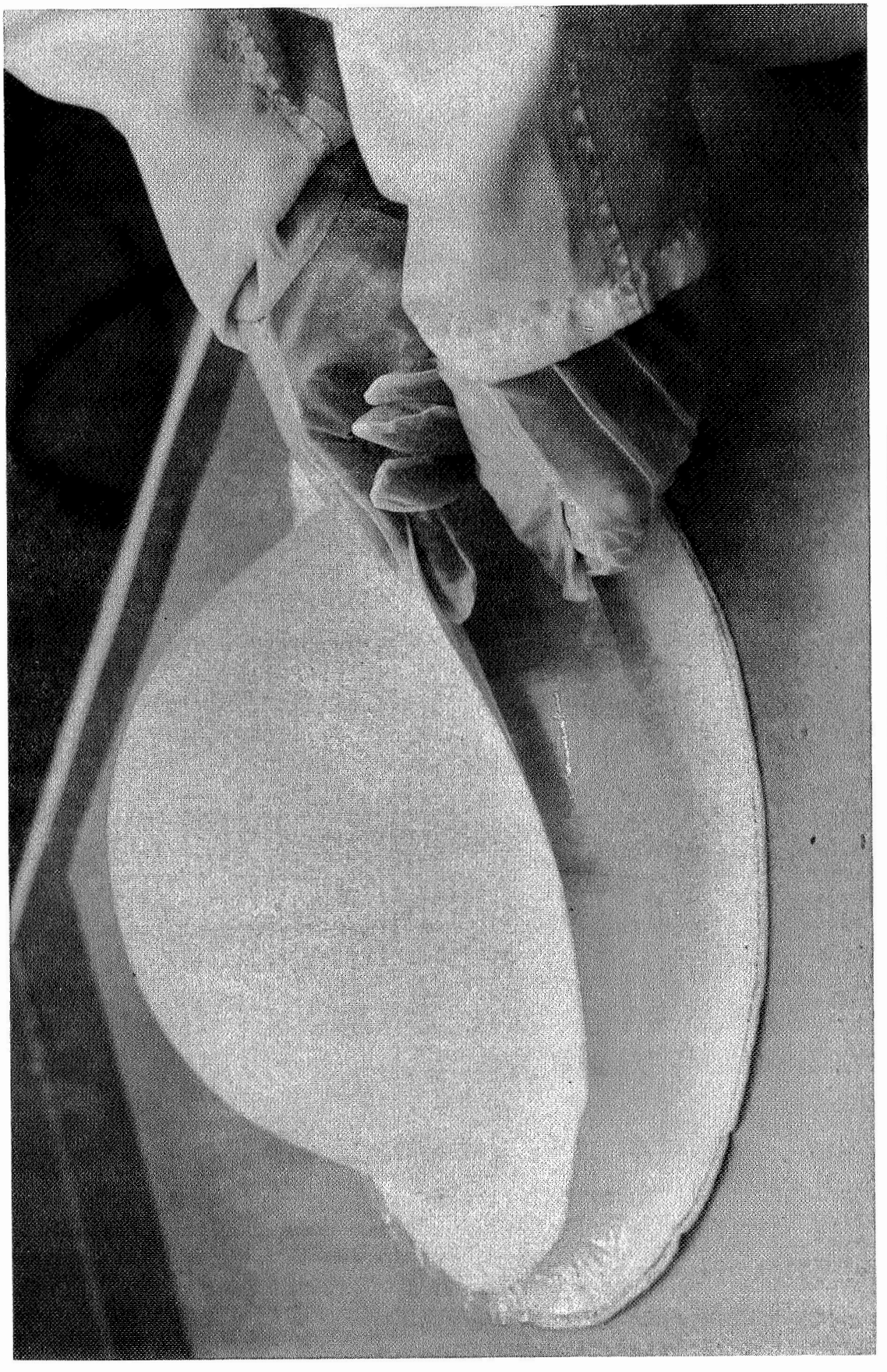

Figure 16: DIAPHRAGM ASSEMBLY SEQUENCE

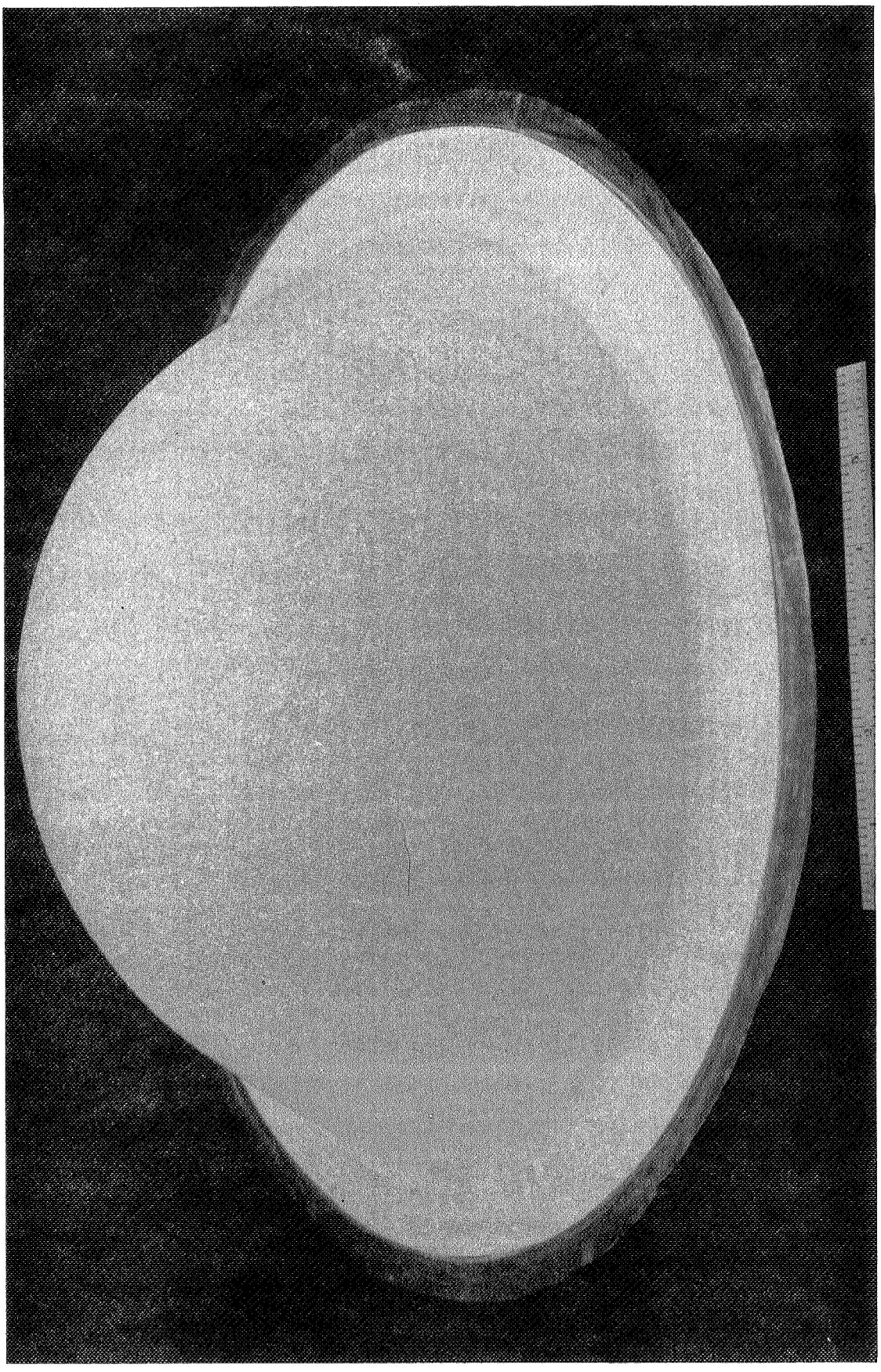

Figure 17: TYPICAL DIAPHRAGM

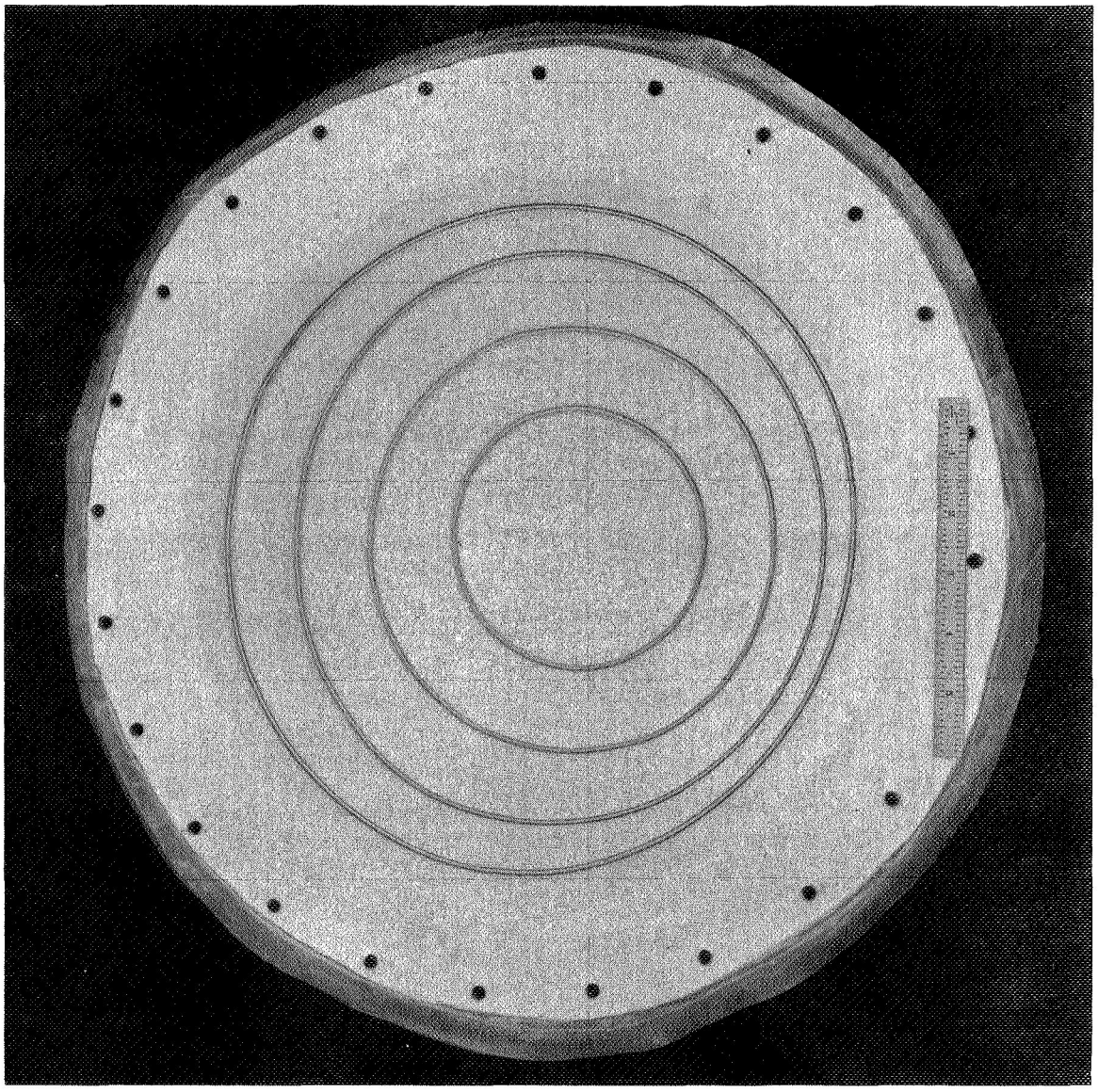

Figure 18: DIAPHRAGM WITH RINGS - RINGS ARE CONCENTRIC

4.0 TEST EQUIPMENT AND TESTING

A schematic drawing of the test facility is shown in Figure 19. The unit was fabricated for upward expulsion of the liquid hydrogen by helium gas which had been conditioned in the upper cryostat.

The test console, visual TV monitor, recorders, and test units are shown in Figures 20 to 23.

4.1 TEST CRYOSTAT

A requirement for the test container was that provision must be made for TV and film coverage of all tests. The original proposed test container and lower cryostat were to have been fabricated of pyrex glass as shown in Figures 24 and 25. This combination would have allowed immersing the cyclic test unit containing the diaphragm in the liquid hydrogen of the vacuum insulated double-walled glass lower dewar. The task of fabricating the units was subcontracted to the vendor who conducted the fabrication on a best effort basis because of the risk involved in fabricating the double walled lower cryostat. The diaphragm containers joined at the flange by a compression ring were fabricated without difficulty. The double-walled cryostat was fabricated successfully after considerable delay. Upon receipt in Seattle at the Tulalip Test Site, a stress crack in the joint of the inner to outer container was discovered during inspection. The vessel was returned to the vendor, who, after attempting repair of the crack recommended the glass concept be dropped and another approach taken to fabricate the lower cryostat.

A series of units were fabricated and tested without success in sequential order as follows:

Plexiglass - Plexiglass Unit---This unit was fabricated of cylinderical sections of plexiglass "Plex II." Each cylinder had a thick flat plexiglass bottom. A stainless steel mating flange with dovetail grooves for plexiglass potting was used. After leak check and LH_2 chill and helium leak check, the unit was tested at the Tulalip Test Site with LH_2 after an initial cooldown with gas from the liquid source. Both bottoms of the inner and outer cylinders were broken off instantaneously when liquid hydrogen contacted the inner container. This unit is shown in Figure 26 after LH_2 cold shock.

A second unit, shown in Figure 27, was fabricated of an inner pyrex glass container, 18-inch diameter, and the same plexiglass outer cylinder potted into a stainless steel base plate dovetailed to receive the unit. Having leak checked and cold shocked the unit with LN_2, the unit was partially filled with LH_2. After approximately one hour the inner pyrex vessel, shown in Figure 28, disintegrated again from differential thermal expansion of the components.

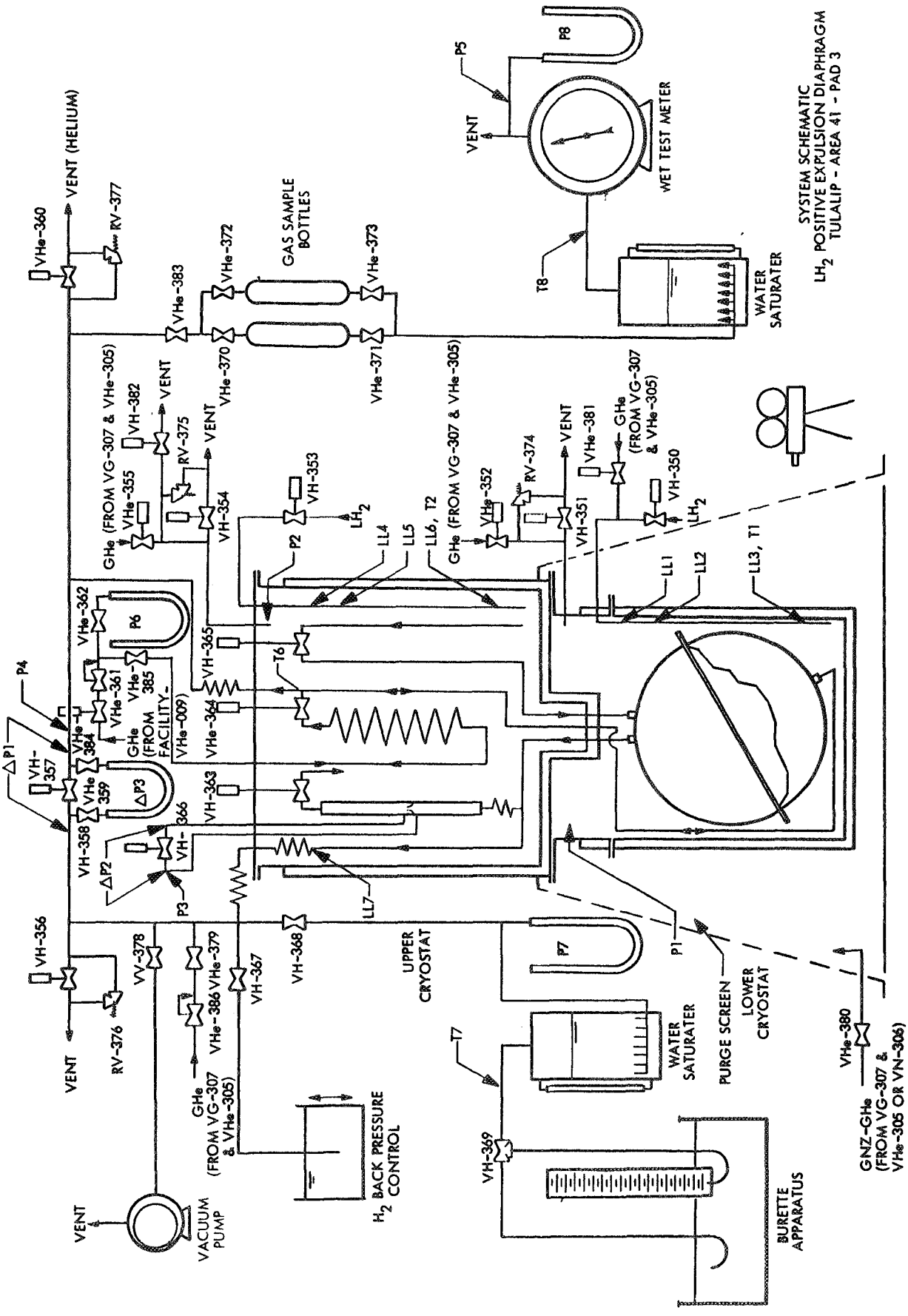

Figure 19: TEST FACILITY SCHEMATIC

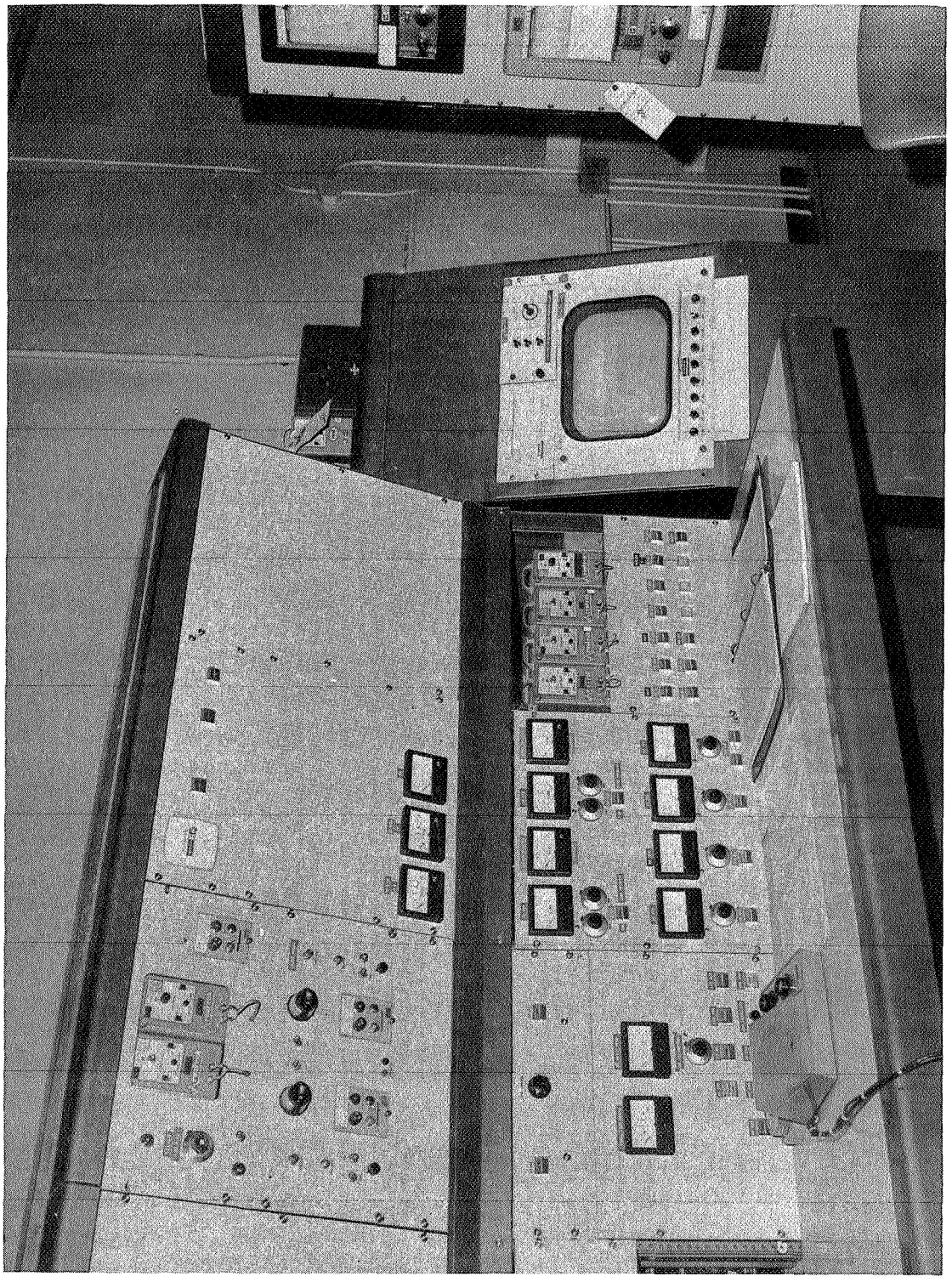

Figure 20: TEST CONSOLE

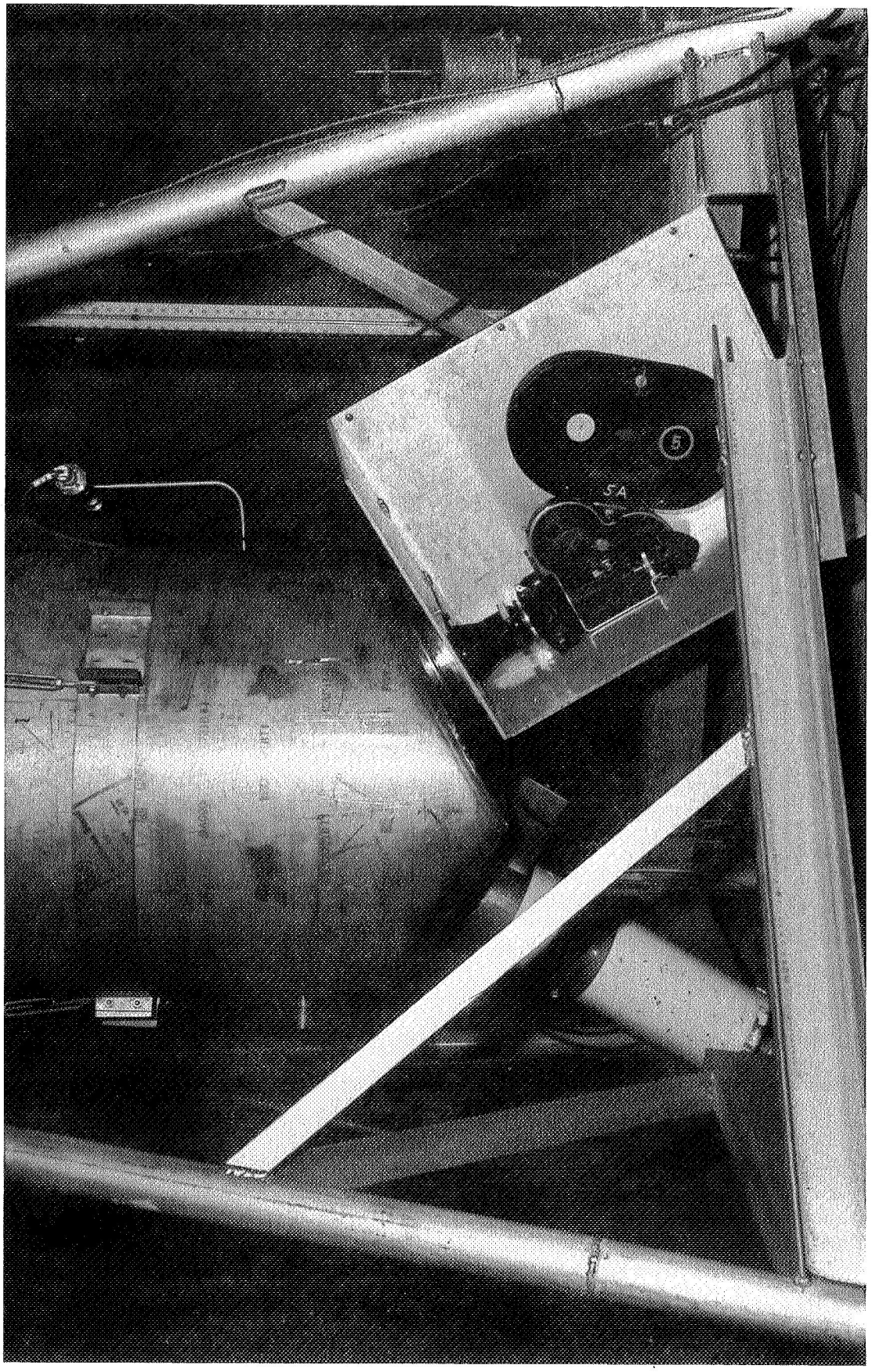

Figure 21: CAMERA AND TV LOCATION

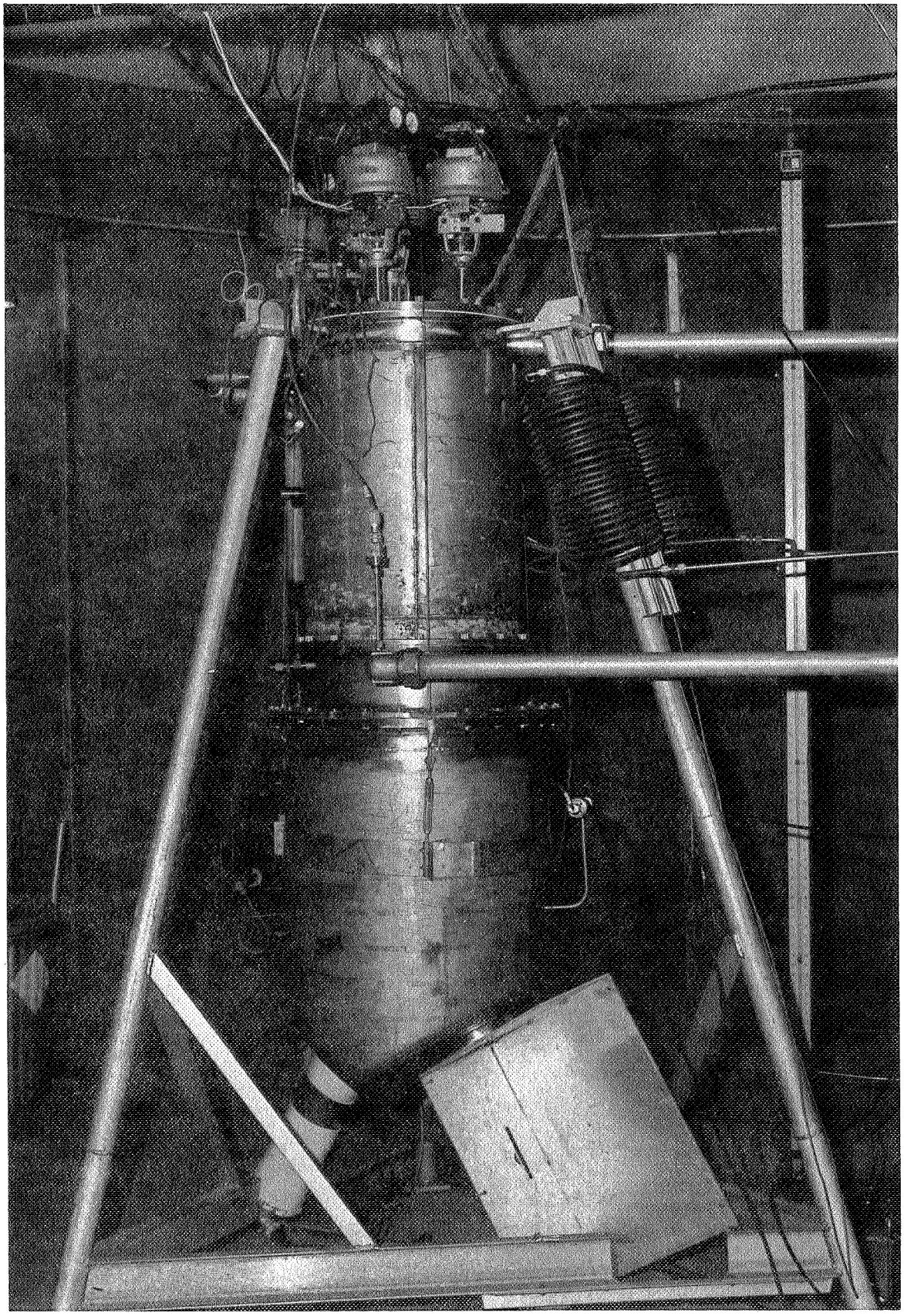

Figure 22: TEST EQUIPMENT

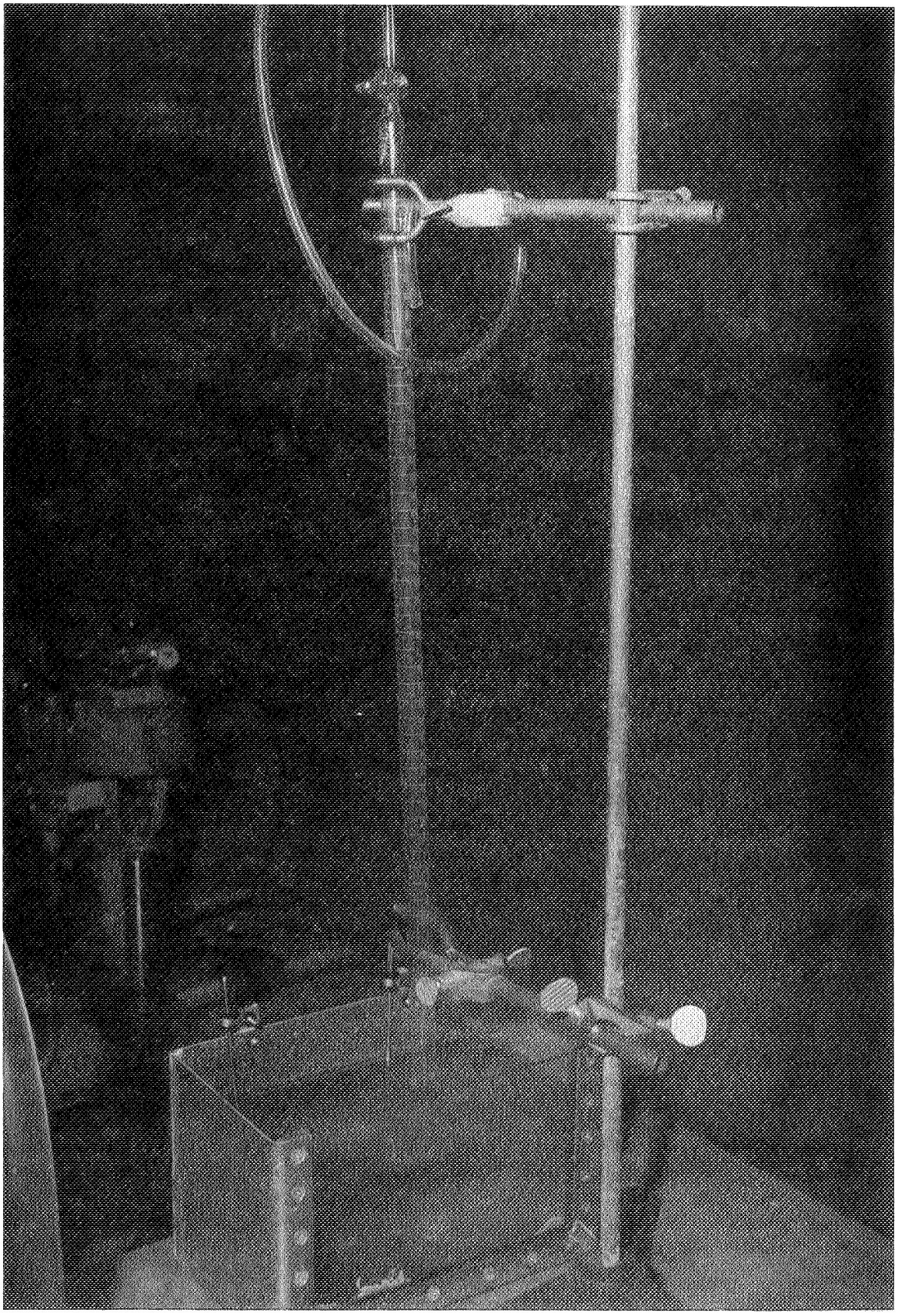

Figure 23: LEAK TEST APPARATUS

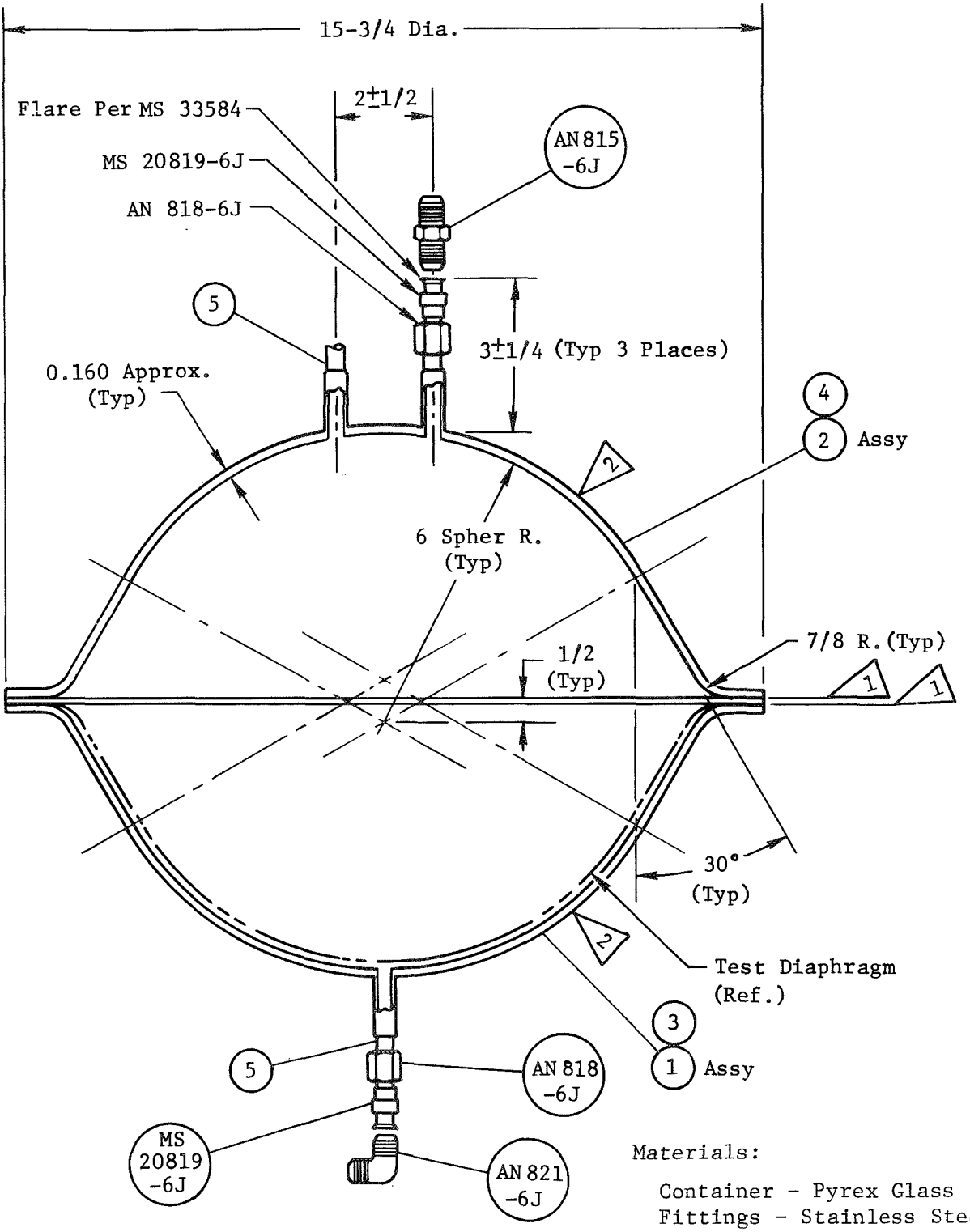

CROSS-SECTION VIEW

Figure 24: TEST CONTAINER

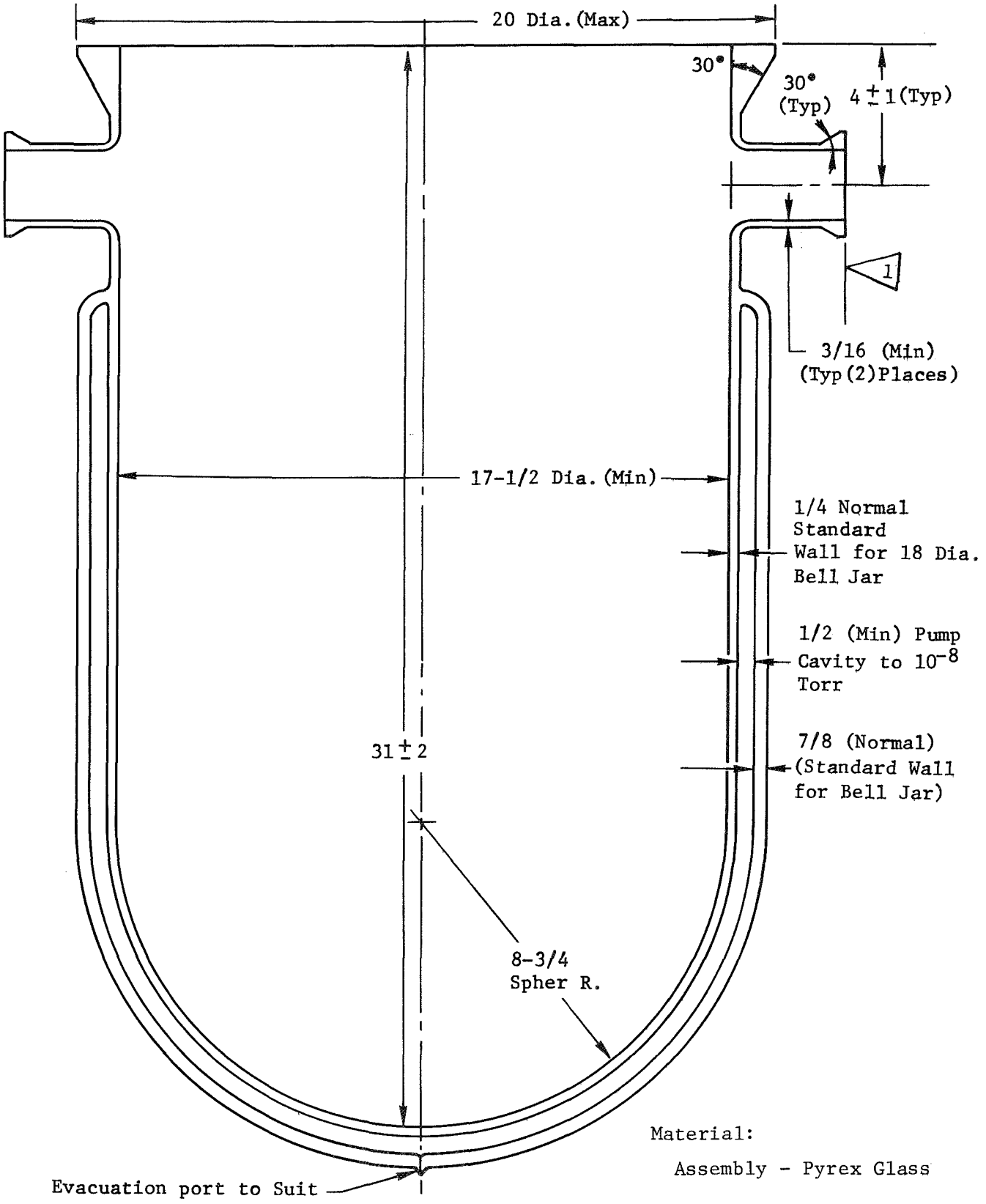

CROSS SECTION VIEW

Figure 25: BELL JAR ASSEMBLY

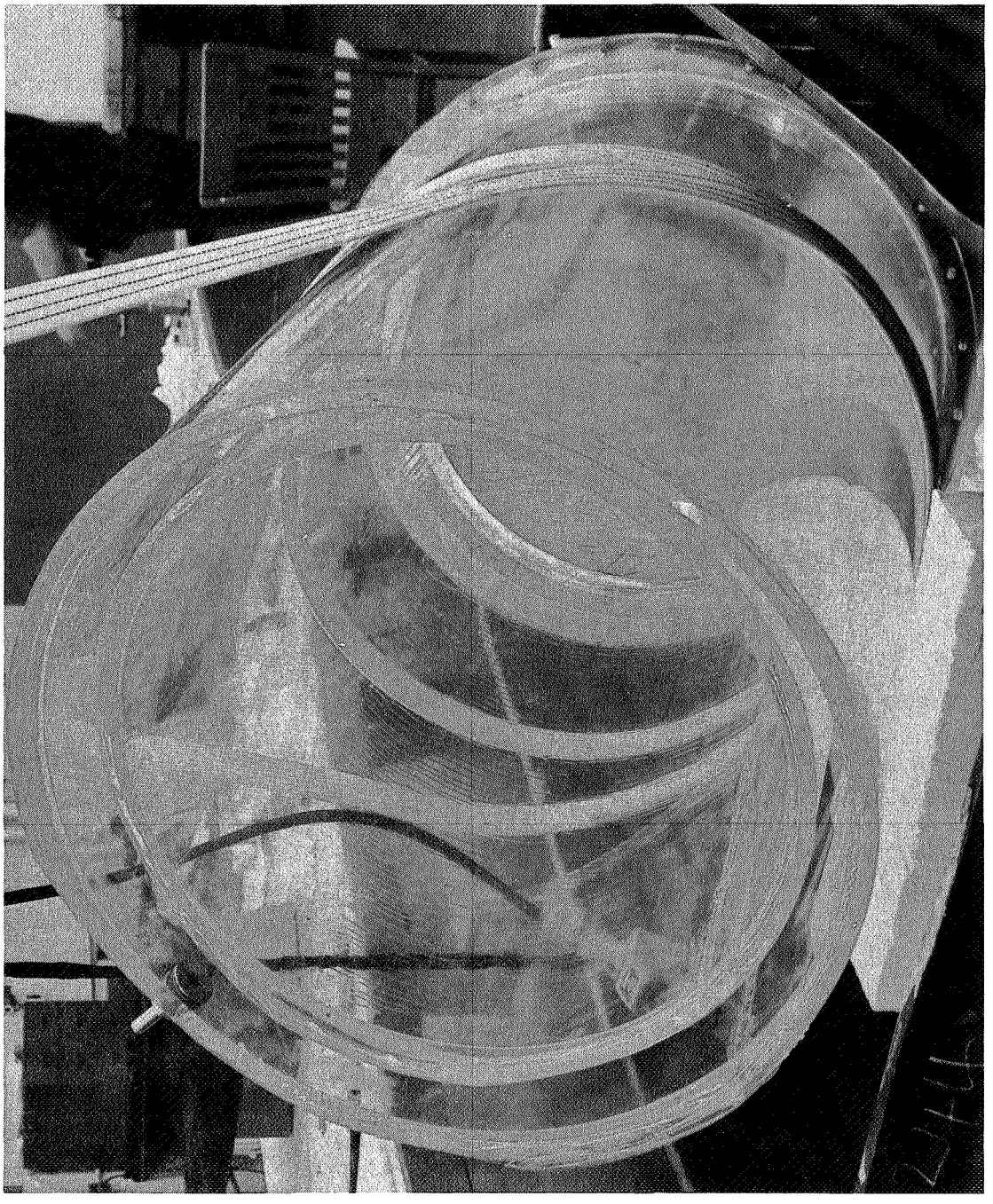

Figure 26: PLEXIGLASS DEWAR

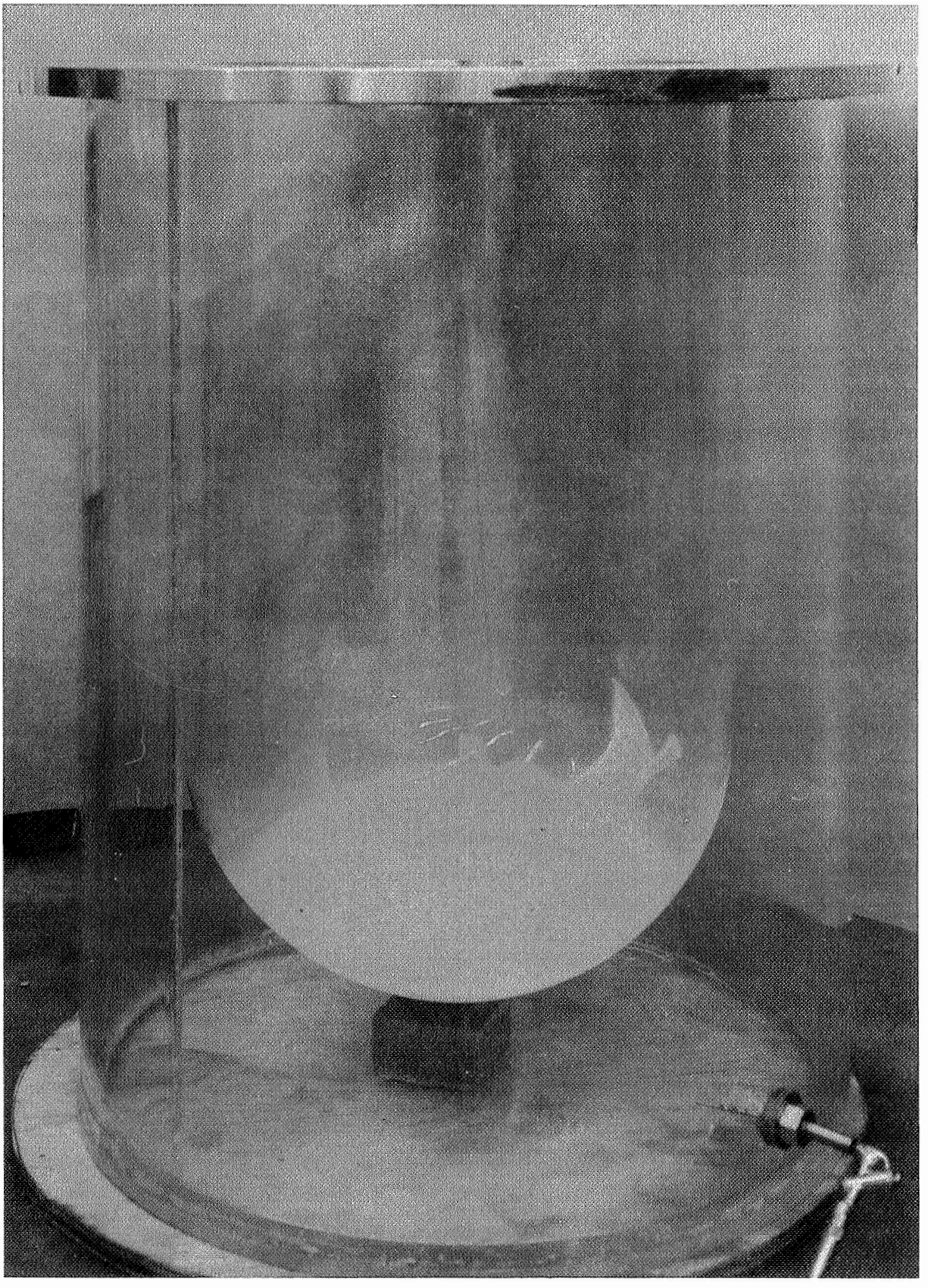

Figure 27: GLASS-PLEXIGLASS DEWAR

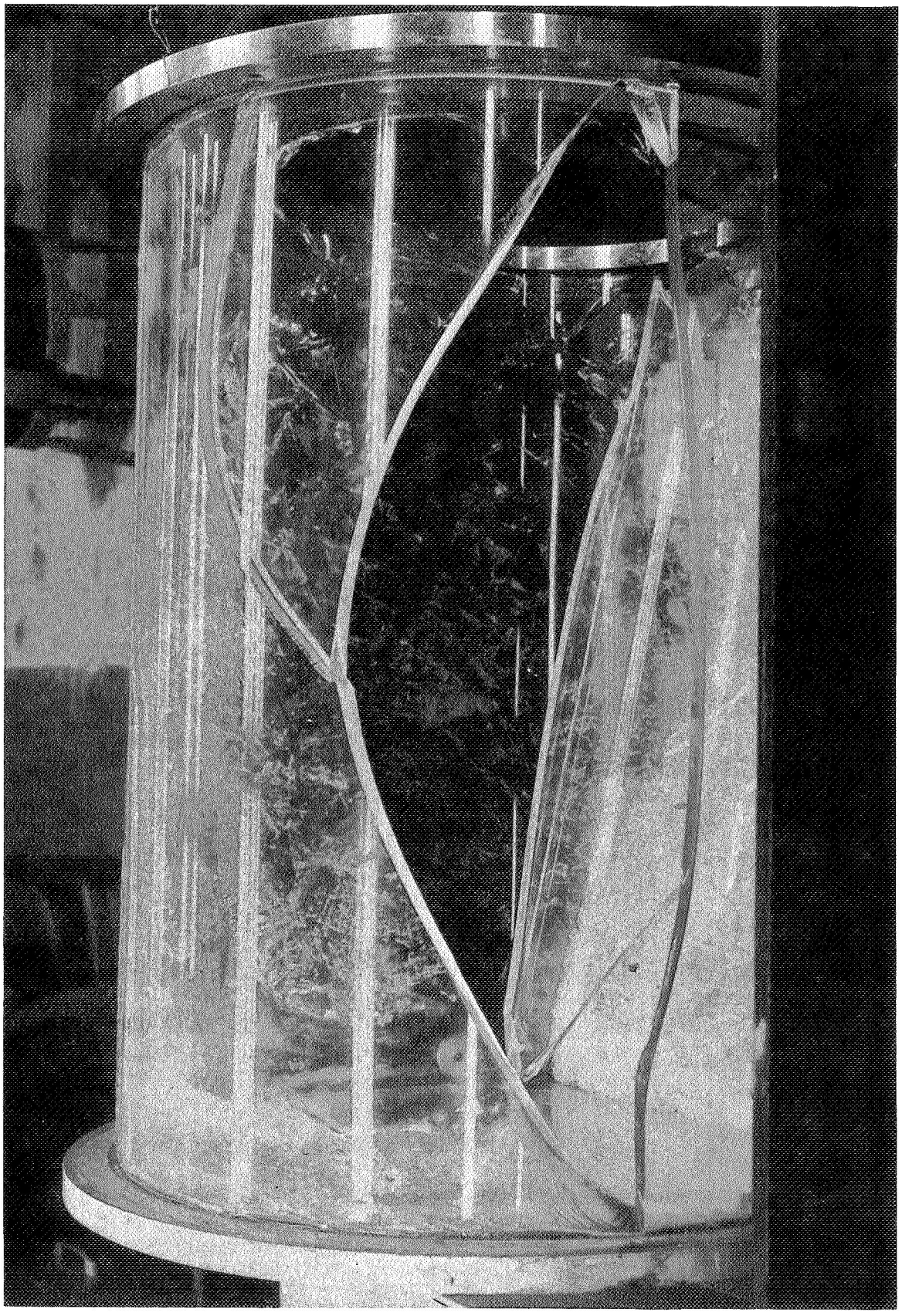

Figure 28: TESTED DEWAR

A third container using an expansion band attaching the inner container to the mating flange and a stainless steel outer container with the view ports was fabricated. The finished dewar is shown in Figure 29. This unit lasted longer with LH_2 in the inner vessel but it also disintegrated.

A mutual decision with the NASA program manager was made to revise the approach to the test unit and fabricate a unit of stainless steel with bolt-in view ports. This unit is shown in Figure 30. The double ports allowed camera coverage through one while the TV camera and light source utilized the second port. The unit was vacuum insulated and the areas above the dome and around the GHe expulsion side were filled with liquid hydrogen. The dome was removable to allow placement of the diaphragms. This unit mated with the existing upper cryostat used for preconditioning of G Helium. The lower cryostat, shown in Figures 31 through 34, was designed for upward expulsion of the liquid hydrogen using preconditioned helium gas on the bottom (camera) side of the test diaphragm.

4.2 UPPER CRYOSTAT

This Boeing test unit mated with the test cryostat to provide conditioning of fluids and gas used in the diaphragm testing. Located in the unit were the folloiing units:

a. The helium pressurization heat exchanger which was used to precondition the gaseous helium to -423°F for porosity measurements and expulsion cycling.

b. The hydrogen vent conditioner located in the ullage volume of the unit was used to prevent liquid hydrogen from reaching the warm vent line during the expulsion tank fill period.

c. The hydrogen expulsion flow section measured and controlled the hydrogen expelled by the diaphragm at one gallon per minute.

4.2.1 Heat Exchangers

The hydrogen and helium heat exchangers were used to increase the temperature of the vent gases to ambient.

4.2.2 Gas Measurement Equipment

A water saturator and a wet test meter were used to measure the quantity of gas evolving from the helium side of the diaphragm during the diffusion test.

4.2.3 Burette Apparatus

This unit was used to measure the porosity of leakage of the diaphragm in the expulsion mode.

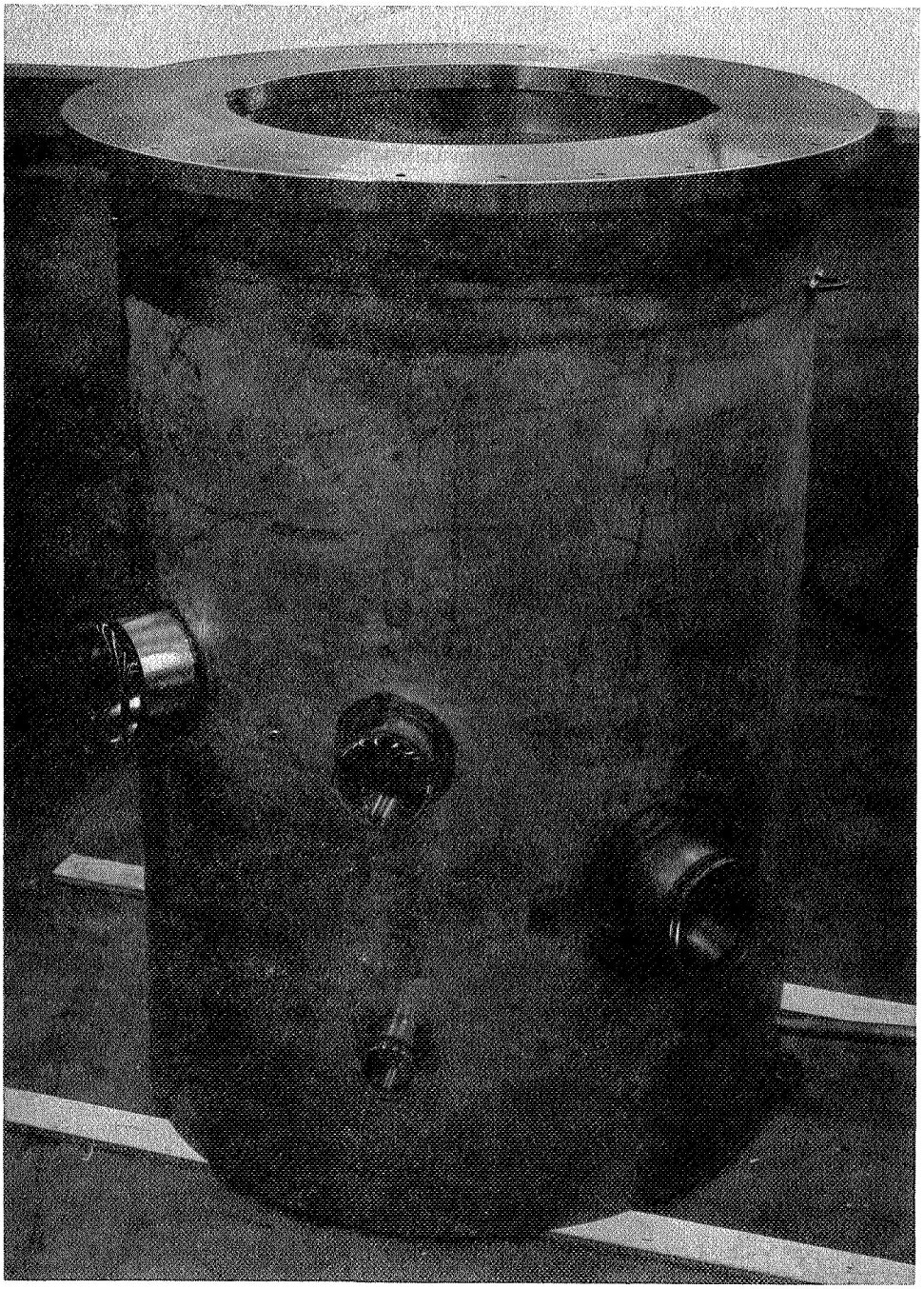

Figure 29: GLASS-STEEL DEWAR

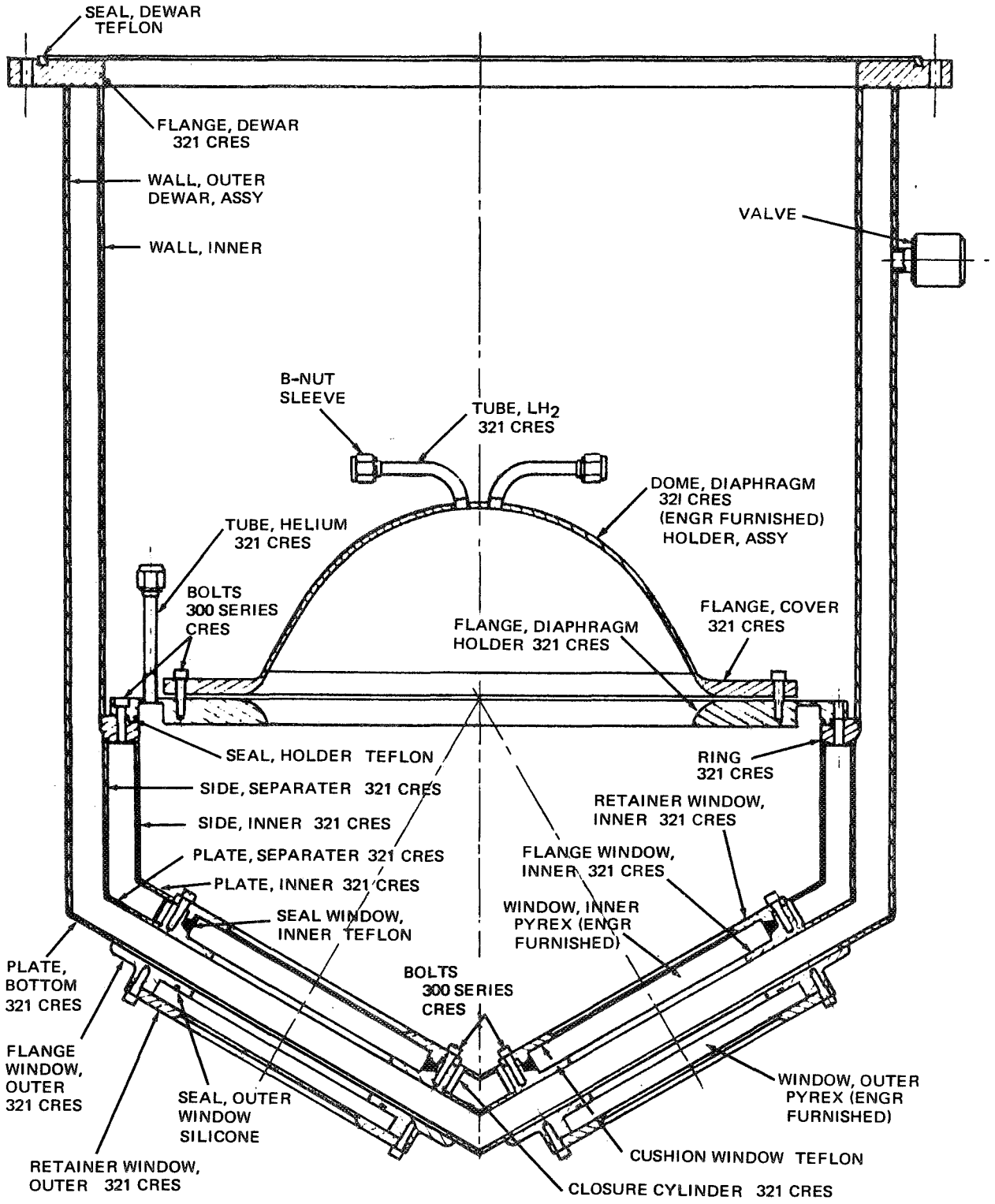

Figure 30: STEEL TEST CRYOSTAT

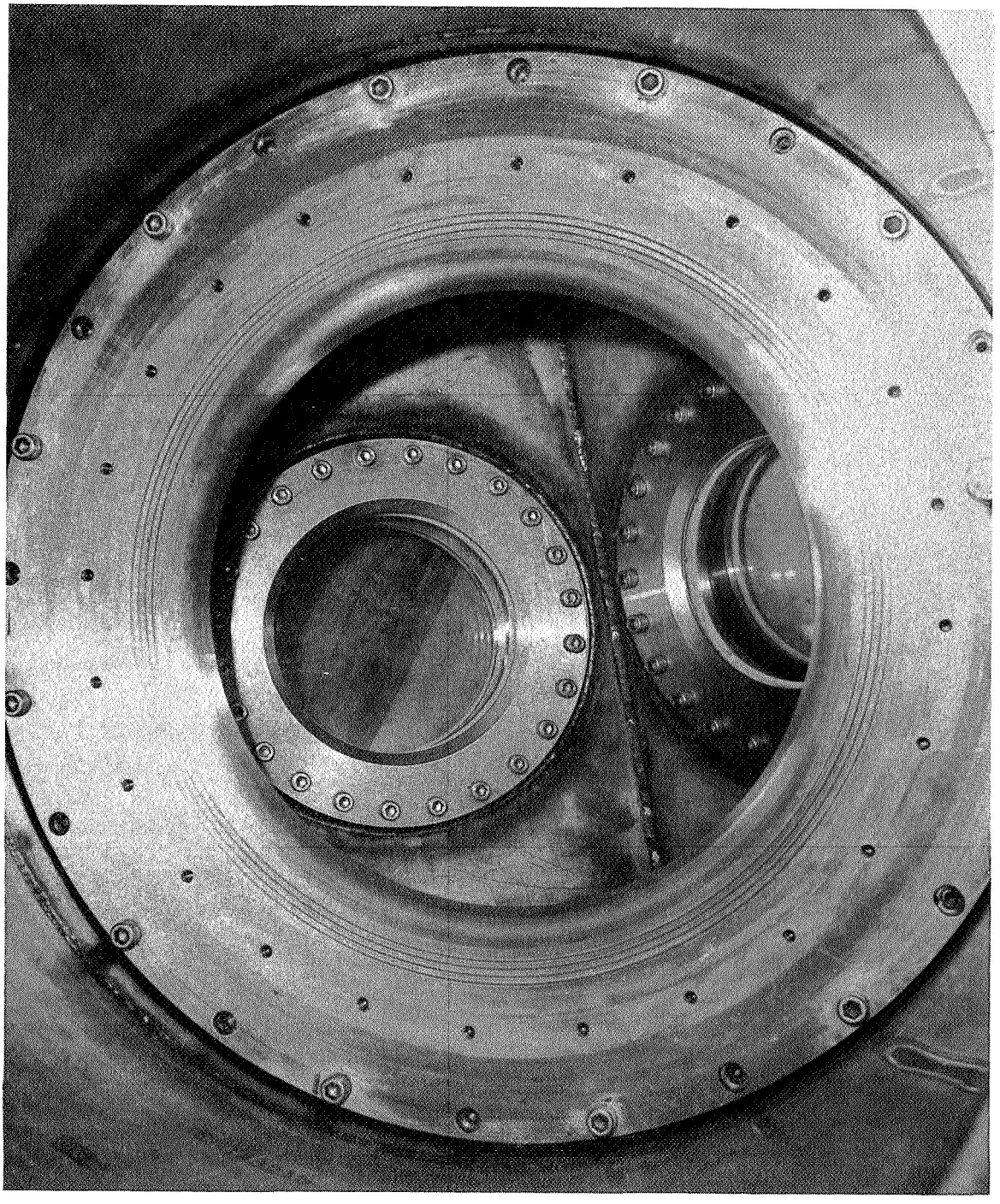

Figure 31: TEST CRYOSTAT VIEW PORTS

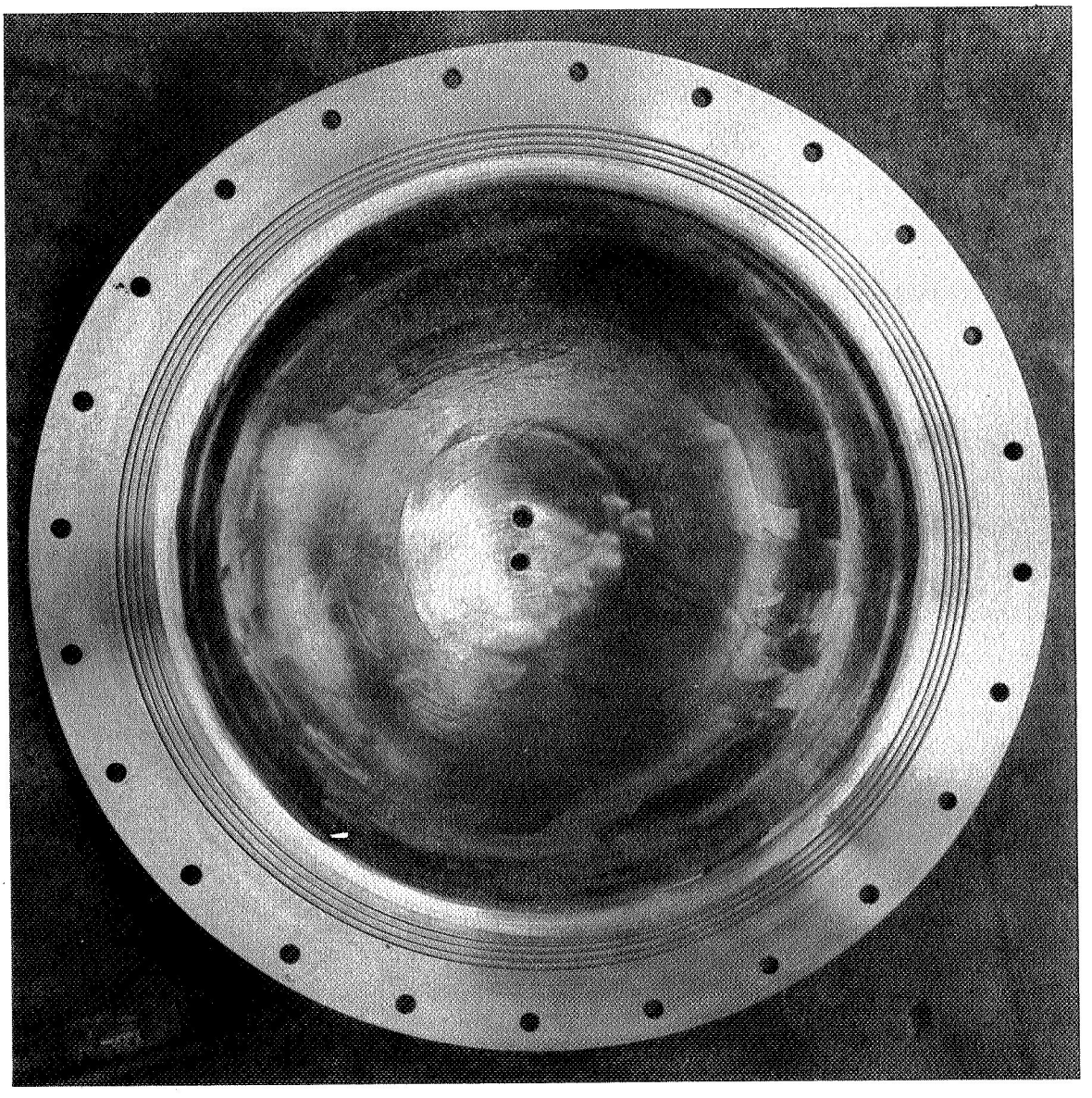

Figure 32: TEST DOME

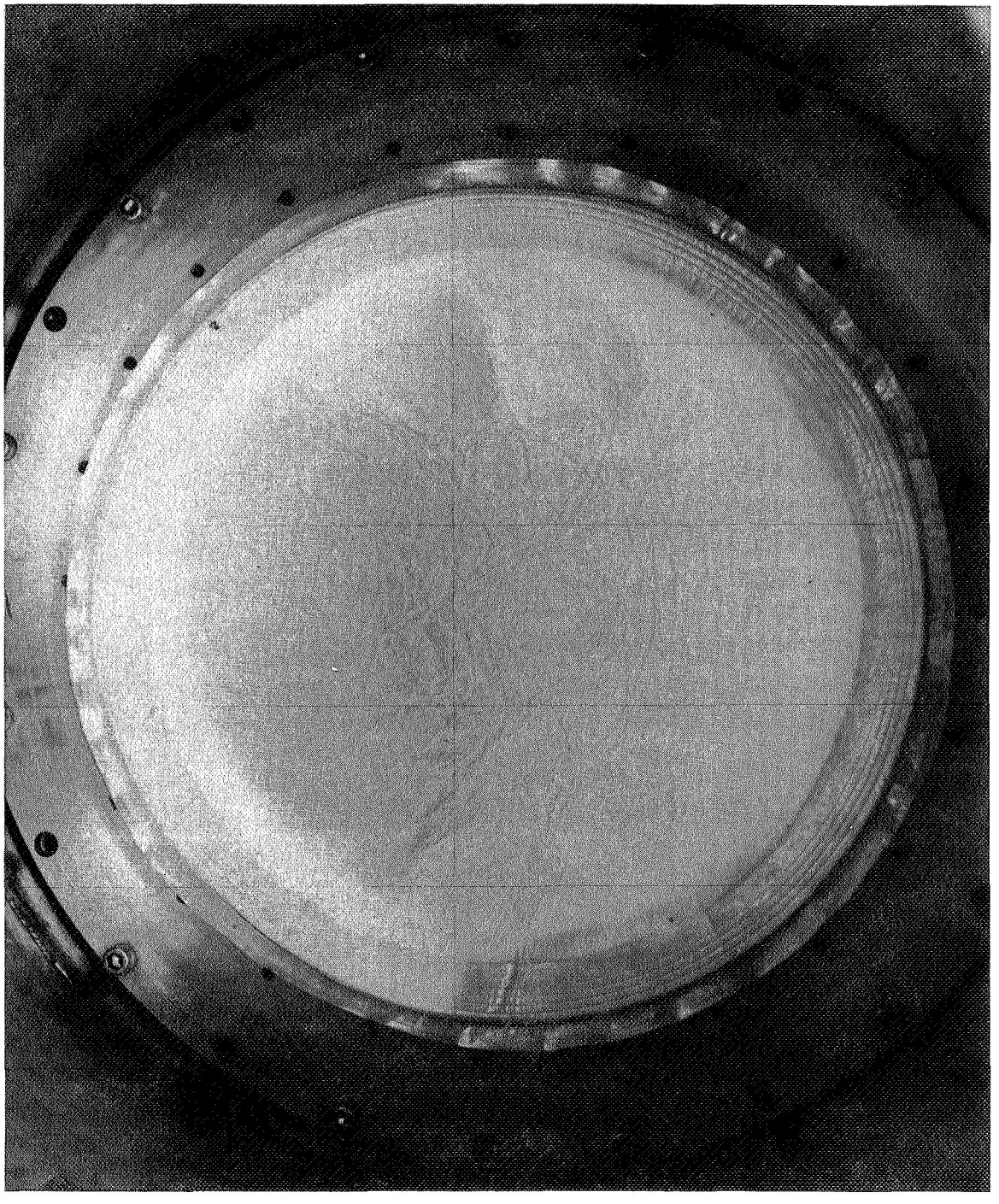

Figure 33: TEST DIAPHRAGM IN CRYOSTAT

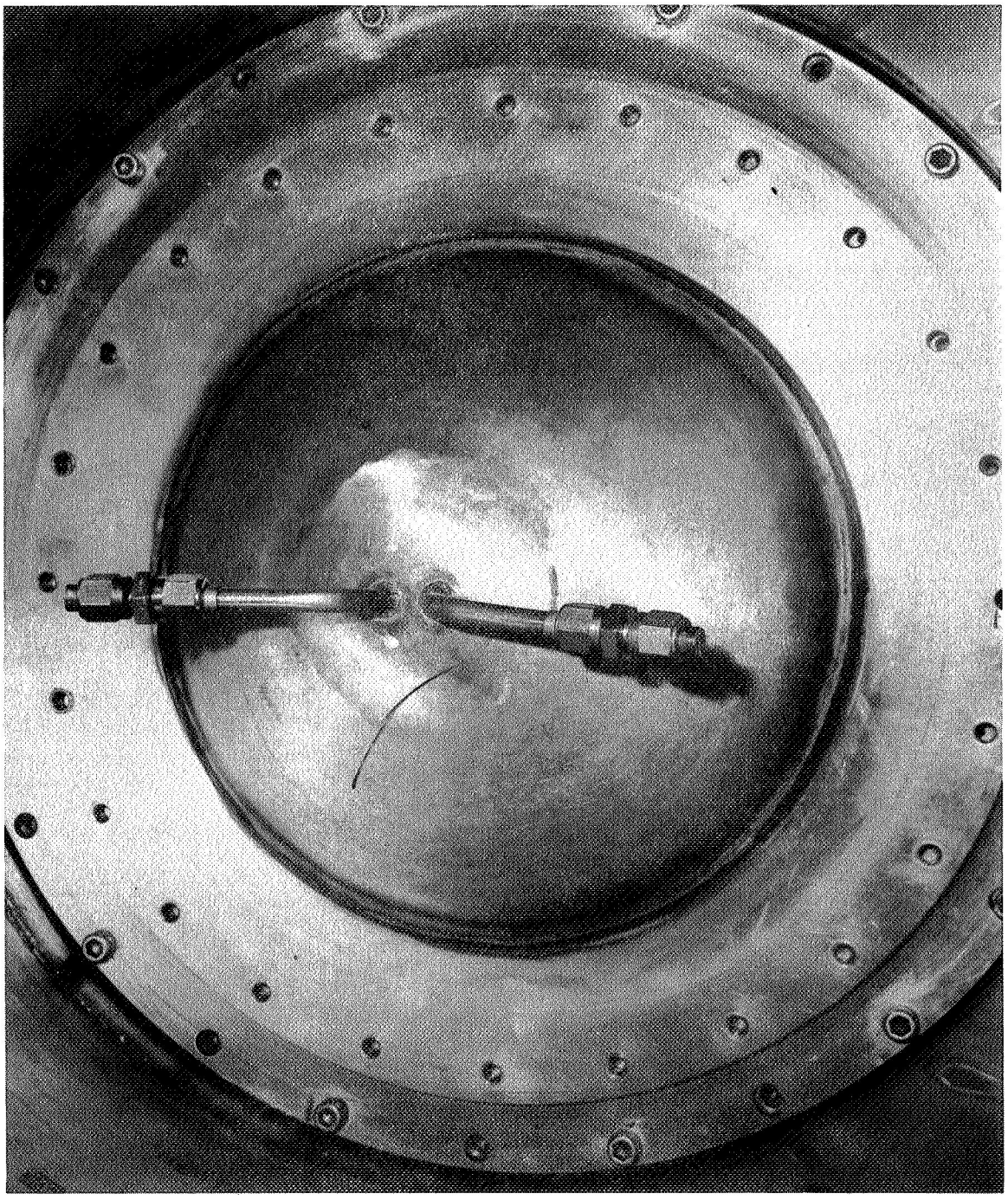

Figure 34: CRYOSTAT ASSEMBLY

4.2.4 Instrumentation

Pressures were sensed by standard strain gage transducers or water manometers. Test temperatures were sensed by copper-constantan or chromel-constantan thermocouple. Liquid levels and control temperatures used carbon resistors as sensors. Outputs were recorded on Leeds and Northrup Speedomax H Strip-Chart recorders. Signal conditioning equipment was Boeing built. All equipment was certified by Boeing's calibration-certification procedures.

Photographic coverage was provided for all expulsion cycles. The film speed was varied from 8 frames per second to as much as 24 frames per second depending upon the fill and expulsion rate. A nominal speed of 12 frames per second gave the best coverage. A "fish-eye" wide angle lens was used on the camera.

A closed circuit television system was used for visually monitoring the tests.

4.3 LIQUID HYDROGEN TESTING

4.3.1 Diaphragm Installation

The diaphragm was inserted in the test unit in the up position so that the diaphragm would not be cycled to conduct the ambient temperature and the liquid hydrogen temperature porosity checks. The hemispherical steel head was positioned and the bolts torqued to 90 inch pounds. An initial leak check was conducted on the flange seal by pressurizing the diaphragm unit with helium gas to one psi, the lower test unit was positioned in place and a room temperature leak check of the diaphragm was measured by means of a burette apparatus shown in Figure 23. Following the room temperature leak test, the cryostat was filled with LH_2 and allowed to stabilize in temperature. A leak check was then conducted at -423°F while pressurizing the diaphragm with one psi of -423°F helium gas.

The leakage through the diaphragm was measured with the burette apparatus. After successfully passing these checks in order, the diaphragms were tested by cyclic expulsion. Maximum acceptable leakage was 10 std. cc/min. prior to test termination.

4.3.2 Expulsion Cycling

Prior to filling the diaphragm with LH_2, the lines and diaphragm head area were vacuum purged to eliminate condensibles. Flow purging with inert gas does not adequately eliminate condensibles.

The diaphragms were filled with liquid hydrogen at a flow rate of approximately one gpm. The fill pressure was adjusted to get the desired flow but the differential pressure across the diaphragms did not exceed two psi.

As the diaphragms filled the unit would reverse itself and be completely filled in the fully extended, down position. The fill rates, pressures, liquid level, differential pressure across the diaphragm were continuously monitored. Closed circuit television allowed visual monitoring of the expulsion cycling. Motion pictures were taken of each diaphragm test. The cyclic tests were terminated when the diaphragm leakage rate exceeded 10 std. cc/min. or physical damage was apparent from visual monitoring.

4.3.3 Post-Test Evaluation Procedures

Following the cyclic testing of each diaphragm, they were removed from the test dewar and subjected to a room temperature leak check and a visual inspection of the disected diaphragm to determine the location and mode of failure of the vapor barrier ply.

The leak check was conducted by clamping the diaphragm in the leak check fixture. The diaphragm was pressurized to one psi internal pressure with helium gas and the external surface probed with a sniffer attachment to the Consolidated Electrodynamics Corporation 24-120A helium mass spectrometer.

After performing the leak test, each diaphragm was disected to remove the leakage areas and these disassembled to determine the mode of failure and to ascertain if there was a pattern to the failures.

5.0 TEST RESULTS

The test result of each diaphragm is discussed below.

5.1 DIAPHRAGM 1A (Gored 1.0 Mil Mylar)

The initial attempt to test diaphragm 1A was aborted when the flange seal leaked during the initial room temperature leak check in the cryostat. Two different seal clamping methods were used. The seal flange of the leak test unit exerted more pressure on the flange area than did the test flange during LH_2 testing which resulted in zero leakage indication during leak check but unacceptable leakage during test. At that time a resealing method was developed to eliminate the helium diffusion through the dacron felt by sealing the Mylar discs to the vapor barrier which eliminated the leak path. After rework, diaphragm 1A was reinstalled for testing. No leaks were recorded during the room temperature check and the test proceeded to the liquid hydrogen temperature leak check. A leak of 9.5 cc/min. was recorded prior to filling the diaphragm with liquid hydrogen. A maximum of 0.75 psid was reached and the diaphragm moved downward a small amount. At this time, liquid hydrogen was visually observed dripping on the inner cryostat window and the test was aborted.

Diaphragm 1A failed in a seam joint of the butted gores as shown in Figure 35.

5.2 DIAPHRAGM 1B (Gored 1.5 Mil Mylar)

This diaphragm was repaired in the flange seal after diaphragm 1A revealed leakage in the flange seal. This modified flange seal was incorporated in all diaphragms in the fabrication phase. There was no leakage in the room temperature leak check in the cryostat and the test proceeded to the liquid hydrogen leak check. Porosity at liquid hydrogen temperature was established at 82 cc/min. which was above the requirement but filling of the diaphragm was attempted. The test was aborted as the differential pressure of one psi could not be developed. At 3.5 minutes after liquid hydrogen filling was started, liquid was observed leaking through the diaphragm. Diaphragm 1B failed due to multiple leaks in the gored seams in the flange radius area as shown in Figure 37.

5.3 DIAPHRAGM 2A (Formed 1.0 Mil Mylar)

Several attempts were made to seal the flange seal in the test cryostat but leakage persisted during the liquid hydrogen leak test. Test was aborted. Attempts to reseal the leak in the flange failed.

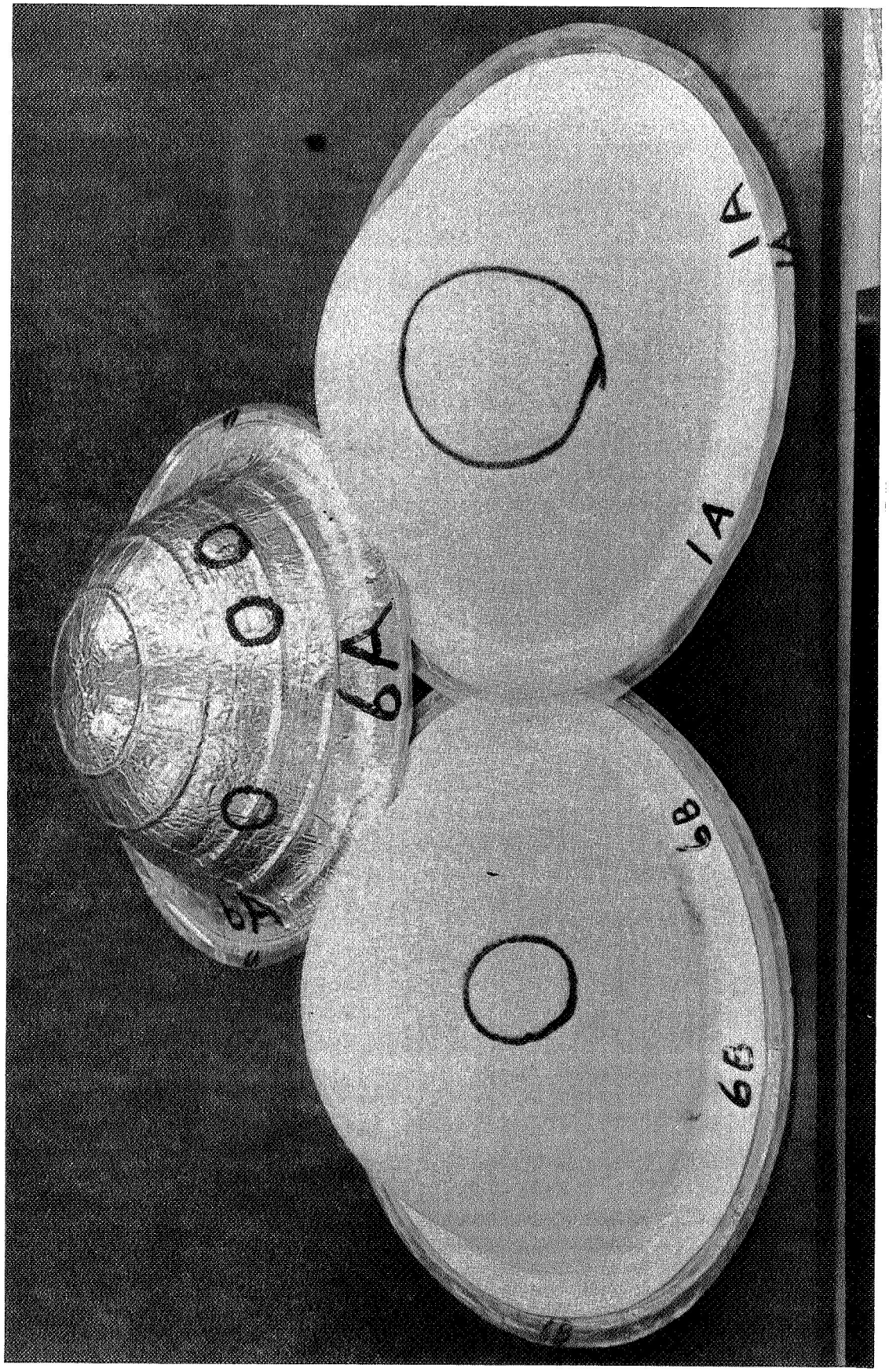

Figure 35: TEST DIAPHRAGM RESULTS

5.4 DIAPHRAGM 2B (Formed 2.0 Mil Mylar)

This unit indicated leakage during the ambient leak check in the test dewar but the tests proceeded on schedule. After the one psi differential was established across the diaphragm the leak rate was determined to be 60 cc/min. An attempt to reverse the diaphragm resulted in liquid hydrogen leaking through the diaphragm onto the cryostat window.

The diaphragm, shown in Figure 36, indicated a large leak area which is a large leak in a three corner fold which had split to give a V-shaped tear.

5.5 DIAPHRAGM 3A (Gored 1 Mil Kapton)

Room temperature leakage of the diaphragm in the test unit was determined to be 7 cc/min. and the tests proceeded to vacuum purging and liquid hydrogen leak test. A leak rate could not be established for the unit and the test was terminated.

The diaphragm with leakage areas located in the flange radius is shown in Figure 36.

5.6 DIAPHRAGM 3B (Gored 2.0 Mil Kapton)

This unit could not be sealed sufficiently in the flange area to proceed past the ambient seal leak check. Attempts to seal the flange area seal revealed the leak existed in the flange radius in an irrepairable area. This unit was flexed in the vacuum purging phase which developed leaks in the diaphragm as shown in Figure 36. The size of the area marked is not an indication of leaks in the total area but a large leak which could not be pinpointed.

5.7 DIAPHRAGM 4A (Formed 1.0 Mil Mylar)

This unit was originally scheduled to have convolute rings but these were eliminated after the results of diaphragm 8A were made available. This unit passed the ambient and liquid hydrogen temperature leak checks and the vacuum purge cycles but when the first liquid hydrogen impinged on the diaphragm leaks developed in the radius and conical sections. The test was terminated.

An effort was made to determine the mode of failure by fabricating a similar unit without the abrasion plies of dacron felts so that the vapor barrier could be observed during cycling. This unit passed ambient and liquid hydrogen leak checks, and the vacuum purge cycles but when the liquid hydrogen contacted the vapor barrier near the apex, the material contracted immediately locally, developed pin holes and leaked liquid into the lower cryostat. Unfortunately the camera did not start and the test was not recorded on film.

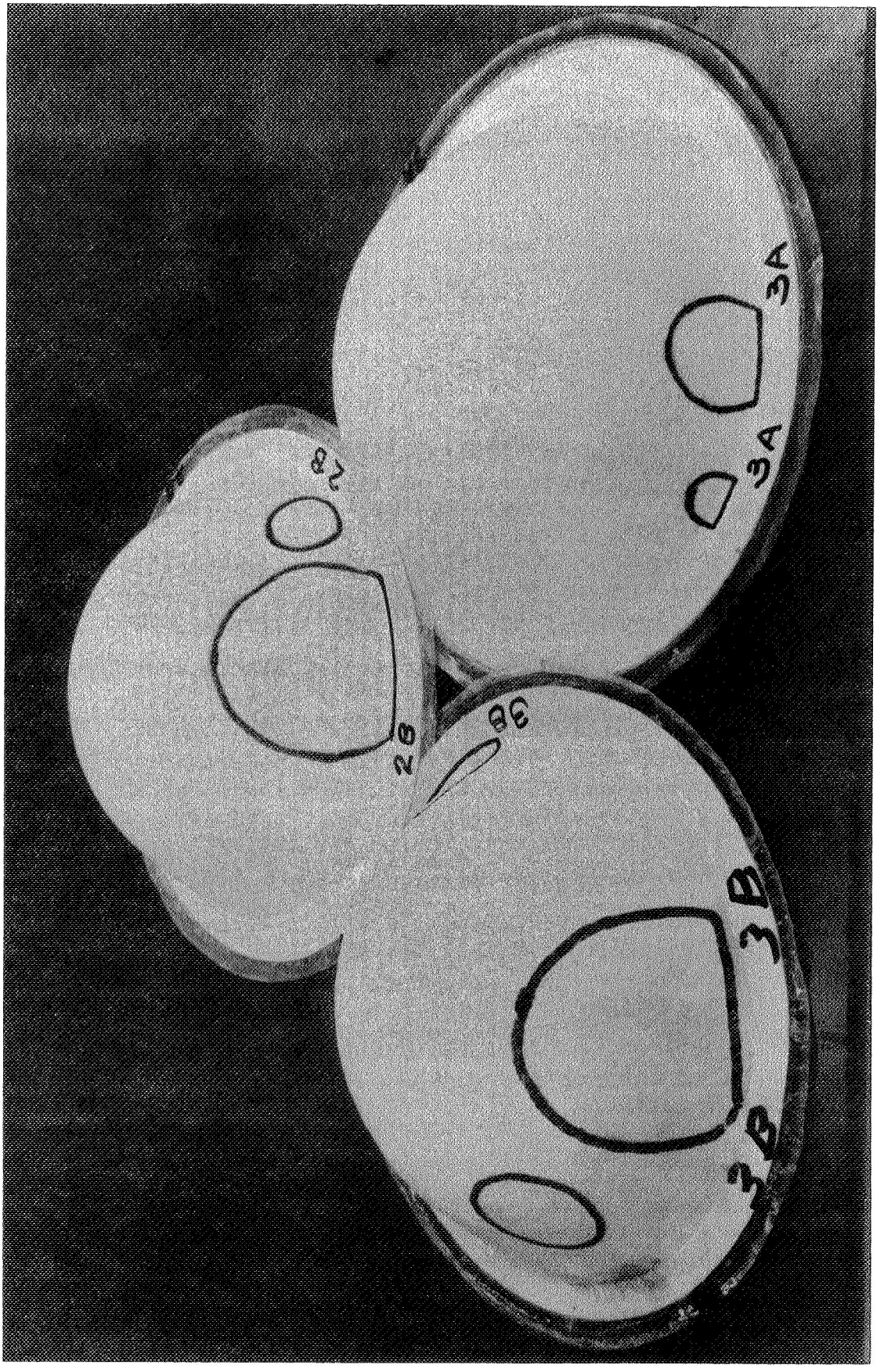

Figure 36: TEST RESULTS

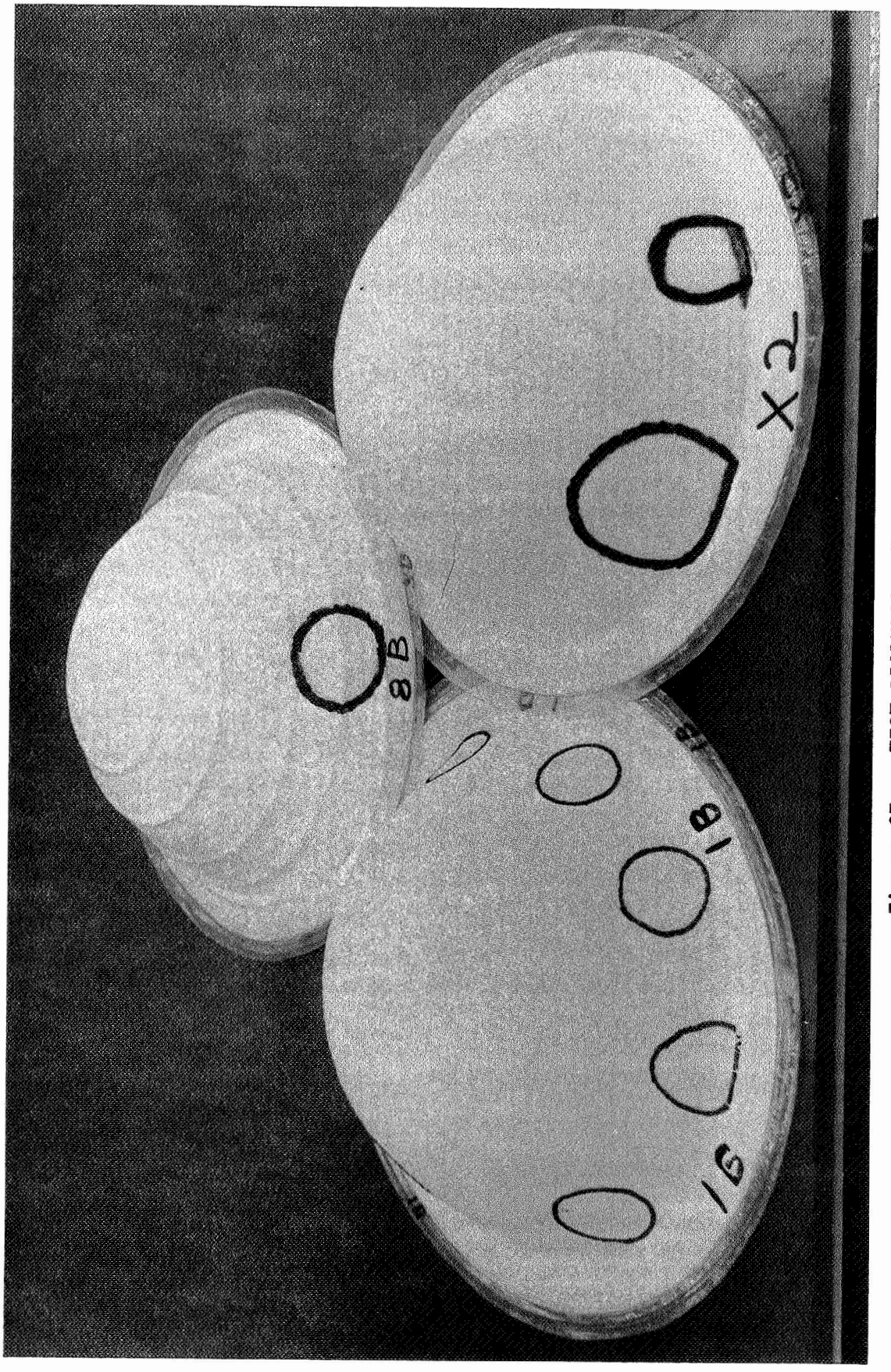

Figure 37: TEST DIAPHRAGM RESULTS

5.8 DIAPHRAGM 4B (Formed 2 Mil Mylar)

This diaphragm developed a leak in the flange seal during installation in the test dewar and was scrapped after attempts had been made to repair the leak. Diaphragm 4BX was fabricated identical to 4B. This unit successfully passed the ambient and cryogenic leak tests with no apparent porosity and the vacuum purging of the system. During the initial fill, the diaphragm moved downward an incremental amount where it remained until liquid droplets were observed in the flange radius area and the test was aborted.

Three leaks were found in the flange radius in the post test analysis.

5.9 DIAPHRAGM 5A (Formed 2 Mil Kapton)

Following installation, ambient leak checks and vacuum purging, the conditions were established for a liquid hydrogen porosity check. The porosity (leak rate) for the diaphragm was determined to be 160 cc/min. Filling of the diaphragm was attempted but a large amount of liquid hydrogen was visible in the helium gas side of the dewar and the test was terminated.

The diaphragm, shown in Figure 38, had a large leak in the conical section of the vapor barrier.

5.10 DIAPHRAGM 5B (Formed 3 Mil Kapton)

The diaphragm passed the flange, ambient and liquid hydrogen leak tests and vacuum purgings with no apparent leakage. Within 13 minutes after initial diaphragm filling began, the test was terminated because of liquid hydrogen leaking through the diaphragm. Only slight motion was apparent.

5.11 DIAPHRAGM 6A (Gored MAM Laminate)

Following the flange leak check, an attempt was made to cycle the test unit from the down (insert) position to the up position for vacuum purging of the line and dewar. After the diaphragm apparently would not reverse at one psi, the pressure differential was increased to 3.8 psi without reversal. The diaphragm moved incrementally but appeared to "lock-up" at a position corresponding to the large ring passing through the diaphragm. The diaphragm was removed from the test dewar and delamination of the felt-convolute ply from the other two plies was observed. The diaphragm was leak checked at room temperature and three leak areas shown in Figure 35 were noted. Testing was terminated on this unit.

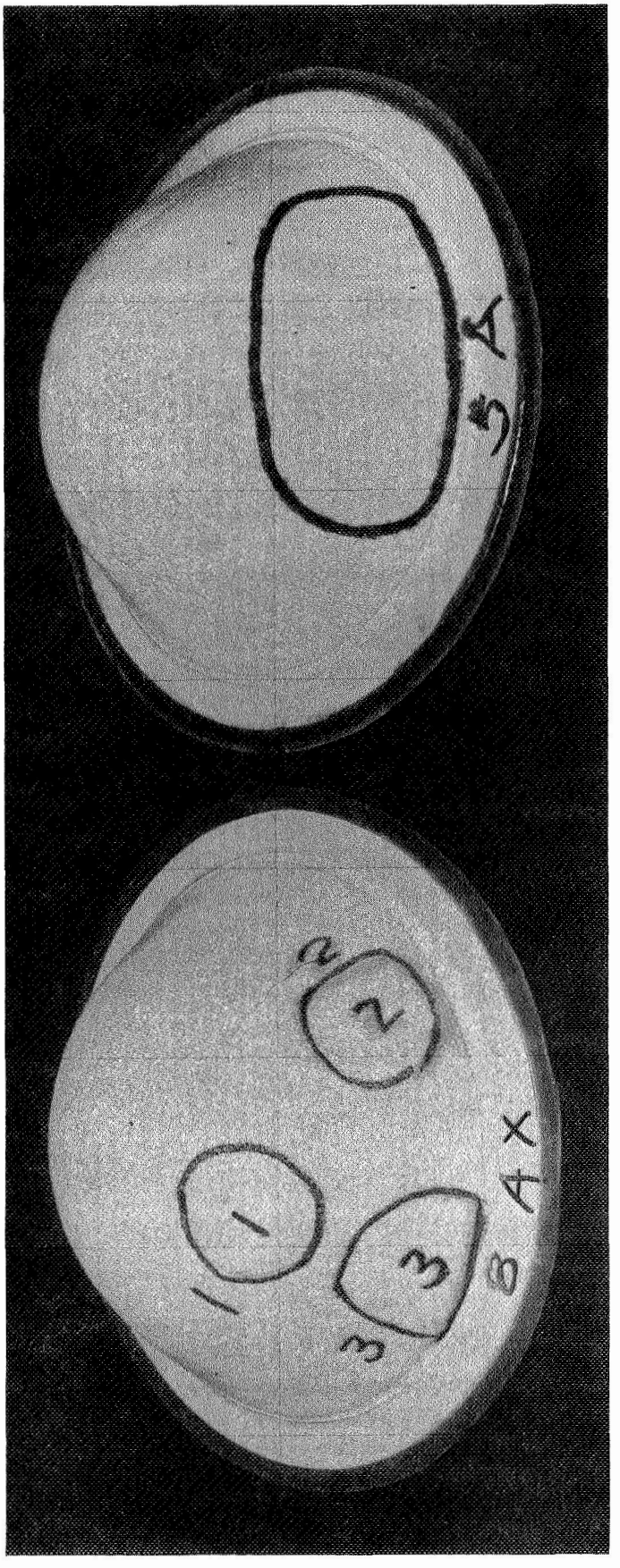

Figure 38: TEST DIAPHRAGM RESULTS

5.12 DIAPHRAGM 6B (Gored MLM Laminate)

Excessive porosity was evident after initial vacuum purge and initial leak checks. As shown in Figure 35 the leakage occurred in the conical-hemispherical head joint area. The leak measuring equipment could not record the flow through the unit.

5.13 DIAPHRAGM 7A (Gored 1.0 Mylar)

This unit was fabricated with new adhesive film because of the possibility of adhesive aging either before or after fabrication of butt joints which had been stored before testing.

Low pressure purging of the lines and diaphragm area with helium gas thereby eliminating the need for vacuum purging was attempted as it was thought that the vacuum cycling may contribute to leakage in the diaphragm. After the initial leak tests and porosity checks, the system was inert gas purged. Conditions were then established for cryogenic porosity but the leakage was too great to measure. An attempt was made to cycle the diaphragm by filling with liquid hydrogen. Dimples appeared in the truncated cone section of the diaphragm but the unit would not cycle because of the lack of differential pressure. Figure 39 shows the leakage areas in the seams of the diaphragm.

5.14 DIAPHRAGM 7B (Gored 2.0 Mil Mylar)

This unit, like 7B, was fabricated as an adhesive test unit. Both the initial flange check and ambient leak checks showed zero leakage but after vacuum purging the cryogenic porosity check yielded 13 cc/min. Fill of the diaphragm was discontinued when liquid hydrogen appeared on the cryostat window. The leakage areas are shown in Figure

5.15 DIAPHRAGM 8A (Formed 3 Mil Mylar)

This diaphragm had convolute rings bonded to the film with abrasion plies on both sides of the vapor barrier.

The leak tests of the flange and ambient porosity checks revealed no leakage but during attempted vacuum purge, it was found that the unit would not reverse. The differential pressure across the diaphragm was increased from 1 psi to 2.5 psi. It was impossible to increase the differential pressure beyond that point without major site rework. Tests were discontinued after the unit failed to move.

Diaphragm 8AX was fabricated identical to 8A but without the convolute rings. The unit showed no porosity during the flange and ambient tests but after vacuum purging the cryogenic leakage rate was 140 cc/min. The diaphragm was filled but the test was discontinued when liquid hydrogen appeared on the test dewar window. This unit is shown in Figure 38.

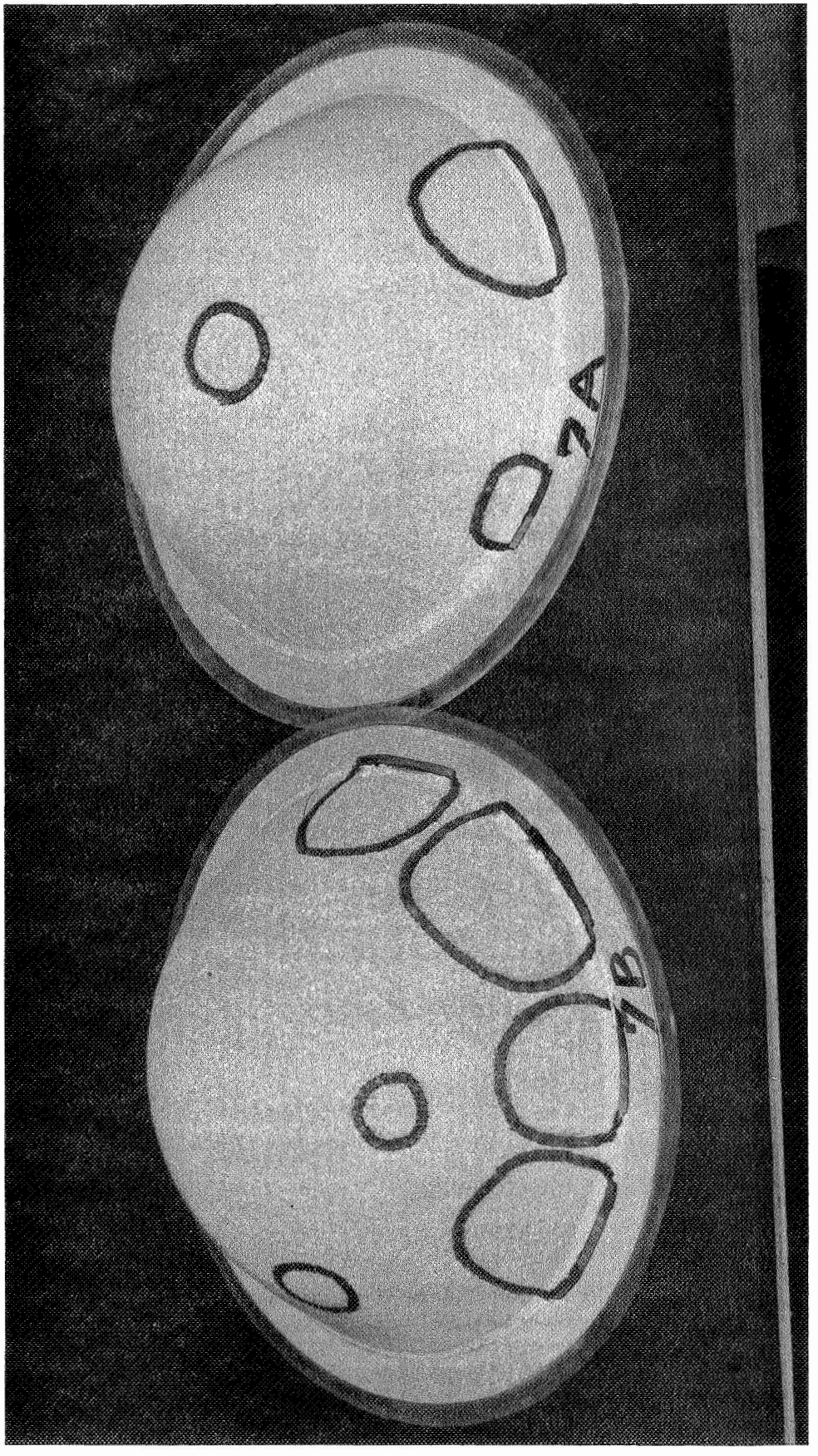

Figure 39: TEST DIAPHRAGM RESULTS

5.16 DIAPHRAGM 8B (Formed 4 Mil Mylar)

The diaphragm had convolute rings bonded to the dacron felt but these were removed after unit 8A failed to cycle because of rings. The unit passed both the flange seal and the ambient leak checks but after conditions were established for the cryogenic porosity check the leakage was in excess of the systems capability to measure and the test was aborted.

As shown in Figure 37, leakage occurred in the conical section near a ring attachment point.

6.0 IMPROVED EXPULSION DIAPHRAGMS

The task was divided into two major parts. The first subtask was the analysis of the results from previous diaphragm tests and the recommendation of two improved diaphragm designs. Analysis of the test results was difficult due to the negative results obtained but it was felt that the design of the diaphragm contributed to the failures in the flange radius and the conical to hemispherical head joint areas. Figure 40 shows graphically that a structural element in the form of a truncated cone existed within the diaphragm unit. This truncated cone (frustrum of a cone) is extremely rigid. As pressure was applied to the hemis pherical section above the conical section, one was attempting to invert concentric circumferences. An additional factor was that the polymeric film vapor barrier became increasingly rigid as the temperature was lowered to that of liquid hydrogen. Observation of the tests by closed circuit television shows the diaphragms to move downward in the flange area initially at which time the motion would cease and liquid hydrogen droplets appeared on the gaseous helium side of the diaphragm. The cone, it appeared, prevented the diaphragm from cycling through as it came into contact with diaphragm test dewar flange radius.

The sequence of the diaphragm unit progress during water expulsion is shown in Figures 41 through 44. The sequence shows that the diaphragm "rim rolls" and has a definite "list" during cycling. It was predicted that the diaphragm would start its reversal at the apex with the flange radius being the last area to reverse. Rim rolling imparts more severe creasing and folding conditions on the film barriers. The "list" of the diaphragm during expulsion had been observed previously in liquid oxygen diaphragms. If a list existed on the LOX diaphragm's initial cycle, this list would be identical in all cycles conducted on that particular diaphragm.

An effort was made in Task IV to eliminate or minimize the structural bridging by redesigning the diaphragm in the conical areas shown in Figure 45 to yield a radius blended diaphragm. It was thought that a great portion of the diaphragms failed because of these elemental joints. Diaphragm fabrication tools were redesigned and fabricated to the new diaphragm design. The selection of materials for the new diaphragm design was made after analysis of the test results of the diaphragms in Tasks II and III. Because the test results were negative the selection was made of the materials which would have the greatest chance of survival in the liquid hydrogen. The units selected were:

1. Gored one mil Mylar
2. Formed one mil Mylar
3. Formed one mil Kapton
4. Three gored layers of 1/2 mil Mylar.

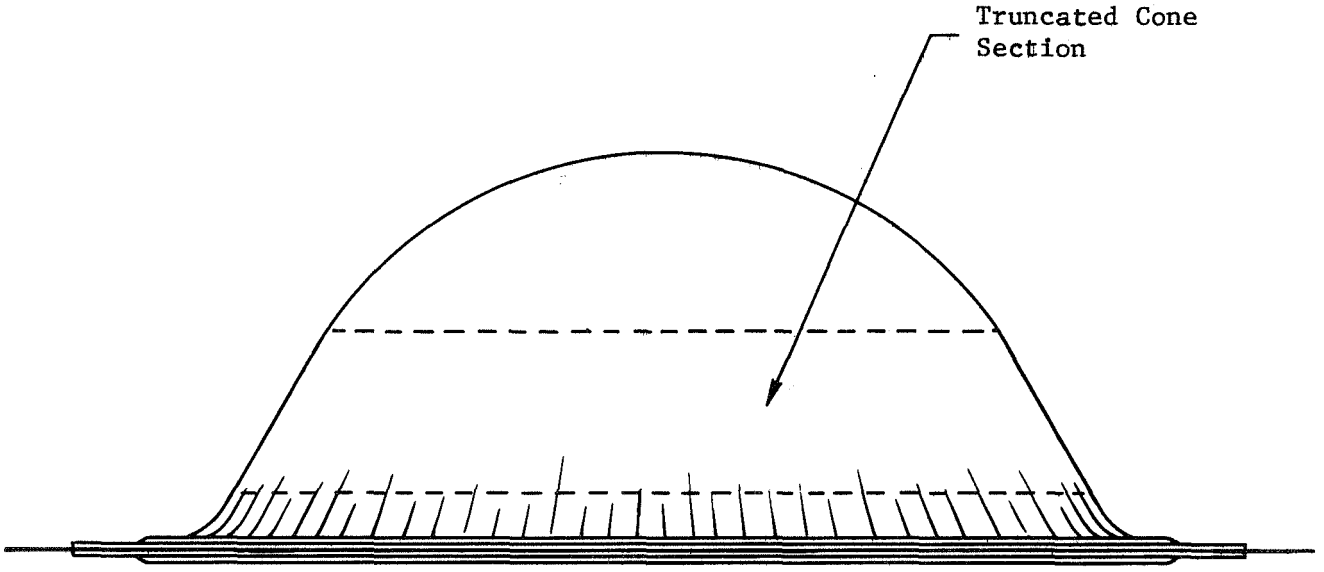

Figure 40: EXPULSION DIAPHRAGM DESIGN

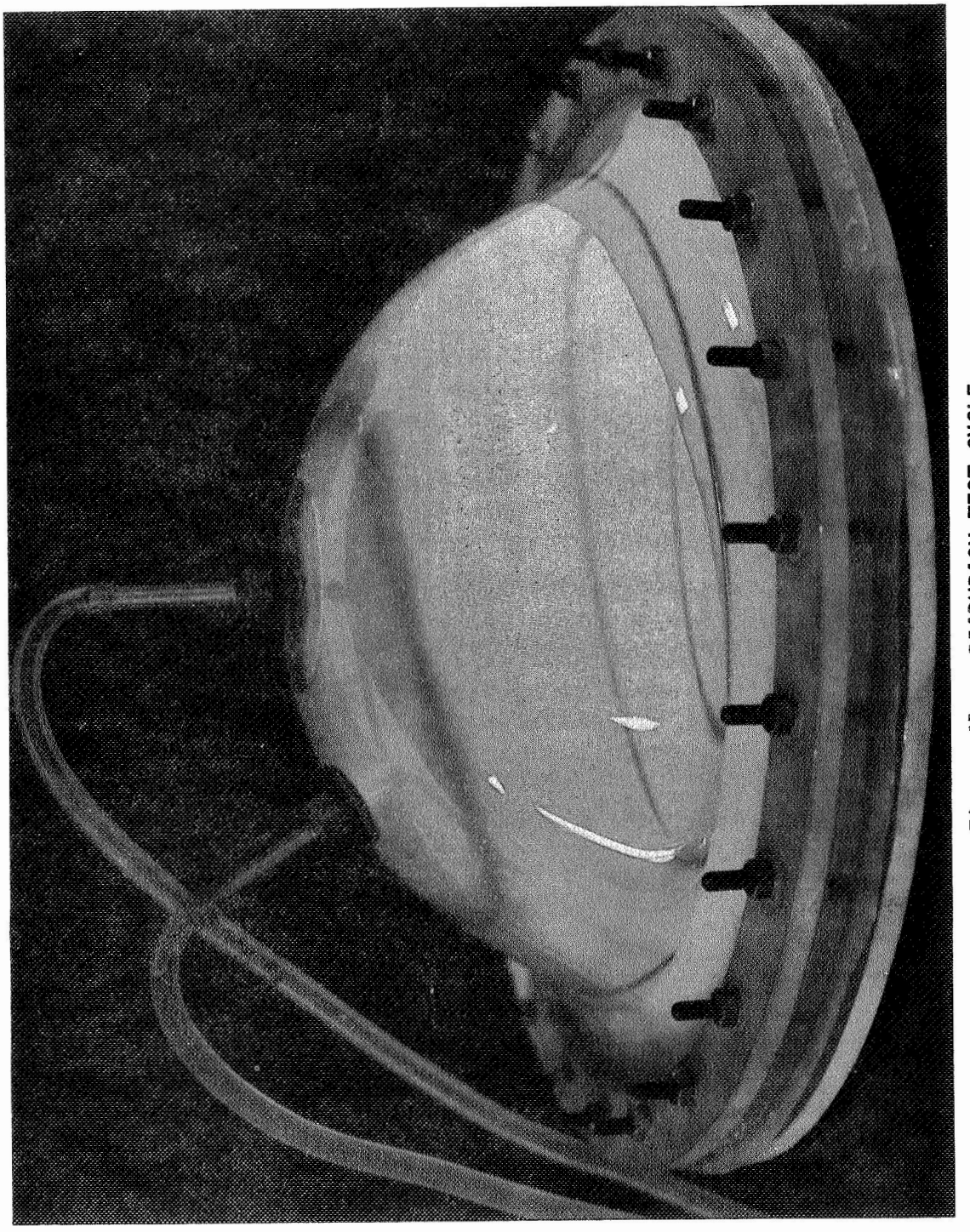

Figure 41: DIAPHRAGM TEST CYCLE

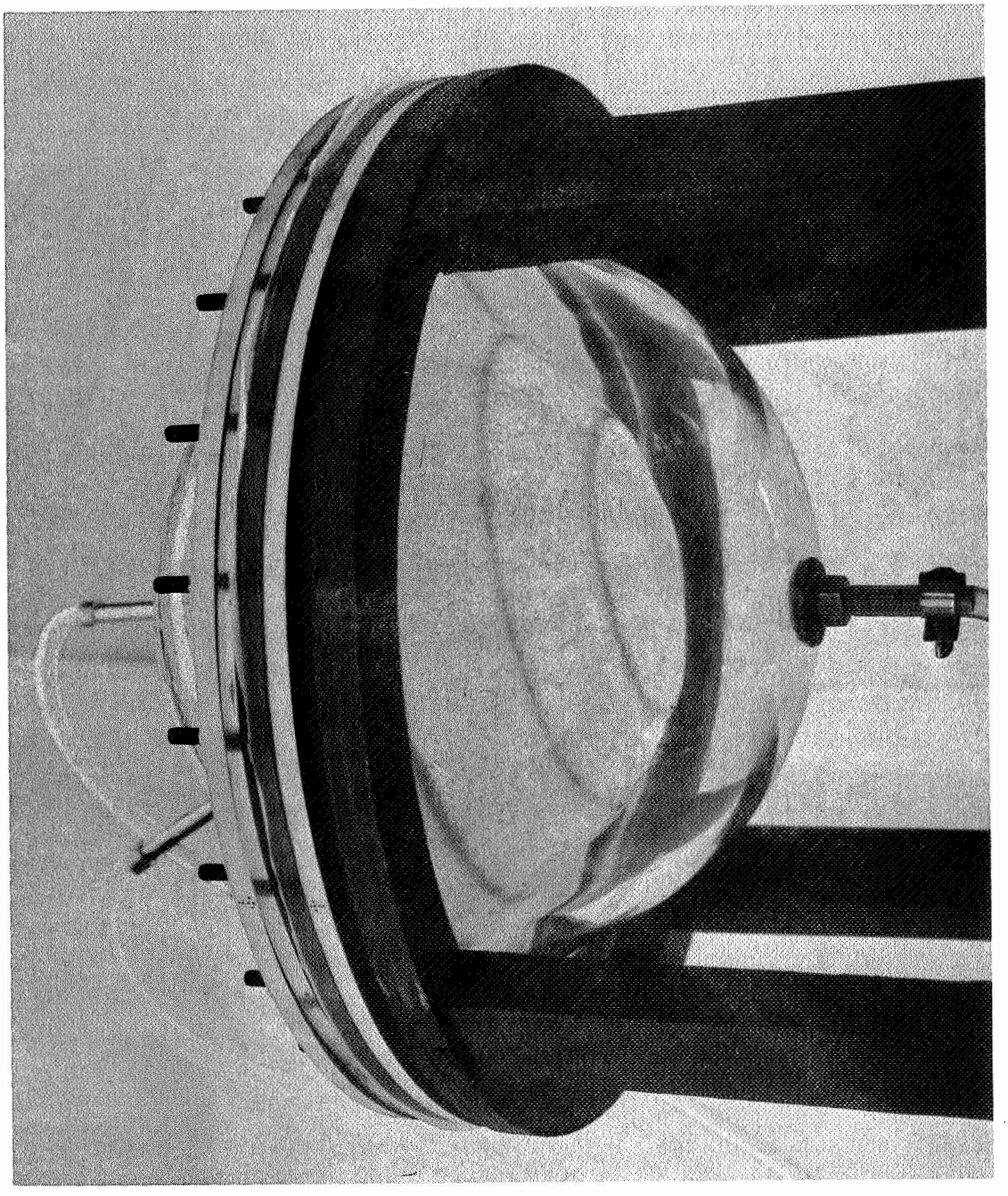

Figure 42: DIAPHRAGM TEST CYCLE

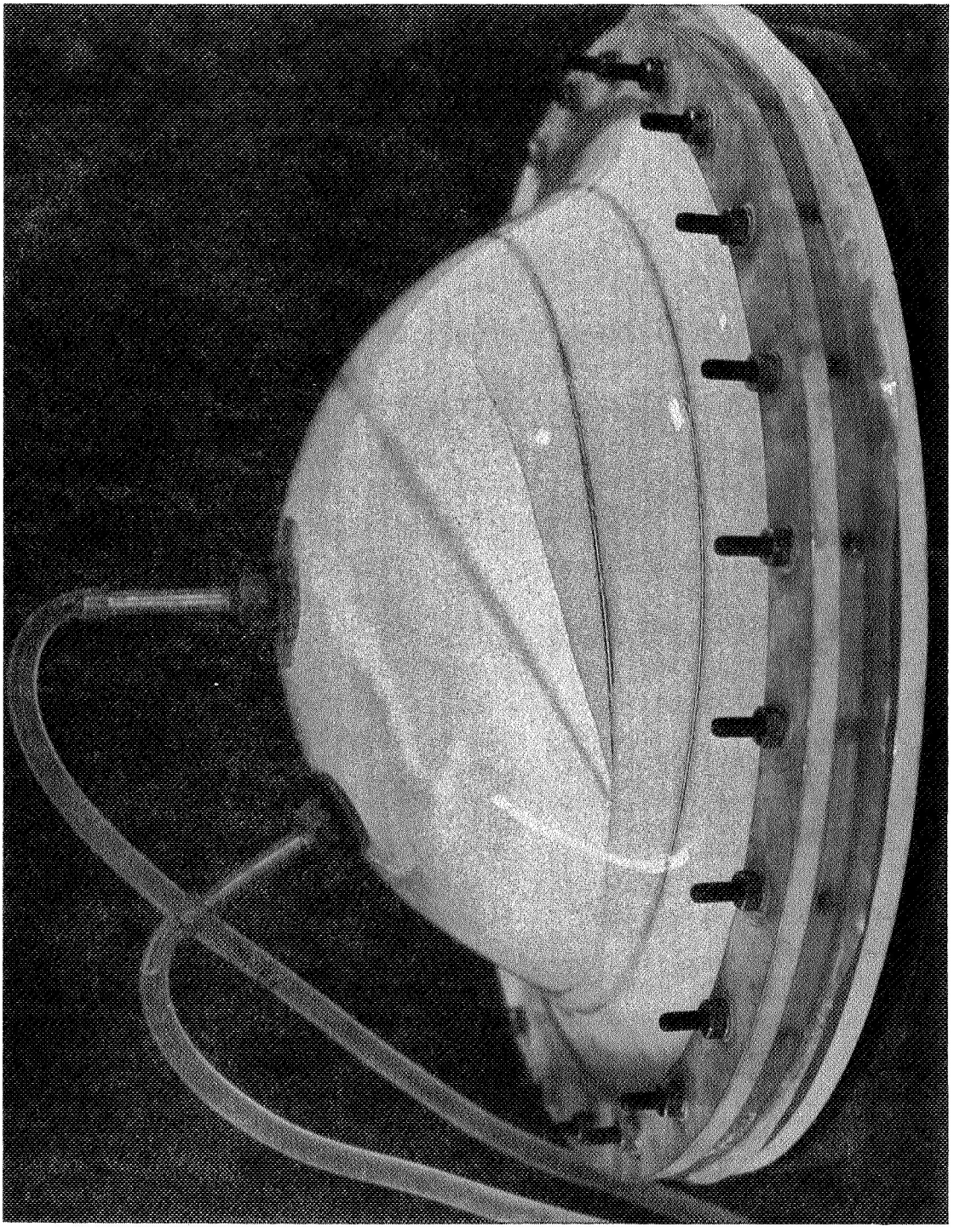

Figure 43: DIAPHRAGM TEST CYCLE

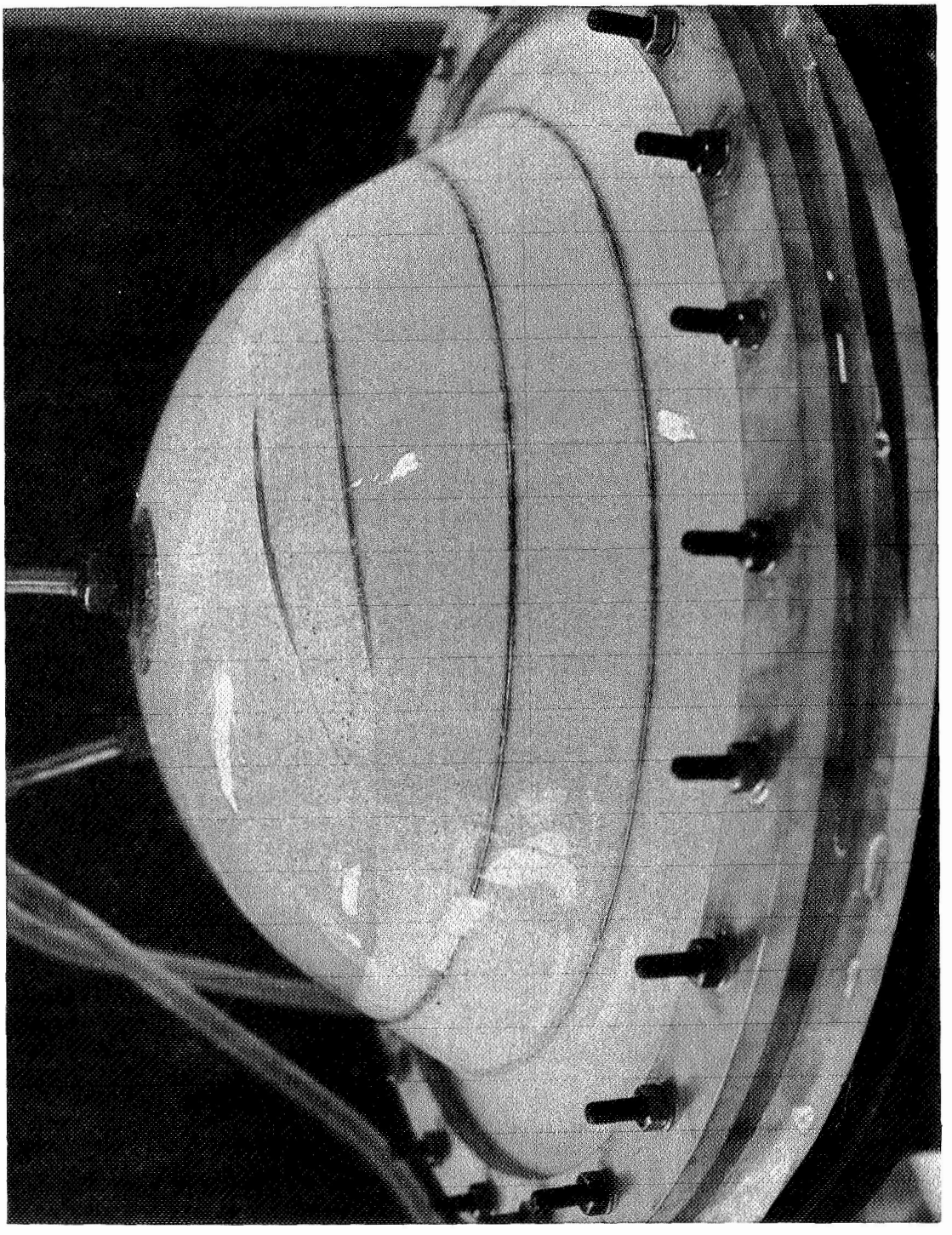

Figure 44: DIAPHRAGM TEST CYCLE

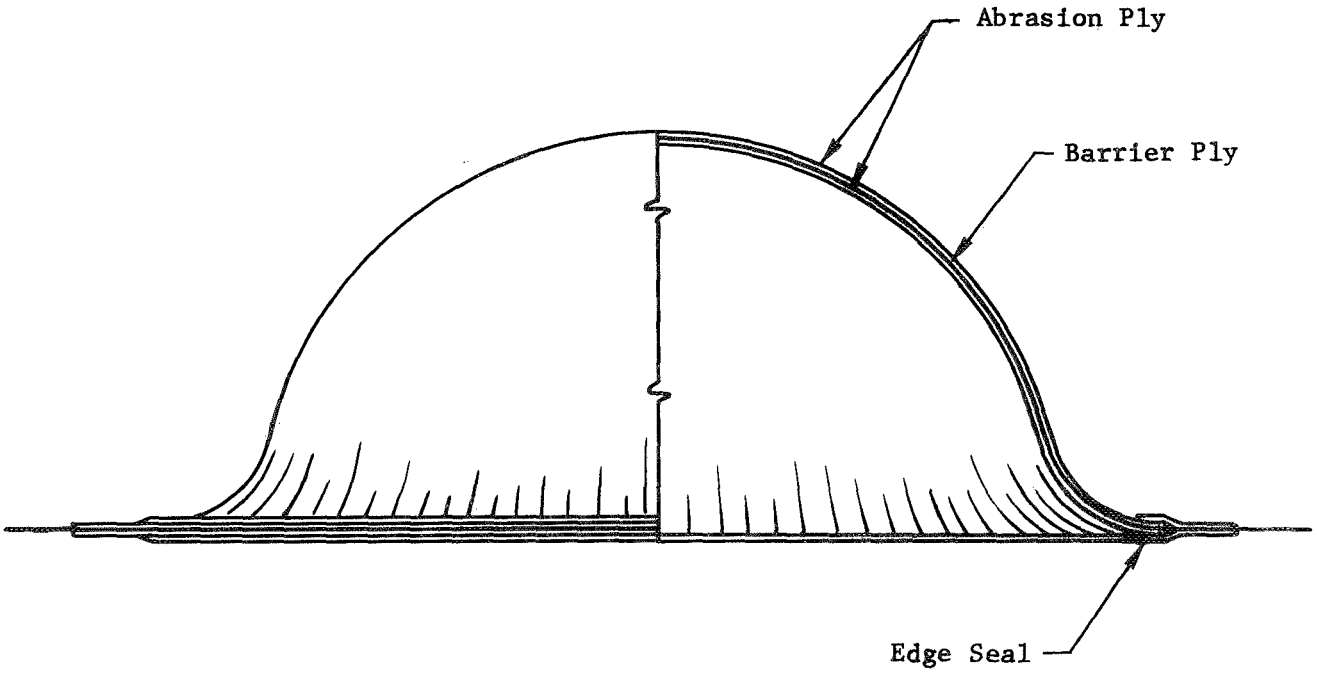

Figure 45: MODIFIED EXPULSION DIAPHRAGM

The final diaphragm was selected as a reference unit as an identical diaphragm (except for geometry) was successfully tested in liquid oxygen.

The diaphragms were fabricated using the procedures established in Phase II of the program and reported in section 3.

6.1 LIQUID HYDROGEN TESTING

The four diaphragms in this phase were tested in the equipment and using the test procedures reported in section 4.3.

6.2 TEST RESULTS

A discussion of the performance of each diaphragm is presented below.

6.2.1 Diaphragm V-1 (One Mil Gored Mylar)

The diaphragm failed in the initial fill cycle after ambient flange test and the initial fill cycle porosity checks. The tests were discontinued when the ambient leak check exceeded the capacity of the test apparatus and when the liquid hydrogen appeared in the window of the cryostat.

6.2.2 Diaphragm V-2 (One Mil Formed Kapton)

This unit failed in the first fill cycle with liquid hydrogen after initially passing the room temperature and cryogenic temperature porosity checks. Although the initial porosity was 10.8 cc/min. and a second at 3.6 cc/min., the test was continued. Liquid hydrogen was introduced into the fill side of the unit but was discontinued 37 minutes later when liquid reached the windows.

6.2.3 Diaphragm V-3 (Formed One Mill Kapton)

Following the ambient and flange porosity checks, the liquid hydrogen temperature porosity test showed a rate of 14 cc/min. Even though the leak rate exceeded the 10 cc/min. acceptable leakage, the diaphragm fill was begun. After 20 minutes of fill, drops of liquid hydrogen were observed on the gaseous helium side of the diaphragm. The test was discontinued when liquid hydrogen was observed on the cryostat window.

6.2.4 Diaphragm V-4 (Three Ply - 1/2 Mil Mylar Gores)

This unit was ambient temperature porosity checked without any measurable leakage but had an initial cryogenic temperature porosity of 21.7 cc/minute. The filling of liquid hydrogen was attempted. After seven minutes of filling, liquid hydrogen appeared in the cryostat window and the test was terminated.

6.3 POST-TEST ANALYSIS

After liquid hydrogen testing, all diaphragms were leak checked using gaseous helium, marked and disected.

The diaphragms, shown in Figures 46 and 47, present a different leak pattern than before in that leaks appeared in the dome area of diaphragm V-3. The leak pattern for the diaphragms fabricated of gores is identical to the failures previously observed. It was surprising that diaphragm V-4 did not perform as expected and failed as rapidly as the single barrier ply units.

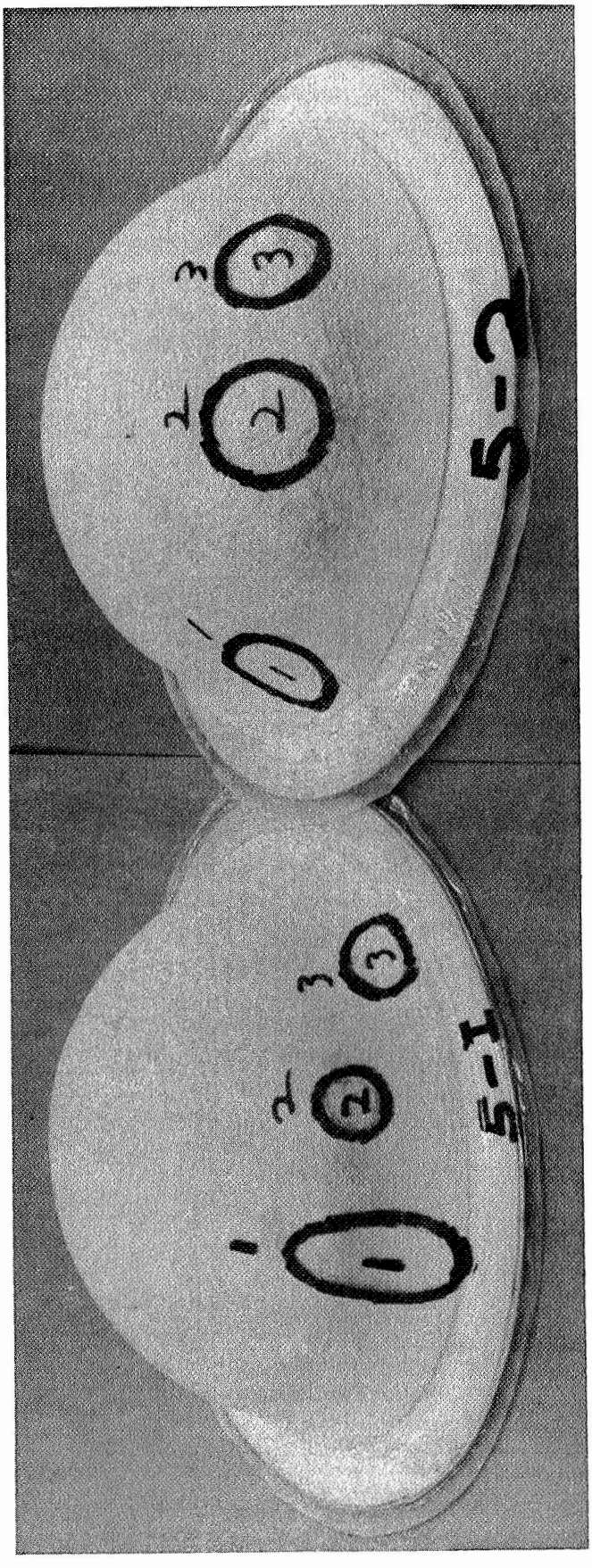

Figure 46: TEST DIAPHRAGM RESULTS

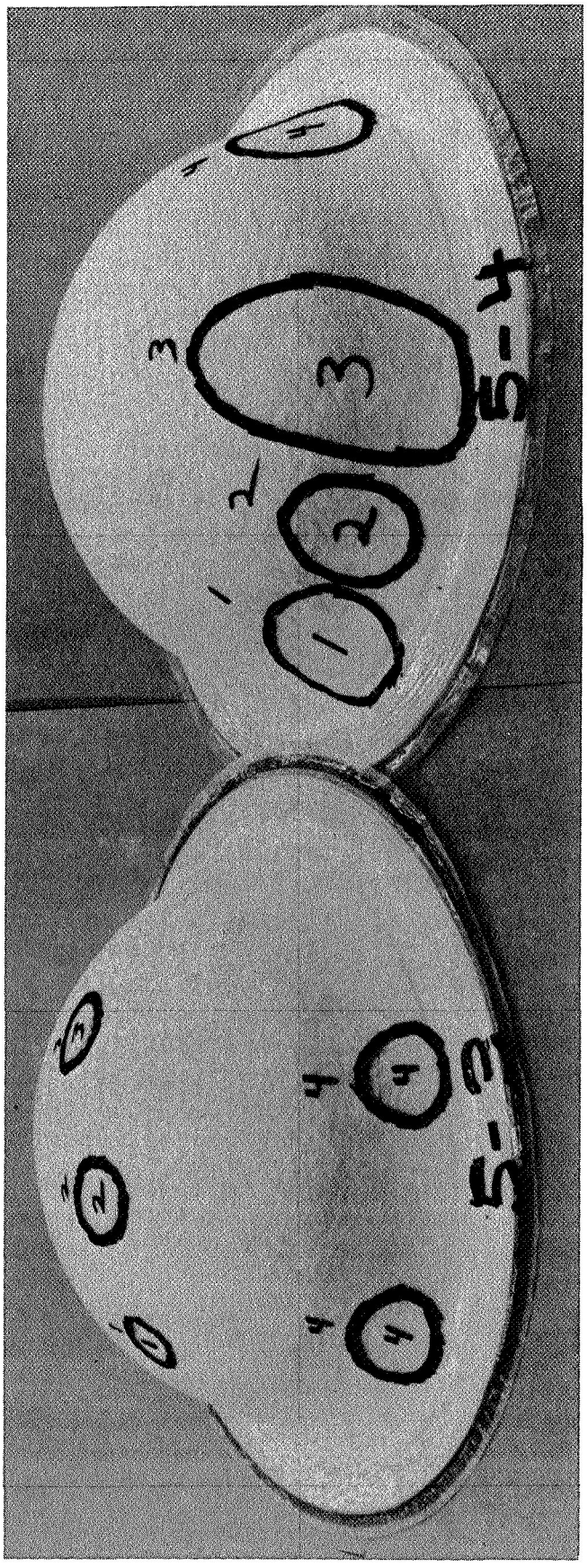

Figure 47: TEST DIAPHRAGM RESULTS

7.0 DISCUSSION OF RESULTS

GENERAL

None of the twenty diaphragms plus alternates performed satisfactorily in liquid hydrogen. A control unit, of identical construction with previous units successfully tested in liquid hydrogen, failed in the initial fill cycle.

Although the program goal of 25 failure free cycles was not approached, the test results gave an insight into diaphragm designs and into previous failures of multiply diaphragms and bladders.

A discussion of each area is given in the following paragraphs.

7.1 DEWAR DESIGN

The initial phase of the program resulted in a stainless steel test dewar which was unique in that the test article could be observed by remote TV and recorded on film during liquid hydrogen testing through windows in the dewar wall. Previous test units utilized observation through boiling liquid hydrogen into which the test article was immersed. Such units distort the image to the eye and to the motion picture camera. Remote site operation and observation of the test article is much simplified which excludes the requirement for personnel near the test unit during operation.

7.2 DIAPHRAGM DESIGN

7.2.1 Geometric Configuration

It is felt that the diaphragm design was the main contributing factor in diaphragm performance. The diaphragm was modified from a full hemispherical unit with the inclusion of a 30 degree conical section blended into the flange. This geometric shape became increasingly rigid at cryogenic temperatures and did not allow the unit to reverse itself. The diaphragms developed were of the type to "rim-roll" and with the conical section adjacent to the flange radius each diaphragm moved downward only slightly before it "locked" in position and leaks developed in the sharp creases. Analysis of the diaphragms in Task III showed great consistency in leaks developing either where the control section joined the flange radius or where it jointed the hemispherical head.

7.2.2 Butt Bonded Seams

An additional geometry factor was the double sealed butt joint of the gage sections diaphragms. Although the GT-300 adhesive was only 1/2 mil thick, two layers bonded together at the joint at liquid hydrogen

temperature created stiffened areas on the diaphragm which increased its resistance to reversing. Ninety percent of the leaks developed in gored diaphragms were in the bonded joints.

Convolute rings, frequently used to control the flexing cycle of diaphragms and bladders, were a hinderance on this program. The rings increased the structural conical section rigidity because of location and processing involved in bonding the rings on the felt or film.

A series of tests were conducted on diaphragms with different ring count and spacing using water as the reversing medium. The result of these tests was the four rings with the spacing shown in paragraph 3.3 which gave the best reversing control of the room temperature diaphragms. The rings prevented diaphragm 8A from reversing until the rings were removed. The rings on diaphragm 8B were removed before testing was attempted because of diaphragm rigidity.

7.3 STRESS GRADIENTS

A control diaphragm with only the formed 1/2 mil Mylar vapor barrier was fabricated and tested so that the liquid hydrogen fill could be observed. Following the initial leak checks, liquid hydrogen was introduced which contacted the diaphragm at the apex. Immediately the formed Mylar crinkled, shriveled, and contracted indicating stress gradients in the formed material. Thermal gradients should not have affected the diaphragm tests because the diaphragm contacted the stainless steel dome of the test dewar during conditioning and sufficient time had elapsed to stabilize the thin film diaphragm. The test shows that Mylar, when thermally formed under heat and vacuum, loses its relatively good characteristics of low permeability and high cycle flexibility in liquid hydrogen.

7.3.1 Film Failure

Analysis of the failures of the diaphragm after pinpointing the leakage areas showed that the majority of diaphragms with gores and butt seams failed in the adhesive joint which is the area of highest stress.

The formed diaphragms failed in three cornered fold areas. The diaphragm is subjected to folds and creases while becoming increasingly rigid at liquid hydrogen temperature. In addition to the film rigidity, the bonding adhesive to join the abrasion plies of dacron felt to the vapor barrier compounded this problem.

8.0 REFERENCES

1. K. E. Wiedekamp, "Development of Liquid Hydrogen Positive Expulsion Bladders," NASA CR-62432
The Boeing Company, Seattle, Washington May, 1968

2. Pope, D. H., Penner, J. E., "Development of Cryogenic Positive Expulsion Bladders," NASA CR-72115
Beech Aircraft Corporation, Boulder, Colorado January, 1968

3. J. T. Hoggatt, "Polymeric Positive Expulsion Bladders for Liquid Oxygen Systems", NASA CR-72418
The Boeing Company, Seattle, Washington June, 1968

9.0 DISTRIBUTION LIST

	No. of Copies
National Aeronautics & Space Administration Lewis Research Center 21000 Brookpark Road Cleveland, Ohio 44135	
Attention: Contracting Officer, MS 77-3	1
Liquid Rocket Technology Branch, MS 500-209	5
Technical Report Control Office, MS 5-5	1
Technology Utilization Office, MS 3-16	1
AFSC Liaison Office, MS 501-3	2
Library, MS 60-3	1
Office of Reliability & Quality Assurance, MS 500-111	1
D. L. Nored, MS 500-209	1
R. F. Lark, Project Manager, MS 49-1	15
E. W. Conrad, MS 500-204	1
R. H. Kemp, MS 49-1	1
R. H. Knoll, MS 501-2	1
Chief, Liquid Experimental Engineering, RPX Office of Advanced Research & Technology NASA Headquarters Washington, D.C. 20546	1
National Aeronautics & Space Administration Ames Research Center Moffett Field, California 94035 Attention: Library	1
National Aeronautics & Space Administration Flight Research Center P.O. Box 273 Edwards, California 93532 Attention: Library	1
National Aeronautics & Space Administration Goddard Space Flight Center Greenbelt, Maryland 20771 Attention: Library	1
National Aeronautics & Space Administration John F. Kennedy Space Center Cocoa Beach, Florida 32931 Attention: Library	1

National Aeronautics & Space Administration
Langley Research Center
Langley Station
Hampton, Virginia 23365
Attention: Library 1

National Aeronautics & Space Administration
Manned Spacecraft Center
Houston, Texas 77001
Attention: Library 1

National Aeronautics & Space Administration
George C. Marshall Space Flight Center
Huntsville, Alabama 35812
Attention: Library 1
Keith Chandler 1
Leon J. Hastings 1

Jet Propulsion Laboratory
4800 Oak Grove Drive
Pasadena, California 91102
Attention: Library 1
L. Toth 1

Defense Documentation Center
Cameron Station
Building 5
5010 Duke Street
Alexandria, Virginia 22314
Attention: TISIA 1

Office of the Director of Defense Research
and Engineering
Washington, D. C. 20301
Attention: Office of Asst. Dir. (Chem. Technology) 1

Chief, Liquid Propulsion Technology, RPL
Office of Advanced Research & Technology
NASA Headquarters
Washington, D. C. 20546 1

Director, Launch Vehicles & Propulsion, SV
Office of Space Science & Applications
NASA Headquarters
Washington, D. C. 20546 1

Chief, Environmental Factors & Aerodynamics
Code RV-1
Office of Advanced Research & Technology
NASA Headquarters
Washington, D. C. 20546 1

Chief, Space Vehicles Structures
Office of Advanced Research & Technology
NASA Headquarters
Washington, D. C. 20546 1

Director, Advanced Manned Missions, MT
Office of Manned Space Flight
NASA Headquarters
Washington, D. C. 20546 1

NASA Scientific & Technical Information Facility
P. O. Box 33
College Park, Maryland 20740 6

Director, Technology Utilization Division
Office of Technology Utilization
NASA Headquarters
Washington, D. C. 20546 1

Arnold Engineering Development Center
Air Force Systems Command
Tullahoma, Tennessee 37389
Attention: Library 1

Advanced Research Projects Agency
Washington, D. C. 20525
Attention: D. E. Mock 1

Aeronautical Systems Division
Air Force Systems Command
Wright-Patterson Air Force Base,
Dayton, Ohio 45433
Attention: Library 1

Air Force Missile Test Center
Patrick Air Force Base, Florida
Attention: Library 1

Air Force Systems Command
Andrews Air Force Base
Washington, D. C. 20332
Attention: Library 1

Air Force Rocket Propulsion Laboratory
Edwards, California 93523
Attention: Library 1
J. Branigan 1

Air Force Office of Scientific Research
Washington, D. C. 20333
Attention: Library 1

Space & Missile Systems Organization
Air Force Unit Post Office
Los Angeles, California 90045
Attention: Technical Data Center 1

Office of Research Analyses (OAR)
Holloman Air Force Base, New Mexico 88330
Attention: Library - RRRD 1

U. S. Air Force
Washington, D. C.
Attention: Library 1

Commanding Officer
U. S. Army Research Office (Durham)
Box CM, Duke Station
Durham, North Carolina 27706
Attention: Library 1

U. S. Army Missile Command
Redstone Scientific Information Center
Redstone Arsenal, Alabama 35808
Attention: Document Section 1

Bureau of Naval Weapons
Department of the Navy
Washington, D. C.
Attention: Library 1

Commander
U. S. Naval Missile Center
Point Mugu, California 93041
Attention: Technical Library 1

Commander
U. S. Naval Weapons Center
China Lake, California 93557
Attention: Library 1

U. S. Naval Ship Research & Development
Laboratory
Annapolis, Maryland 21402
Attention: C. Hershner, Code A-731 1

Commanding Officer
Naval Research Branch Office
1030 East Green Street
Pasadena, California 91101
Attention: Library 1

Director (Code 6180)
U. S. Naval Research Laboratory
Washington, D. C. 20390
Attention: Library 1

Picatinny Arsenal
Dover, New Jersey 07801
Attention: Library 1

Air Force Aero Propulsion Laboratory
Research & Technology Division
Air Force Systems Command
United States Air Force
Wright-Patterson AFB, Ohio 45433
Attention: RPRP (Library) 1
R. Quigley 1

Propulsion Division
Aerojet-General Corporation
P. O. Box 15847
Sacramento, California 95803
Attention: Technical Library 2484-2015A 1

Aeronautic Division of Philco Ford Corporation
Ford Road
Newport Beach, California 92663
Attention: Technical Information Department 1

Boeing Company
Space Division
P. O. Box 868
Seattle, Washington 98124
Attention: Library 1

Chemical Propulsion Information Agency
Applied Physics Laboratory
8621 Georgia Avenue
Silver Spring, Maryland 20910
Attention: T. Reedy 1

Curtiss-Wright Corporation
Wright Aeronautical Division
Woodridge, New Jersey
Attention: Library — 1

University of Denver
Denver Research Institute
P. O. Box 10127
Denver, Colorado 80210
Attention: Security Office — 1

Fairchild Stratos Corporation
Aircraft Missiles Division
Hagerstown, Maryland
Attention: Library — 1

Research Center
Fairchild Hiller Corporation
Germantown, Maryland
Attention: Library — 1

General Dynamics/Convair
P. O. Box 1128
San Diego, California 92112
Attention: Library — 1

Missiles and Space Systems Center
General Electric Company
Valley Forge Space Technology Center
P. O. Box 8555
Philadelphia, Pa. 19101
Attention: Library — 1

General Electric Company
Flight Propulsion Laboratory Department
Cincinnati, Ohio
Attention: Library — 1

Martin-Marietta Corporation (Baltimore Division)
Baltimore, Maryland 21203
Attention: Library — 1

Denver Division
Martin-Marietta Corporation
P. O. Box 179
Denver, Colorado 80201
Attention: Library — 1
R. Fearn — 1

Rocketdyne Division
North American Rockwell Inc.
6633 Canoga Avenue
Canoga Park, California 9134
Attention: Library, Dept. 596-306 — 1

Space & Information Systems Division
North American Rockwell
12214 Lakewood Blvd.
Downey, California
Attention: Library — 1

Northrop Space Laboratories
3401 West Broadway
Hawthorne, California
Attention: Library — 1

Radio Corporation of America
Astro-Electronics Products
Princeton, New Jersey
Attention: Library — 1
Y. Brill — 1

TRW Systems Inc.
1 Space Park
Redondo Beach, California 90278
Attention: Tech. Lib. Doc. Acquisitions — 1

TRW Incorporation
TAPCO Division
23555 Euclid Avenue
Cleveland, Ohio 44117
Attention: Library — 1

United Aircraft Corporation
Corporation Library
400 Main Street
East Hartford, Connecticut 06108
Attention: Library — 1

United Aircraft Corporation
Pratt & Whitney Division
Florida Research & Development Center
P. O. Box 2691
West Palm Beach, Florida 33402
Attention: Library — 1

United Aircraft Corporation
United Technology Center
P. O. Box 358
Sunnyvale, California 94038
Attention: Library 1

Vought Astronautics
Box 5907
Dallas, Texas
Attention: Library 1

Garrett Corporation
Air Research Division
Phoenix, Arizona 85036
Attention: Library 1

Garrett Corporation
Air Research Division
Los Angeles, California
Attention: Library 1

Grumman Aircraft Engineering Corporation
Bethpage, Long Island, New York
Attention: Library 1

Honeywell, Inc.
Aerospace Division
2600 Ridgeway Road
Minneapolis, Minnesota
Attention: Library 1

I IT Research Institute
Technology Center
Chicago, Illinois 60616
Attention: Library 1

Kidde Aerospace Division
Walter Kidde & Company, Inc.
567 Main Street
Bloomfield, N.J.
Attention: Library 1

Ling-Temco-Vought Corporation
P. O. Box 5907
Dallas, Texas 75222
Attention: Library 1

Lockheed Missiles and Space Company
P. O. Box 504
Sunnyvale, California 94087
Attention: Library 1

Aerospace Corporation
2400 E. EI Segundo Blvd.
Los Angeles, California 90045
Attention: Library-Documents 1

Astropower Laboratory
McDonnell-Douglas Aircraft Company
2121 Paularino
Newport Beach, California 92163
Attention: Library 1

ARO, Incorporated
Arnold Engineering Development Center
Arnold AF Station, Tennessee 37389
Attention: Library 1

Susquehanna Corporation
Atlantic Research Division
Shirley Highway and Edsall Road
Alexandria, Virginia 22314
Attention: Library 1

Battelle Memorial Institute
505 King Avenue
Columbus, Ohio 43201
Attention: Report Library, Room 6A 1

Beech Aircraft Corporation
Boulder Facility
Box 631
Boulder, Colorado
Attention: Library 1
L. Thompson 1

ARDE', Inc.
19 Industrial Avenue
Mahwah, New Jersey 07430
Attention: D. Gleich 1